TECHNISCHE UNIVERSITÄT WIEN

MASTER'S THESIS

# Analyses of LASI (Light Absorbing Snow Impurities) within samples of snow pits collected in an high alpine environment

Conducted at the Institute of Chemical Technologies and Analytics

At the TU Wien

In the research group Environmental Analytics

Under the supervision of ao. Univ. Prof. Dipl.-Ing. Dr. techn. Anne Kasper-Giebl

and

Projektass. Dipl.-Ing. Daniela Kau, BSc.

By Jakub Bielecki, BSc.

_____ _____

Date Jakub Bielecki, BSc.

# Acknowledgements

I would like to express my sincere thanks to Ao. Univ. Prof. Dr. Anne Kasper – Giebl for the supervision and facilitation of this thesis. Additionally, I am very thankful to Daniela Kau, Michaela Zuckerhut and Hong Huang who taught me the appropriate techniques, regarding the handling of various instruments. I also wish to thank the ZAMG (Central Institution for Meteorology and Geodynamics) for the taking and providing of the samples for this thesis.

I am also equally grateful to my other colleagues; Bernadette Kirchsteiger, Karoline Rieger, Christine Hochwartner, Thomas Riedlberger, Felix Happenhofer, Andjela Vukicevic, Gurpreet Gill, Thomas Rosa-Steinkogler, Clea Danlos and Peter Redl. Their support and creation of a positive work environment helped me through a lot while working on my master's thesis.

Special thanks go to the research group of Univ. Prof. Dr. Andreas Limbeck for making it possible to perform the elemental analysis, their enduring support and help. I am also very thankful to Andjela for providing data from her bachelor's thesis.

I would also like to thank my parents, brother and friends for the permanent support during my education.

# Table of Contents

# List of Figures

# List of Tables

# Abstract

Global warming is impacting the earth way faster than expected. Several processes take part in global warming and thus may enhance or reduce the impacts. One of them is the Albedo, which is the fraction of solar light that is reflected by a surface and therefore contributes to the prevention of further warming. Fresh snow shows a high albedo, but the presence of Light Absorbing Snow Impurities (LASI) leads to faster melting snow, because the impurities heat up. This leads to less snow and therefore to less albedo.

This thesis is dedicated to analyzing three different groups of LASI. Water Insoluble Organic Carbon (WIOC), Elemental Carbon (EC) and Mineral Dust (MD). The analysis of carbon is achieved through a thermal - optical analyzer (TOA). For MD, Inductively Coupled Plasma - Optical Emission Spectroscopy (ICP – OES) was applied. To compare the samples taken from different positions at the glacier, cation - chromatography was used.

Based on the calcium and especially the ammonium concentrations, a comparison of the snow samples investigated within this thesis with earlier samples collected nearby was possible. The data showed good agreement, regarding the seasonal trend as well as absolute concentration values. Therefore, the two data sets can be merged for future investigations. A comparison of the WITC (Water Insoluble Total Carbon), WIOC and EC data with studies conducted in other regions, allowed to discuss agreement and differences regarding elevation, vicinity of emission sources and remoteness of the site. Except of 2020, all carbon depth profiles do not show a seasonal trend. For all other years elevated concentrations could be seen at different times, throughout the year. Besides carbon parameters, data for thirteen elements was analyzed. With those concentrations, a mass balance of fifteen MD samples was done.

With the data gathered in this thesis, WITC, WIOC, EC and MD concentrations representing the accumulation periods of the years 2017 - 2022 from the Austrian Alps are available and can be used for comparison and modeling. Additionally, a method for the correction of the TOA for samples containing MD has been elaborated and looks very promising. Three criteria for the determination whether a sample contains MD or not, were tested and evaluated. MD accounts for the majority of the mass of insoluble particles, being much more prominent than organic matter.

# 1. Introduction

## 1.1 LASI (Light Absorbing Snow Impurities)

LASI (Light Absorbing Snow Impurities) summarize several compounds which decrease snow albedo. Albedo is the fraction of solar light that is reflected by a surface and therefore contributes to the prevention of further warming. Fresh snow has a high albedo (~ 80 % reflection),[10] but the presence of Light Absorbing Snow Impurities (LASI) leads to faster snow melt, because the impurities heat up. This leads to less snow and therefore to less albedo. [11] There are many different impurities that can have this effect on the snow albedo. Examples are black carbon (BC), mineral dust (MD), volcanic ash, soil organics, algae, and other biological organisms. [1] In literature several additional terms to characterize LASI exist like light-absorbing impurities (LAIs) [1] or light-absorbing particles (LAPs) [2].

A carbonaceous material in aerosol particles is often classified as black carbon (BC) and organic carbon (OC). BC itself was already introduced as an important contributor as LASI. Regarding OC a number of constituents have also been mentioned before as part of LASI, i.e. soil organics, algae and other biological organisms. Still, not all of OC is light absorbing. The source of BC is mainly the combustion of fuel and biomass, while OC has various sources and can either be emitted or is formed in the atmosphere. [4]

The amount of these impurities in the snowpacks depends on different factors. The first one is wet deposition, which is the input via snowfall. Concentrations in precipitation and the snowfall rate determine the deposition load. The second one is the amount deposited on the surface through dry deposition, i.e. the direct input of particulates or gaseous compounds without the aid of precipitation. The third one is the redistribution of these impurities through post-depositional processes. Examples for these processes are wind driven drifting, wind pumping, snow sublimation and scavenging during snowmelt, which leads to a lower amount of LASI at melt time. [1] But impurities are not the only factor which influences snow albedo, also the physical properties of the snow microstructure are important, especially in the near infrared. These properties are highly relevant for the density and specific surface area, which means that it is very important to take them into account.

Because of the global occurrence of LASI, their effects on snow albedo and therefore snowpack evolution and melt are global problems. The impact on the presence of snow cover varies on a local scale, which means that local LASI observations are recommended. [3] It is also important to not only focus on BC when looking at the radiative impact of LASI, because other constituents are responsible for up to 50 % of the absorption. Other studies have shown that dust is also a very important factor for snow radiative forcing which can lead to a total melt out by up to 50 days. [1] BC and mineral dust

are suspected to have the biggest influence on snowpack evolution in the European Alps. It is even so big, that BC was probably one of the causes why the Little Ice Age in the Alps ended. [1]

Saharan dust depositions in the Alps mostly happen between April and August and give snow layers a reddish or yellowish color. These events, i.e. the time when dust particles are airborne lasts only a few hours but they lead to a significant amount of mineral dust in the snowpacks, which influence snow melt and eventually snowpack stability. [2]

Typical regions where measurements of LASI concentrations have been done are the Himalaya, North America and the Artic, while just a few investigations were performed in the French Alps. [4, 2, 17, 22] There have been less measurements of LASI concentrations in seasonal snow in the European Alps than in long-term measurements from ice cores. Still, measurements of seasonal snow are very important for the research of the seasonal evolution of LASIs at lower altitudes. [2]

There are two ways to gather information regarding the radiative impact of LASIs in seasonal snow. The first one is to determine the concentrations of various snow impurities in the samples with different chemical measurement techniques. Afterwards the relation between the concentration and the LASI absorption is determined using the mass absorption efficiency (MAE), which is the absorption efficiency of the LASI. Another method to determine the radiative impact of LASIs in snow samples, is spectral measurements of the snow reflectance. [2] As this work will contribute to the first approach, the analytical methods available for analyses of snow samples will be discussed a bit further.

To determine black carbon (BC), methods like the thermal-optical analysis (TOA) and the single particle soot photometer (SP2) are common. [2, 19] Use of TOA allows to evaluate the concentrations of water insoluble OC (WIOC) as well. It has to be noted, that the presence of MD in the samples leads to issues during the determination of OC and EC. The optical properties of hematite change during the temperature program of the thermal – optical analysis (TOA). This leads to a change in the transmittance and reflectance of the laser and therefore to wrong EC and OC values, because of the wrong positioning of the OC / EC split point. [9]

There are a few methods to determine the concentration of dust in snow, for example, particle counters, gravimetry or analysis based on dust mineralogical properties. However, measuring uncertainties of dust concentrations are still a problem because research on mineral dust is not getting as much attention as on BC. [2] Going back to the analysis of the major elements this approach needs a calculation via a mass balance. For this purpose, Ca, Fe, Al, Si and Ti concentrations are used in the following equation to evaluate the concentrations of MD in the collected samples.

$$MD = (1.41\ x\ Ca + 2.09\ x\ Fe + 1.9\ x\ Al + 2.15\ x\ Si + 1.67\ x\ Ti)\ x\ 1.16$$

*Equation 1: Calculation of the mineral dust (MD) content [12]*

If not all elements are analyzed other relationships need to be used. A common problem is, that Si cannot be determined since the quartz fiber filters contain silicon. Therefore, the average ratio of Si/Al = 2.5 can be used to calculate the Si in the collected sample. [12]

Analyzing the chemical composition of MD is also a way to determine its origin. The average composition of Saharan dust samples, which have been sampled in Spain, is: 64 % silicate, 14 % sulfates, 6 % quartz, 5 % calcium – rich particles, 1 % hematite, 1 % soot and 9 % other carbonaceous material. [7]

While the analyses of metals is a quite straightforward method, there are additional ways to find out if there is MD in the snow sample. Three possibilities which will be used within this work are explained in the following. The first one is visual inspection of the water insoluble material filtrated from the molten snow sample. The reddish color of the sampled filters, due to hematite, becomes visible. This is most evident after TOA, when all carbonaceous compounds have already been removed.

The second one is the rising transmissions signal at the end of the TOA, which happens due to the cooling of the hematite and the change of its' optical properties and was already mentioned above as an interference for TOA.[9]

The third one is described in Greilinger et al. (2018) and refers to analyses of the liquid samples. The criterion for a marked MD content is defined by a pH > 5.6 and a $Ca^{2+}$ concentration > 10 µeq/l. [8]

Since no pH measurements were conducted, it was necessary to use data of a series of samples taken parallel but analyzed already earlier. The comparability of the data sets had to be shown via the analyzes of the cations using ion chromatography. If the values are similar, the pH values can be used for the samples examined in this thesis.

## 1.2 Aim of this work

This thesis is dedicated to analyzing two groups of LASI (light absorbing snow impurities) in snow samples collected from 2017 until 2022 at two glaciers near the Sonnblick Observatory. These two groups are Elemental Carbon (EC) and Mineral Dust (MD). Furthermore, Water Insoluble Organic Carbon (WIOC) is evaluated. Part of WIOC will also contribute to LASI, but no clear correlation is possible. The snow profiles evaluated here complement and extend an independent data set of snow profiles obtained annually for soluble inorganic anions and cations, pH and conductivity since more than 30 years. The profiles for the determination of LASI were taken in close vicinity to the profiles of the long-term monitoring. To ensure, that the data of both profiles is well comparable the analysis of soluble cations was repeated for the samples analyzed within this thesis. The results obtained for EC; WIOC and MD will allow further investigations concerning the deposition flux of LASI and their impact on the surface albedo.

The analysis of carbon (EC and WIOC) is achieved by thermal – optical analysis. The identification and quantification of MD was done via the combination of several methods including thermal-optical analysis, Inductively Coupled Plasma – Optical Emissions Spectroscopy (ICP – OES) and based on the results obtained for inorganic ions and pH.

# 2. Experimental

## 2.1 Sampling

Every year at the end of the winter accumulation period, usually in April, snow samples are taken at the Glaciers. For this purpose, a snow pit is dug and samples, with a vertical resolution of 20 cm, are taken by the ZAMG (Central Institution for Meteorology and Geodynamics). To do this a stainless-steel cylinder with a length of 20 cm is pushed into the snowpack vertically to collect the respective snow segments. Masks and gloves were used to avoid contamination of the samples during this process. Then the samples are stored in PE bags (WhirlPak). The samples are transported frozen to TU Wien, where they were stored in a deep freezer until analysis.

In parallel to these samples with a vertical resolution of 20 cm, additional snow profiles with a vertical resolution of 10 cm were obtained every year to analyze pH, conductivity and inorganic ions. This time series was actually started already in the 1980s. Sampling of the 20 cm increments to additionally analyze LASI, was started in 2017. As both profiles were sampled within one snow pit it can be expected that the chemical composition of the profiles is well comparable. Still the layering of the snow can show some variation spatially already at small distances. To evaluate possible differences and to prove the agreement of the profiles part of the analysis of the 10-cm profile, i.e., the analysis of inorganic cations, was repeated for the 20 cm profile.

The snow samples, which are analyzed in this work, were collected at two different glaciers. They are called Kleinfleißkees (FLK) and Goldbergkees (GOK), near the Hoher Sonnblick (SBK). Both are located in the Austrian National Park “Hohe Tauern” in the Eastern Alps at about 3100 m a.s.l.. Figure 1 shows the exact locations.

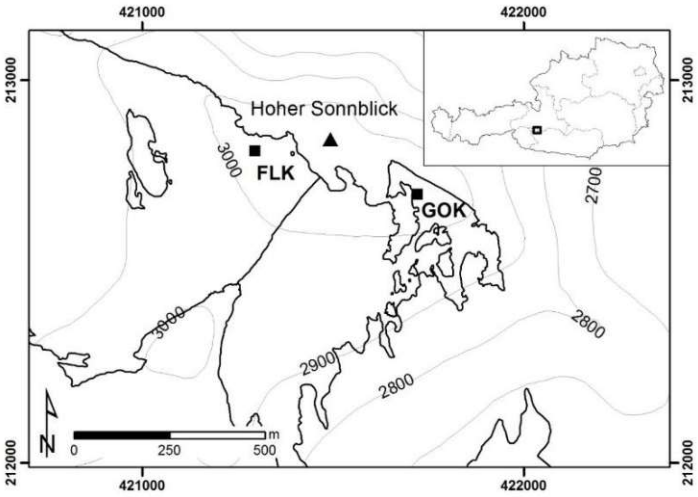


*Figure 1: Location of the glaciers Kleinfleißkees and Goldbergkees (source: Marion Greilinger)*

## 2.2 Preparation of quartz fiber filters and filtration

Before the snow samples are filtered through quartz fiber filters (PALLFLEX Membrane Filters), the filters must be prepared. Firstly, circular punches with a diameter of 27 mm are cut and then placed in a muffle furnace for 24 hours to be cleaned. Afterwards they are put in a desiccator above demineralized water to cool off. This saturates the reactive surface of the filter material with water vapor, instead of carbon containing vapors. Then the weight of the filters was determined using an analytical balance (Sartorius MC 210 P).

The snow samples are melted in a glass beaker using a microwave (600 W) and weight after extracting 1 mL for the cation chromatography measurement with a pipette. The following Figure 2 shows the used filtration setup.

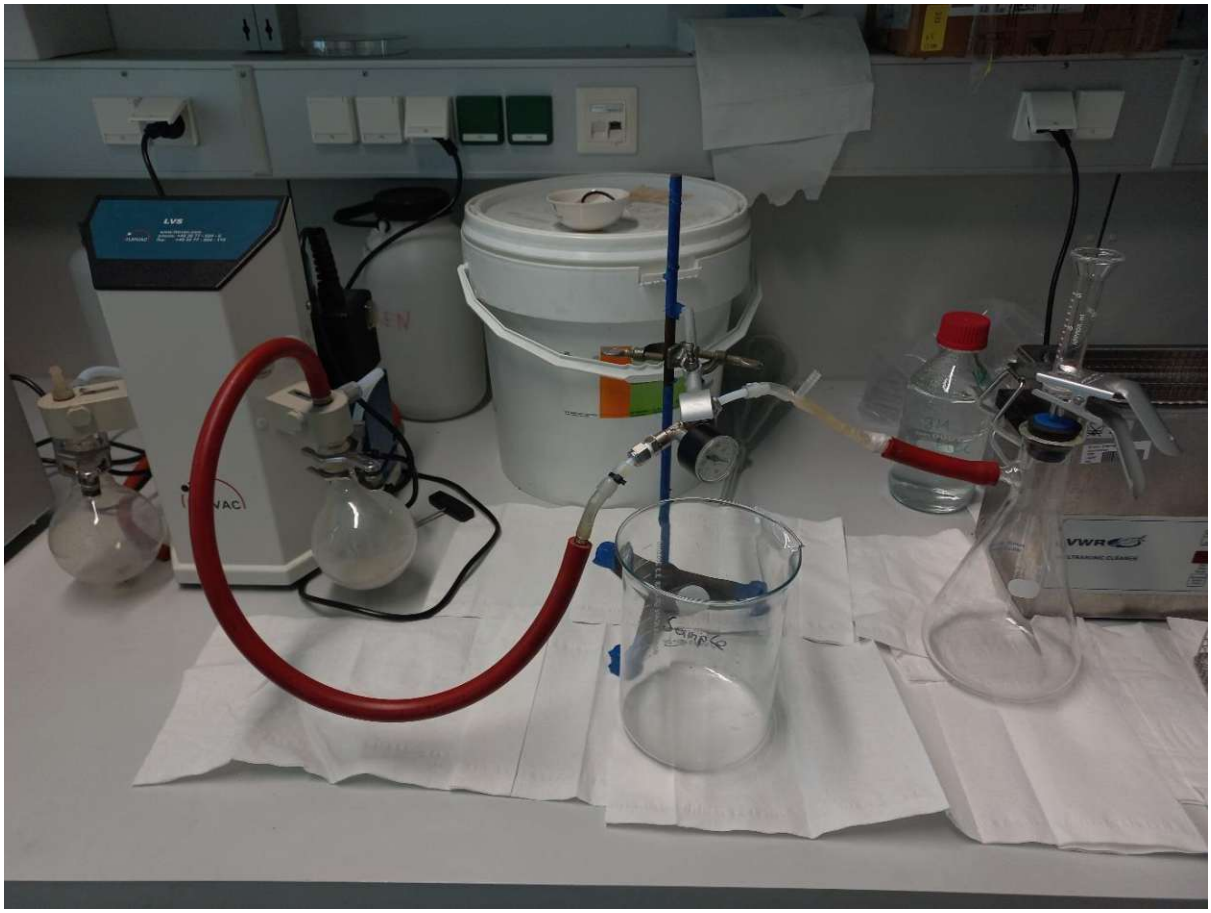

*Figure 2: Filtration setup*

The actual filtration setup consists of a side-arm flask, a frit, a clamp and a funnel. It is connected to a manometer, a T-piece and a vacuum pump. The filter is placed between the frit and the funnel, and the clamp is holding everything in place.

Firstly 5 mL of Milli-Q water are poured onto the filter in order to moisten it, so the particles, contained in the actual sample, are distributed more evenly on the filter. The molten snow sample is poured into

the funnel and the sample flow is regulated by adjusting the vacuum by closing the T-piece. Additionally, it was important to apply a slight vacuum only. Pressures between 0.1 and 0.7 bar showed in a previous master's thesis the best results. [9] After the whole sample volume was filtered, the beaker was rinsed with 25 mL of Milli-Q water to remove residues of the sample from its walls. This water was filtrated as well, and the filter is dried by drawing some air at a lower pressure for about 10 seconds.

Then the loaded filters are dried in a desiccator above silica gel, for at least 24 hours. Afterwards the weight of the loaded filters was determined again.

Even though the filters have a diameter of 27 mm, only an area of 16 mm was loaded. For subsequent analysis, a punch of 17 mm was made which comprised the whole loaded area. This punch was cut in two halves to fit onto the glass spoon of the thermal-optical analysis. Consequently, two analytical runs had to be performed for every sample. The overall load was determined as the sum of both runs. Therefore, it was not necessary to guarantee a correct separation of the loaded area in two halves of equal area.

## 2.3 Thermal-optical analysis (TOA)

The Sunset Laboratory Inc. OC/EC instrument is used for the thermal-optical analysis of OC/EC and is a recognized and widely used method to determine elemental and organic carbon collected on quartz fiber filters. The whole instrument is made of three sectors which are connected to each other. The first one is the main oven box, which contains the motherboard, the front oven and the back oven, which is filled with an oxidizing agent called $MnO_2$. The combination of front and back oven is called main oven. The second sector contains the methanator oven, which is filled with a heated nickel catalyst, and the flame ionization detector (FID). The third and last sector is the computer for data processing.

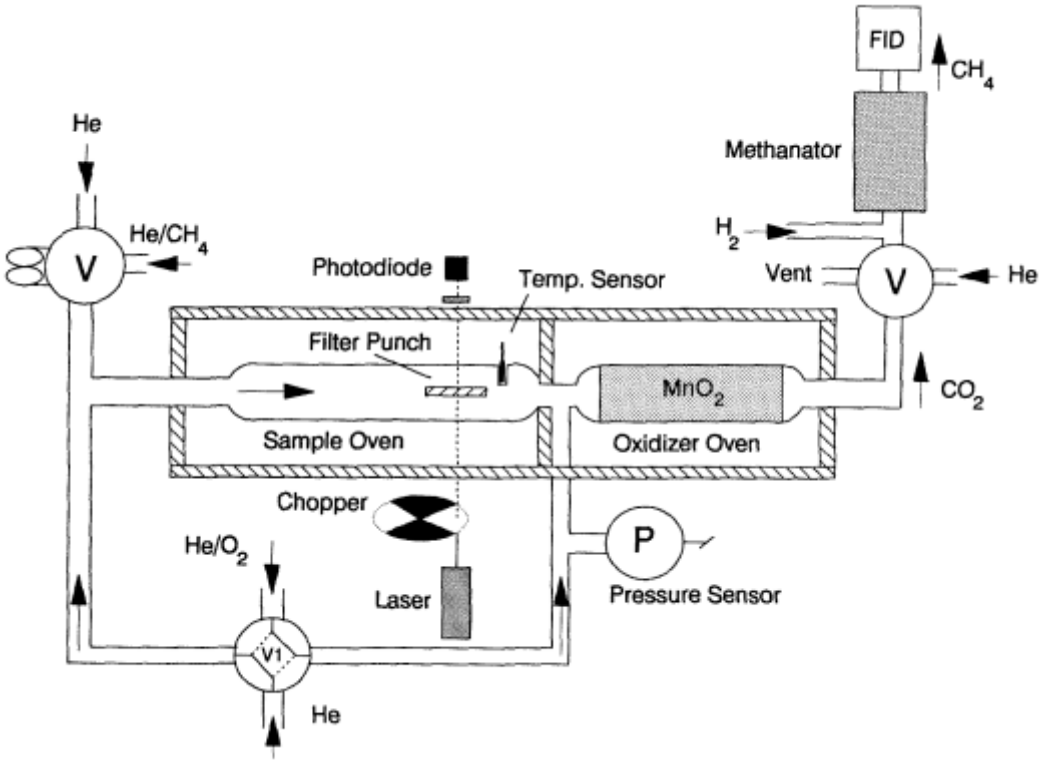


*Figure 3: Schematic diagram of the OC/EC Analyzer [13]*

For the thermal-optical analysis seven different gas flows, with different flow rates, are used. They are set in the range of possible flow rates, which are shown in Table 1. In the inert atmosphere He is used as the carrier gas and in the oxidizing atmosphere it is a He/$O_2$-mixture (10 vol % $O_2$). The calibration gas is a mixture of He and 5 vol % $CH_4$ and is measured at the very end of every measurement. For the

detection via FID $H_2$ and synthetic air is used. The same gas bottle is used for He1, He2 and He3 but they have different gas lines and are introduced at different positions.

*Table 1: Gases and gas flow rates used by the Sunset OC/EC Analyzer*

| Gas | Lowest flow rate (cc/min) | Highest flow rate (cc/min) |
|---|---|---|
| Synthetic air | 280 | 300 |
| $H_2$ | 50 | 54 |
| He1 | 48 | 52 |
| He2 | 7 | 9 |
| He3 | 63 | 67 |
| He / $O_2$ | 7 | 9 |
| Calibration gas | 10 | 15 |

The results were obtained in µgC/cm² for each measured filter half. These values were added up and converted to the loading of the entire filter area (i.e. divided by two and multiplied by 2.01 to get the result in µg on the sampled area). In the last step, the value was divided by the sample weight (g of snow filtrated onto the filter) and then multiplied by 1000 to obtain the end result in ng/g.

### 2.3.1 Thermal protocol EUSAAR.2

The thermal protocol used for the measurements is EUSAAR.2. Even though it is optimized for the analysis of carbonaceous aerosols at European regional background sites [14], it has proven to be applicable for the analysis of water insoluble carbonaceous compounds in snow samples as well [17,18] Figure 4 shows the desired temperature of EUSAAR.2 as a function of time.

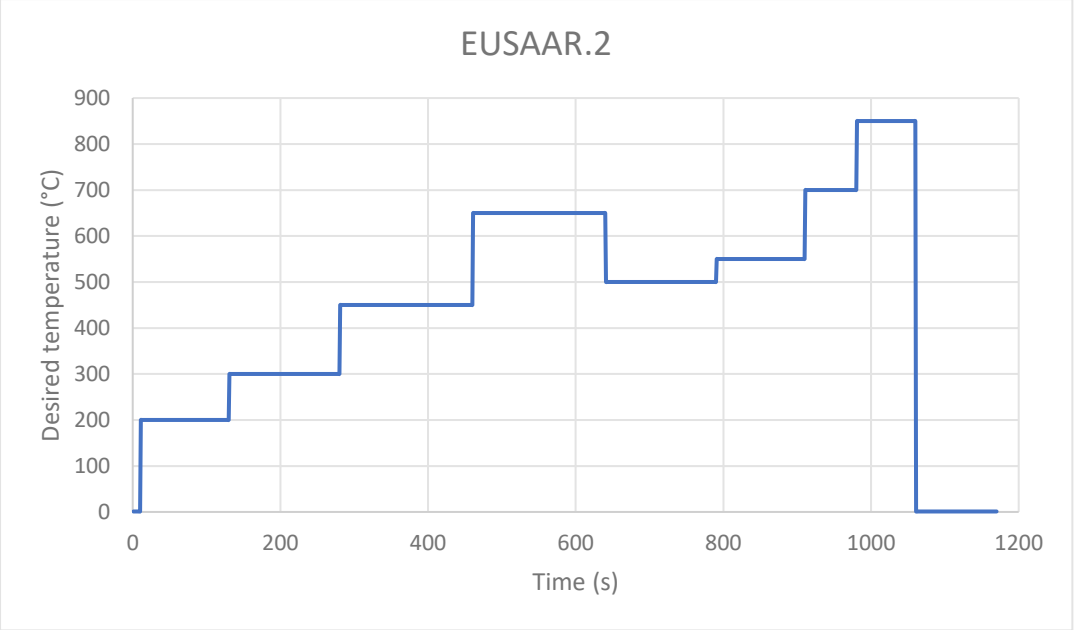


*Figure 4: Desired temperature of EUSAAR.2 as a function of time*

In the following Figure 5 is a TOA thermogram shown.

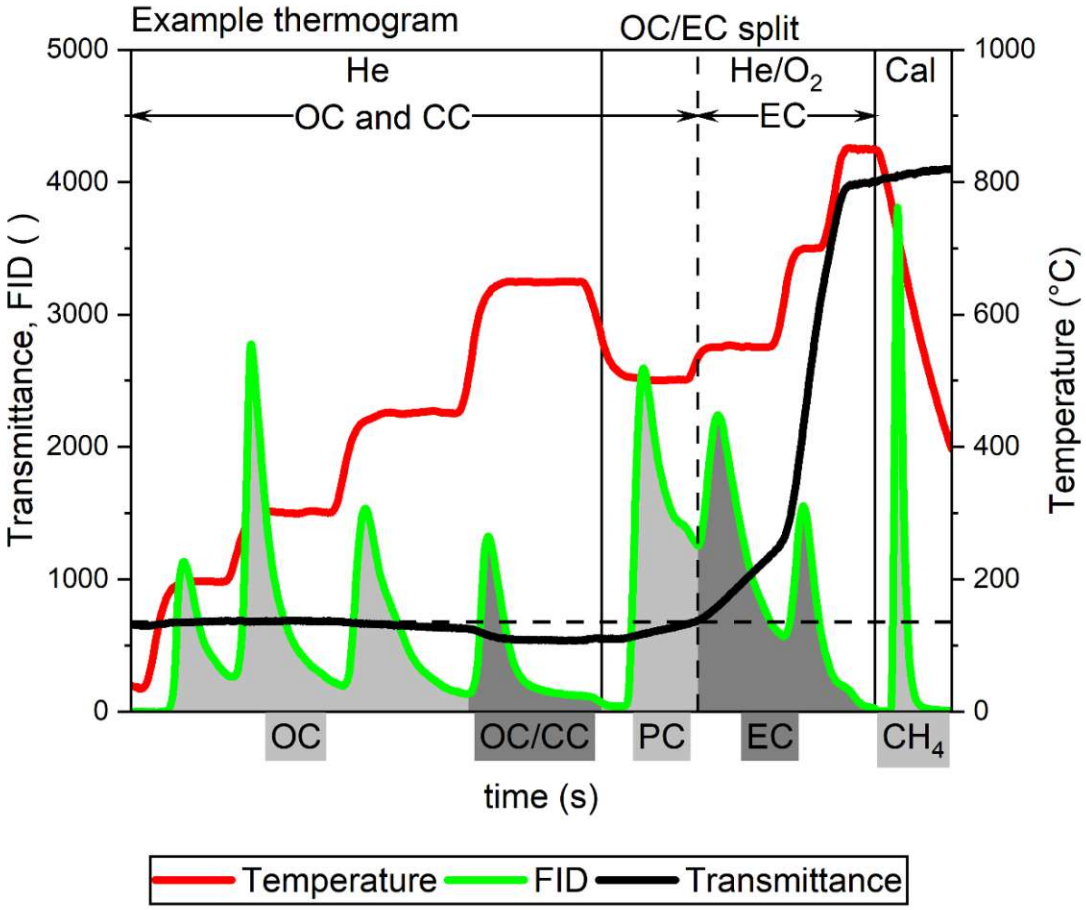


*Figure 5: TOA thermogram (source: Daniela Kau)*

The FID signal, temperature and transmittance are shown. Additionally, to the obtained measurement data, the used carrier gas (He and 2% $O_2$/He) and the OC-EC split (split point), which separates the OC and EC values, are given in the diagram. The four different carbon fractions OC (organic carbon), CC (carbonate carbon), PC (pyrolytic carbon) and EC (elemental carbon) and the calibration gas ($CH_4$) are shown.

The back-oven is heated to 870 °C and the methanator oven to 500 °C. The filter punch is placed on a quartz spoon in the front oven, so that it is in the path of the laser (λ = 658 nm). Photodiodes record the initial transmittance and reflectance of the filter sample and the changes during the whole measurement so that pyrolytic and elemental carbon can be distinguished. The measurement is started and the temperature of the front-oven increases according to the thermal protocol. Then the organic compounds are thermally desorbed, combusted and / or pyrolyzed. They are transported with He as the carrier gas and pass the main oven, where they are quantitatively converted to $CO_2$. The $CO_2$

is transported further with the carrier gas, which is now mixed with $H_2$, until it reaches the methanator oven. It is now quantitatively converted to $CH_4$ and is measured when it reaches the FID.

When the maximum temperature in the front oven is reached, the oven is cooled according to the temperature program and the carrier gas is changed to a helium / oxygen mixture. Another temperature ramp is initiated, and the elemental and pyrolytic carbon is oxidized and transported further through the instrument.

### 2.3.2 TOA - quality assurance

For quality assurance purposes, a sucrose solution with a concentration of 5 gC/l is analyzed. A clean run must be done beforehand, so that no carbon residues are left from the last analysis. After that, 10 µL of the sucrose solution are pipetted on a clean filter punch and a method is selected, that dries the filter in the front oven at a maximum temperature of 123 °C. Then the right thermal protocol is selected, which is the one that is used for the upcoming sample measurements. EUSAAR2 was used for the sucrose and sample measurements. The acceptable range of the sucrose measurements is 50 ± 2 µgC. After the measurement, the calibration area and the result are added to a control chart, which is used to get a quick overview of possible malfunctions of the instrument.

According to Sunset Laboratory Inc., 2020 the limit of detection (LOD) of the Sunset Laboratory OC / EC instrument is 0.2 µgC/cm². To get values for the limit of detection (LOD) and limit of quantification (LOQ) of this specific instrument, and the use of the quartz fiber filter, measurements of filter blanks have been performed by Daniela Kau for her master's thesis "Determination of elemental carbon and mineral dust in snow and ice samples". [9] The results are 2.49 µgC/cm² for the LOD and 7.48 µgC/cm² for the LOQ of OC or TC. For EC the LOD is 0.14 µgC/cm² and 0.42 µgC/cm² for the LOQ.

### 2.3.3 Correction of the split point

The mineral dust, especially the hematite, leads to issues during the placement of the OC / EC split point, as already mentioned before. Due to the presence of MD, the transmittance and reflectance of the laser are changed, this leads to wrong EC and OC values, because of the wrong position of the OC / EC split point. To correct this error, two different ways were used. The first one was used for the samples of 2017 – 2020, the transmittance at 700 °C was noted and the difference between this transmittance and the one at the very end of the cooling phase was calculated. The obtained difference was added to every transmittance data point of the oxidizing phase. The same procedure was done with the transmittance at 800 °C instead of 700 °C. To do a manual positioning of the new split point, the highest transmittance during the first 250 seconds was noted and compared to the corrected transmittance signals. The time when both values were the same or almost the same was used as the new split point. To decide whether to use the difference calculated for 700 °C or 800 °C,

the temperature at the new split point was looked at. If the temperature at the split point was closer to 700 °C, the difference calculated for 700 °C was used, the same applies to 800 °C.

The difference for the samples of 2021 and 2022 is that the values from a second measurement of the same sample filter punch are used to correct the transmittance of the first measurement. These evaluations are discussed in detail within the bachelor's thesis of Andjela Vukicevic [23].

## 2.4 Cation chromatography

A cation exchanger is used to separate selected mono- and divalent cations. The exchanger is a part of the solid phase in the separator column and retains the cations due to their different electrostatic interactions with the anionic anchor groups in the cation exchanger. [5] A 38 mM methanesulfonic acid (MSA) solution is used as the eluent and is transported through the separator column and the suppressor until it reaches the conductivity detector. The cations in the sample interact with the anchor groups in the exchanger, thereby combining with the ions of the MSA eluent. Because of the different strengths of the electrostatic interactions, the cations with the weakest interaction leave the column first and the strongest as last. The purpose of the suppressor is to exchange the counterions of the eluent, which has the advantage of a lower background conductivity which leads to increased sensitivity.

In the following Table 2 the parameters of the cation chromatography are shown. The following cations were analyzed: $Na^+$, $NH_4^+$, $Mg^{2+}$, $K^+$, $Ca^+$.

*Table 2: Parameters of cation chromatography*

| | |
|---|---|
| Instrument | Dionex-Aquion |
| Column | Dionex Ion Pac CS16A |
| Guard column | Dionex Ion Pac CG16A |
| Eluent | 38 mM MSA |
| Flow rate | 1 mL/min |
| Suppressor | Dionex CSRS 500 – 4mm (electrochemical) |
| Regenerant | Eluent |
| Sample loop | 150 µL |
| Detection | Conductivity detector |
| Integrationsystem | Chromeleon 7.2.9 |

### 2.4.1 Cation chromatography quality assurance

In the following Table 3, the seven calibration standards (STD1 – STD7) and three control standards (CSTD1 – CSTD3) for quality assurance purposes are shown.

*Table 3: Concentrations of the cation standards used for calibration*

| Cationstandards (µg/ml) | | | | | |
|---|---|---|---|---|---|
| **Standard** | **$Na^+$** | **$NH_4^+$** | **$K^+$** | **$Mg^{2+}$** | **$Ca^{2+}$** |
| **STD1** | 0.05 | 0.05 | 0.05 | 0.04 | 0.05 |
| **STD2** | 0.10 | 0.10 | 0.075 | 0.08 | 0.10 |
| **STD3** | 0.50 | 0.50 | 0.10 | 0.12 | 0.50 |
| **STD4** | 0.75 | 0.75 | 0.50 | 0.40 | 0.75 |
| **STD5** | 1.00 | 1.00 | 0.75 | 0.70 | 1.00 |
| **STD6** | 2.00 | 3.00 | 1.00 | 1.00 | 3.00 |
| **STD7** | 5.00 | 4.50 | 2.00 | 2.00 | 7.00 |
| **CSTD1** | 0.04 | 0.05 | 0.10 | 0.05 | 0.10 |
| **CSTD2** | 0.20 | 0.25 | 0.50 | 0.25 | 0.50 |
| **CSTD3** | 2.00 | 2.50 | 5.00 | 2.50 | 5.00 |

After the analyses the results are added to a control chart. To get a quick overview of possible malfunctions of the instrument, the curve and the slope of the calibration function of each ion are recorded. Furthermore, the calculated concentrations of the control standards are registered in the control chart and checked with the respective target values. The target value of the measurements is the average concentration µ and respective deviations of ± 5 % are considered as acceptable.

The LODs for all the cations mentioned above are 0.01 µg/ml. They are determined by conducting at least 10 measurements of a low concentrated standard (0.01 µg/ml) and evaluation of the standard deviation of these measurement series. The LOD is three times the standard deviation. For quality assurance such measurements are repeated yearly within the research group and were not performed within this thesis.

As already mentioned in chapter 2.2 cation analysis was performed from liquid snow sample, prior to filtration. To do so, aliquots of 1 ml of the molten snow sample are pipetted into a 1.5 mL vial. This vial is centrifuged and 800 µL are transferred carefully into an autosampler vial. After that, the sample is ready for the measurement.

## 2.5 Elemental analysis (ICP-OES)

Inductively coupled plasma (ICP) is used to produce excited atoms and ions, which emit electromagnetic radiation (Optical Emission Spectroscopy – OES) at certain wavelengths, which are characteristic of different elements.

The plasma reaches temperatures between 6000 and 8000 K and is typically made of ionized Argon. It is produced in the high frequency field of an induction coil, which surrounds a quartz tube. A peristaltic pump transports the liquid sample into a nebulizer, where droplets are formed and are transported further into the plasma torch. To achieve a high stability of the excitation source and thereby the resulting signals, it is important to get rid of bigger droplets.

There are a few different designs, but basically the emitted electromagnetic radiation is focused by one or more lenses on a diffraction grating, where it is diffracted to give an emission spectrum. Afterwards the light intensity of the characteristic wavelength is measured by a photomultiplier. [6]

### 2.5.1 ICP – OES measurements

To gather quantitative information, seven standard solutions with an elemental concentration in the range of 0.05 to mg/L and are shown in **Fehler! Verweisquelle konnte nicht gefunden werden.**. The analyzed elements are Ca, Mn, Co, P, Ti, Ni, Sr, Mg, Cr, Fe, Pb, Al and K. The following stock solutions were used in this process: ICP multi-element standard solution VIII (100 mg/L, certipur©); Indium ICP standard (1000 mg/L, certipur©); Phosphorus, plasma standard solution 1000 mg/L (specpure™).

*Table 4: ICP-OES standard solutions*

| Standard | Std. 1 | Std. 2 | Std. 3 | Std. 4 | Std. 5 | Std. 6 | Std. 7 |
|---|---|---|---|---|---|---|---|
| Concentration (mg/L) | 0.05 | 0.1 | 0.2 | 0.5 | 1 | 2 | 5 |

The ICP-OES instrument used for these samples is the iCAP 6500 ICP-OES spectrometer, Thermo Scientific.

The measured values determined by the ICP-OES were in µg/ml. After multiplying them with the dilution factor and the sample weight, they were expressed in µg/filter. At this point the values were corrected with the blank average. Afterwards, the end result (µg/g snow) was calculated by dividing them by the weight of the snow sample.

### 2.5.2 Microwave assisted chemical digestion

The filters probably loaded with mineral dust, are chemically digested using a microwave system (Multiwave 5000, Anton Paar). For this purpose, filters, which have already been analysed with TOA are used. They are put in teflon vessels and 3 mL $HNO_3$ (65 % for analysis, EMSURE®, Supelco), 1.684 mL Milli-Q water and 1.315 mL $HBF_4$ (38 %, ultra-pure, Chemlab NV) are added. The used temperature program is called “Characterization of waste – Digestion for subsequent determination of aqua regia soluble portion of elements” (EN 13657) and is commonly used in environmental chemistry. After the digestion, the solution is transferred in tared vials and the teflon vessels are rinsed with Milli-Q water, which leads to a final solution volume of about 15 mL. The obtained digestion solution is then diluted 1:10 for the ICP – OES measurement.

Due to a contaminated $HBF_4$-solution (50%, Apollo Scientific), the samples from 2019 and 2020 couldn’t be measured with the ICP-OES.

# 3. Results

## 3.1 EC, WIOC and WITC depth profiles

The following figures Figure 6 to Figure 32 show the yearly depth profiles of WIOC, EC and WITC of both glaciers.

Due to a very high carbon content, some samples are not displayed in the following figures. This applies to (2017) FLK 20 and (2021) GOK 25 (only EC). Sample (2021) GOK 25 contained stones, as it was at the deepest point of the sampling site. Thus a correct analyses is not feasible. In case of (2017) FLK an insect was found in the sample. It was removed, but still the sample showed very high carbon values, which are regarded as contaminated. As both samples are at the bottom of the respective profiles, no gaps become visible in the respective graphs. The numbering of the samples starts at the surface. Thus sample FLK 20 refers to the profile at Kleinfleißkees and a depth of 380 to 400 cm. Some samples were missing ((2020) GOK4, (2021) FLK1, (2022) FLK 9) therefore no data is shown in the figures.

Samples containing mineral dust show a reddish to brownish color on the filter, as was already mentioned before. To identify these samples in the depth profiles the respective bars are plotted in orange. As deposits or iron oxides like hematite introduce an artefact to TOA, a correction of the split point was performed according to the procedure given in the chapter 2.3.3. The blue bars adjacent to the orange ones represent the corrected value. As expected, the correction leads to an increase of EC concentrations and a corresponding decrease of OC values. It is just the different scaling of the graphs and the fact that the OC concentrations are usually higher than EC concentrations, which give the impression of higher differences for EC than for OC. The correction could not be performed for all samples. If there is only one orange bar shown, no correction was performed, because it was either not necessary or not possible. Note that a correction is only necessary for OC and EC values, as just the position of the split point is concerned. WITC values remain unaffected and thus just one (orange) bar is given in the graphs for WITC.

The samples were taken from 2017 to 2022, but only in 2017, 2021 and 2022 both glaciers were chosen as sample locations. The number of samples taken was in the range between 16 and 25 and the depth of the snow pits was between 320 and 500 centimeters. Note that in 2019, the snow pits could have been deeper, but due to the weather, the sampling had to be stopped before the surface of the glaciers, i.e. the ice, was reached.

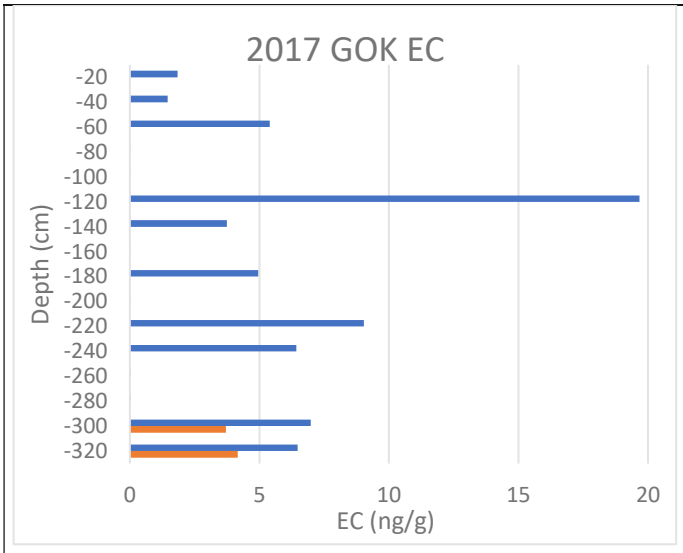


*Figure 6: Depth profile 2017 GOK EC*

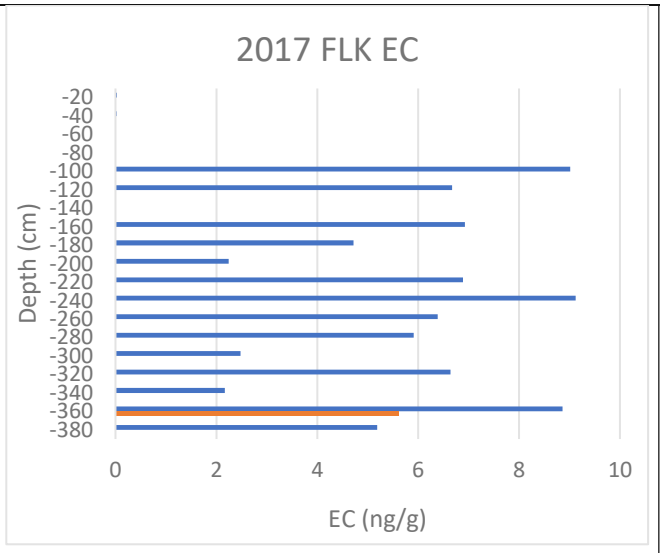


*Figure 7: Depth profile 2017 FLK EC*

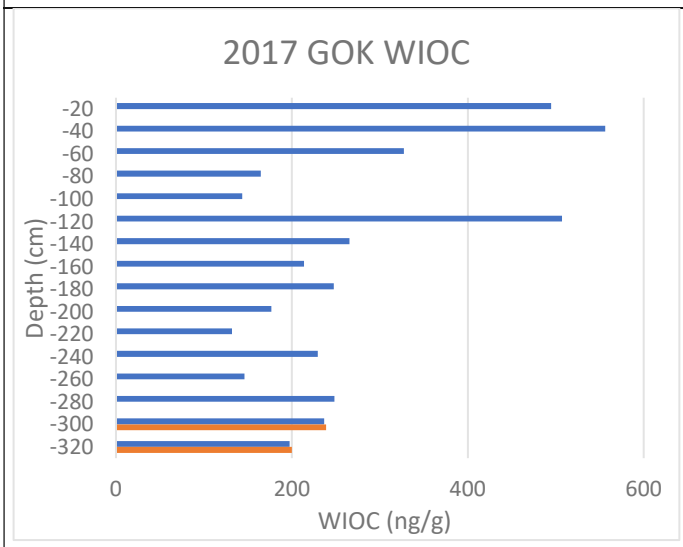


*Figure 8: Depth profile 2017 GOK WIOC*

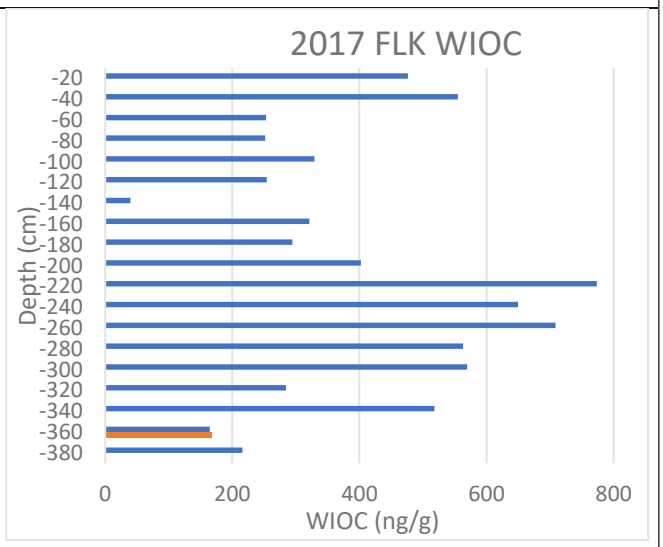


*Figure 9: Depth profile 2017 FLK WIOC*

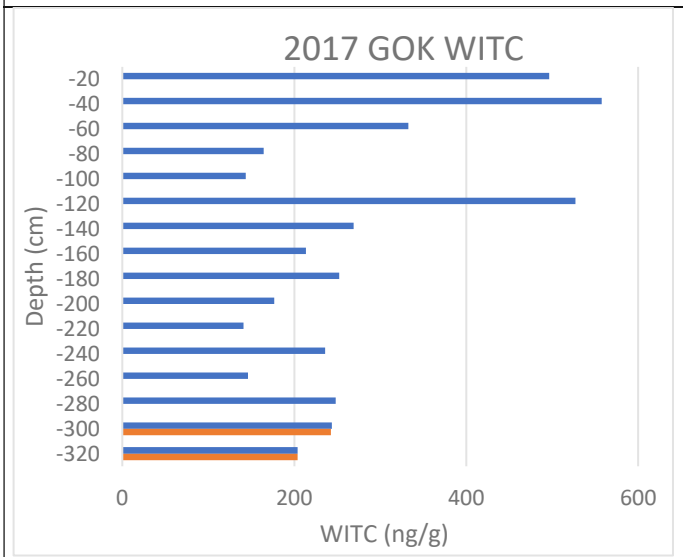


*Figure 10: Depth profile 2017 GOK WITC*

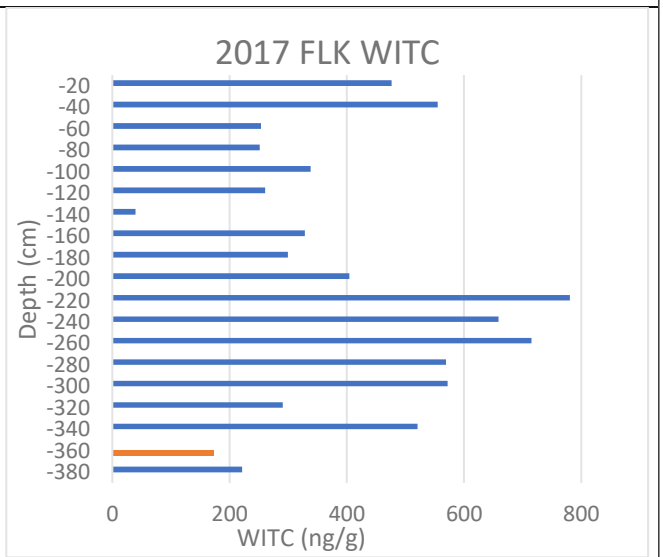


*Figure 11: Depth profile 2017 FLK WITC*

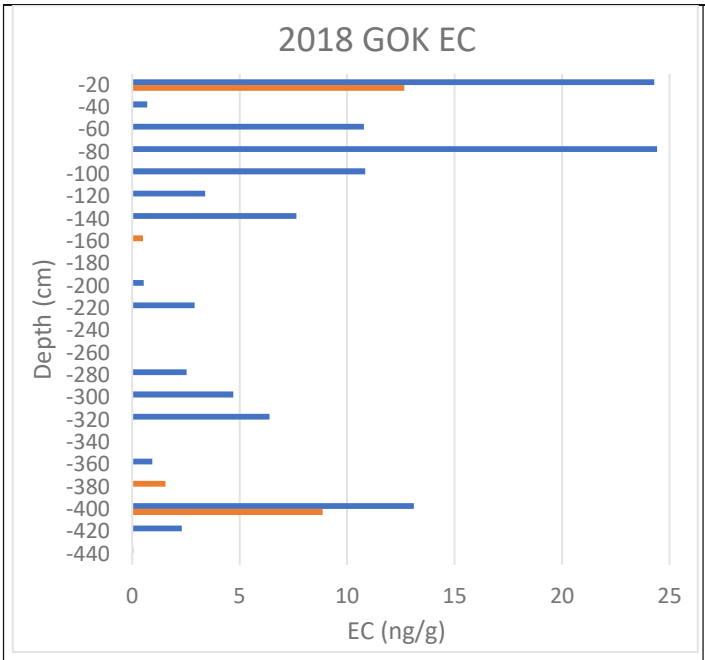


*Figure 12: Depth profile 2018 GOK EC*

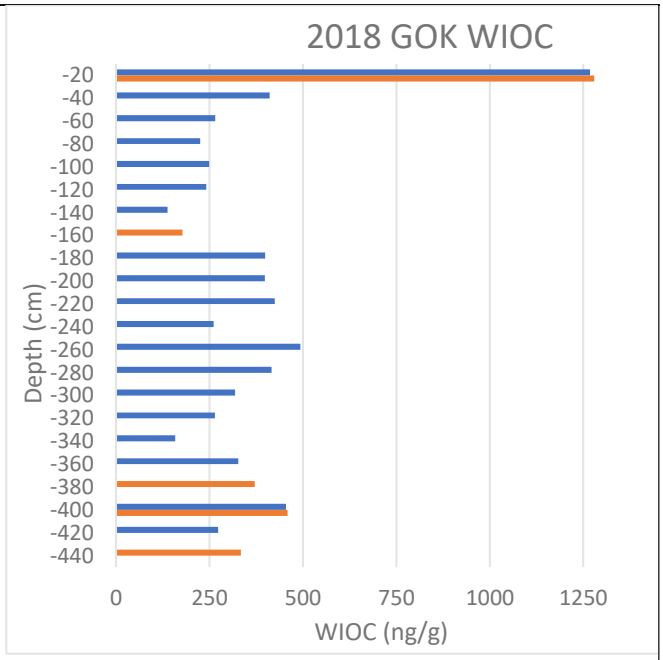


*Figure 13: Depth profile 2018 GOK WIOC*

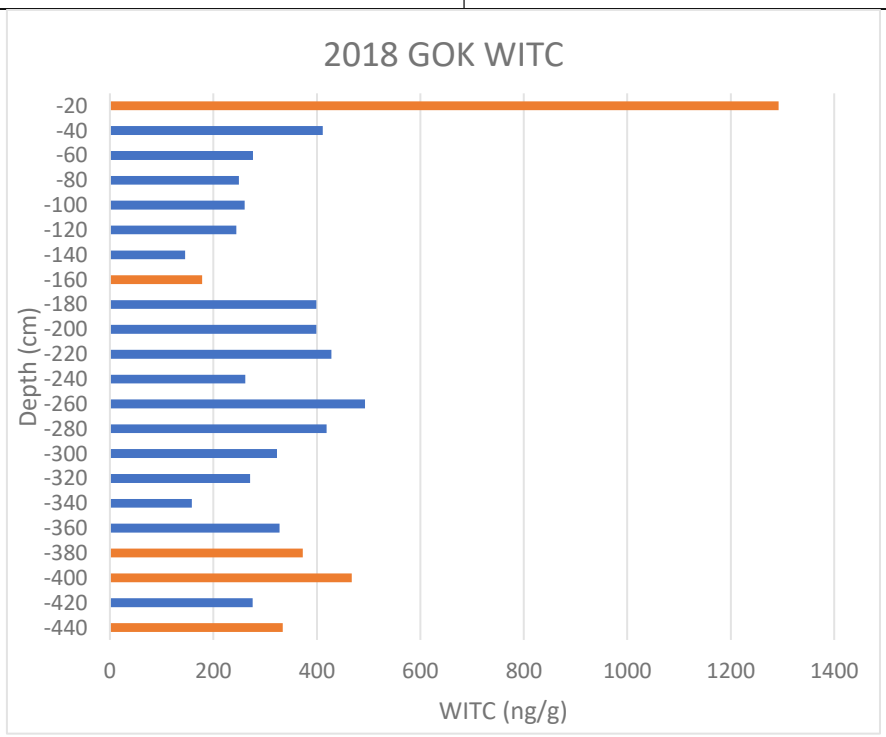


*Figure 14: Depth profile 2018 GOK WITC*

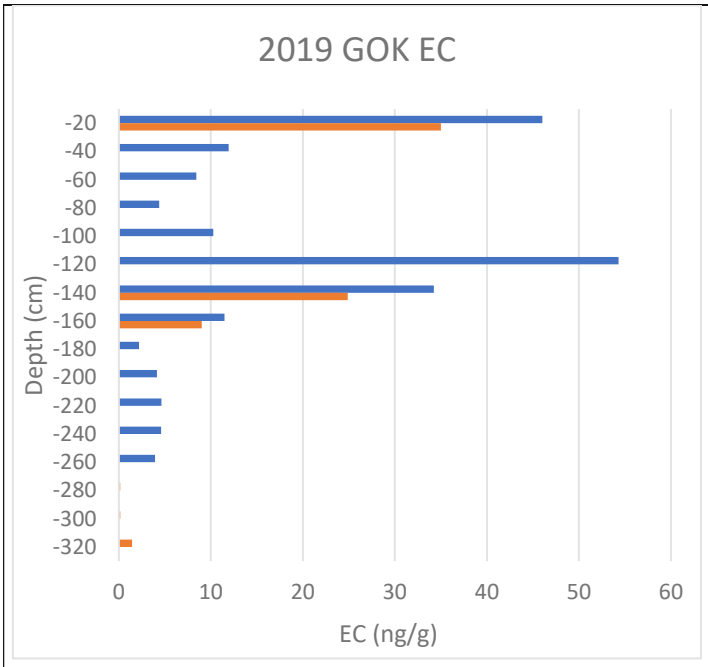


*Figure 15: Depth profile 2019 GOK EC*

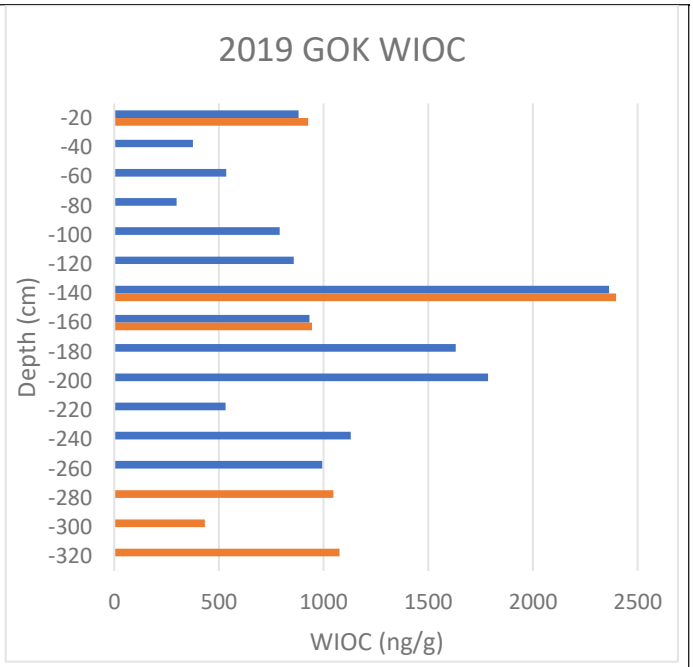


*Figure 16: Depth profile 2019 GOK WIOC*

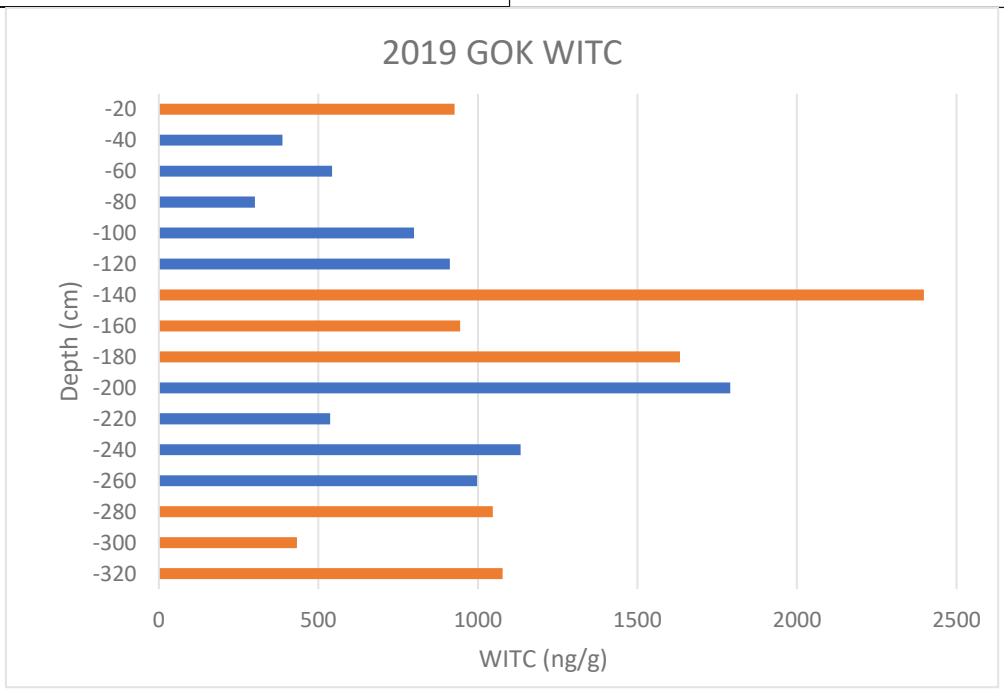


*Figure 17: Depth profile 2019 GOK WITC*

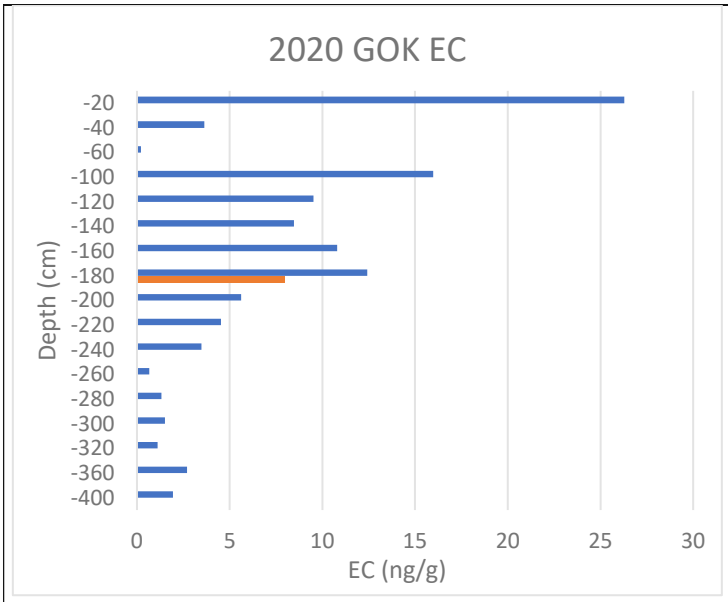


*Figure 18: Depth profile 2020 GOK EC*

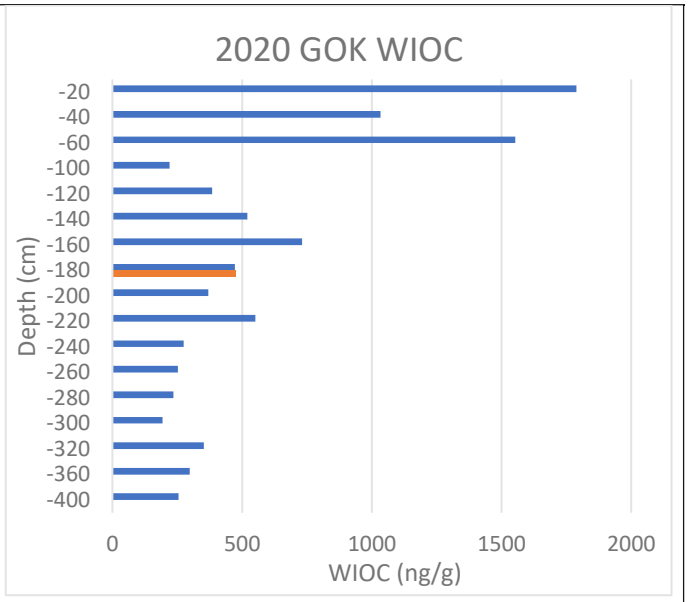


*Figure 19: Depth profile 2020 GOK WIOC*

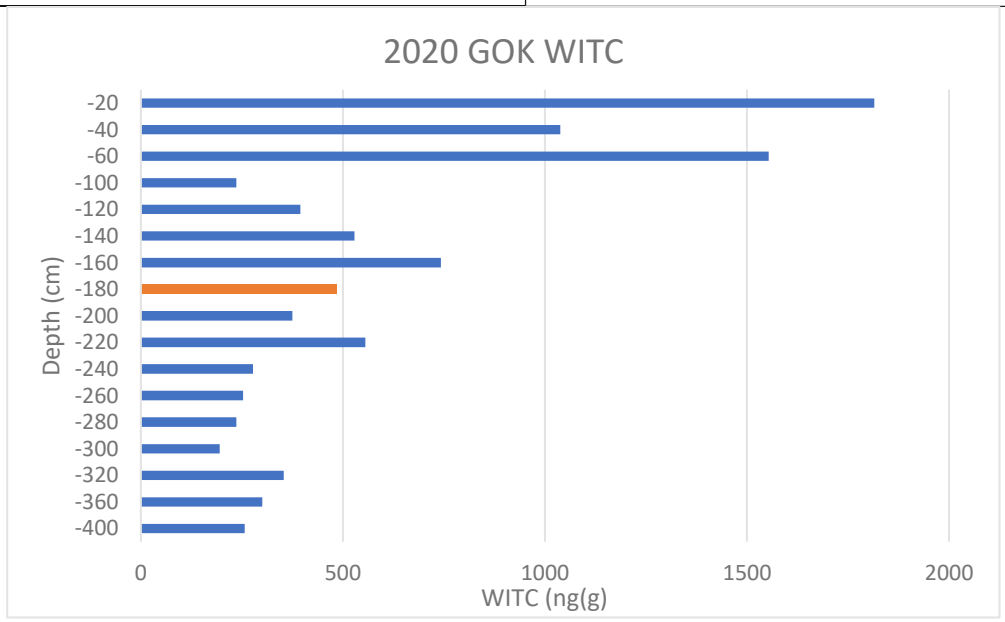


*Figure 20: Depth profile 2020 GOK WITC*

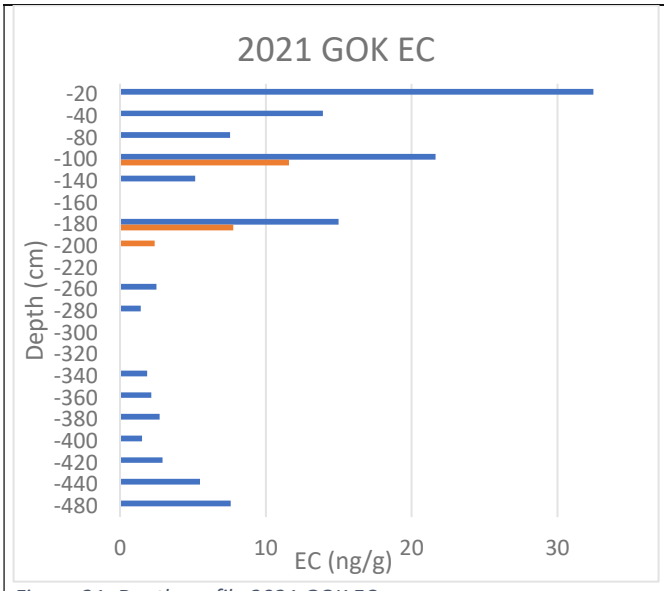


*Figure 21: Depth profile 2021 GOK EC*

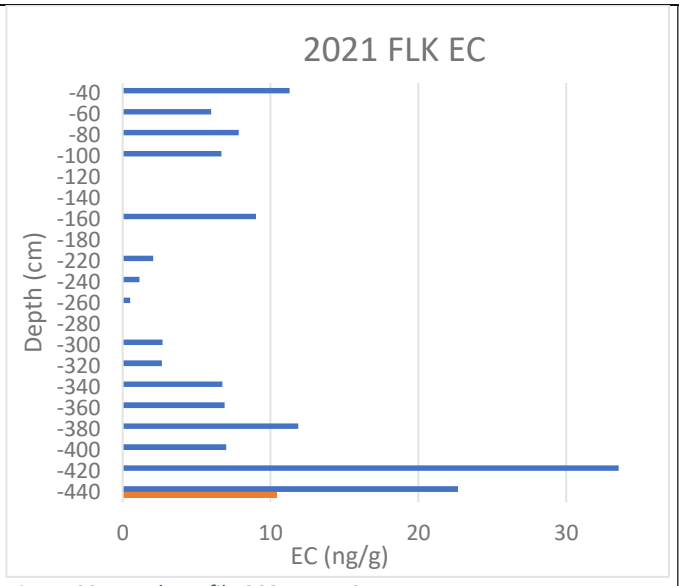


*Figure 22: Depth profile 2021 FLK EC*

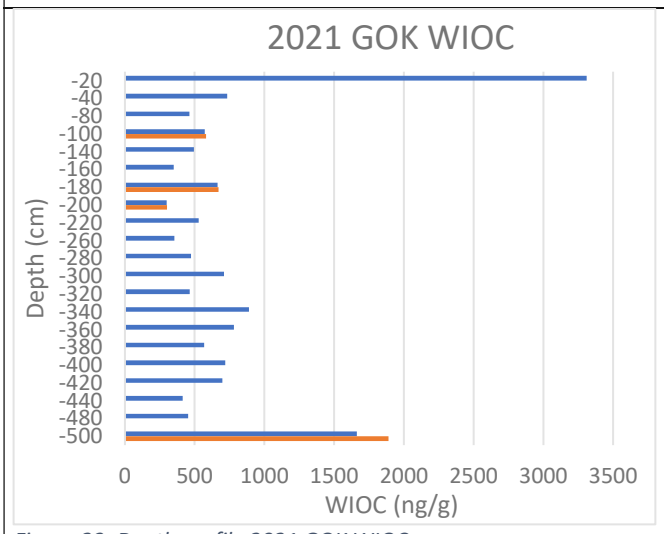


*Figure 23: Depth profile 2021 GOK WIOC*

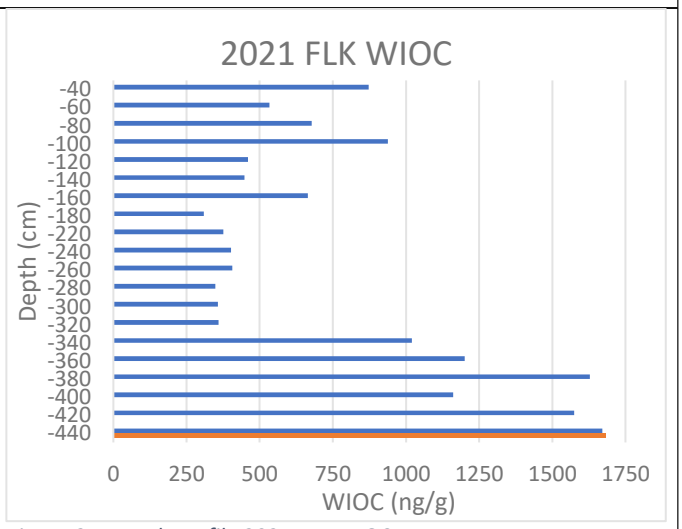


*Figure 24: Depth profile 2021 FLK WIOC*

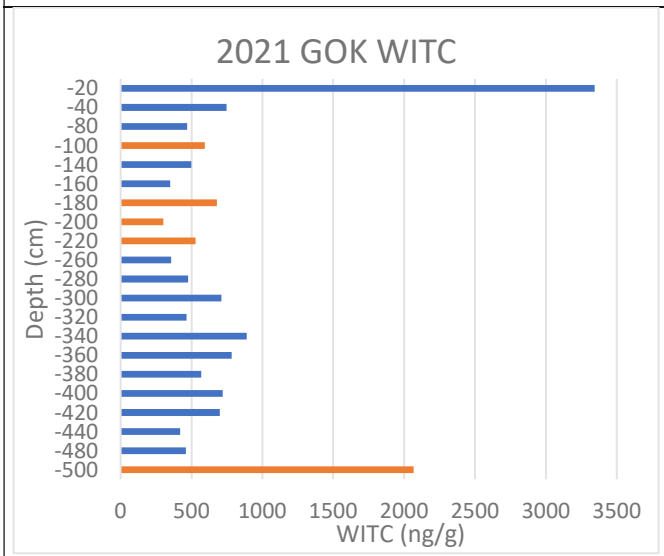


*Figure 25: Depth profile 2021 GOK WITC*

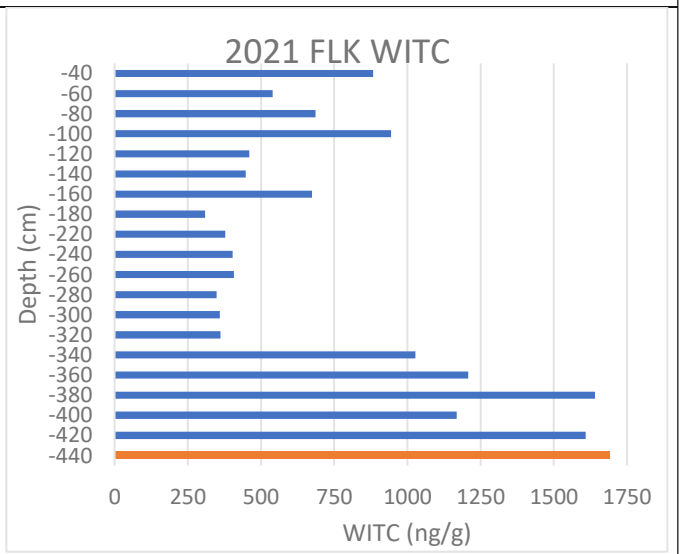


*Figure 26: Depth profile 2021 FLK WITC*

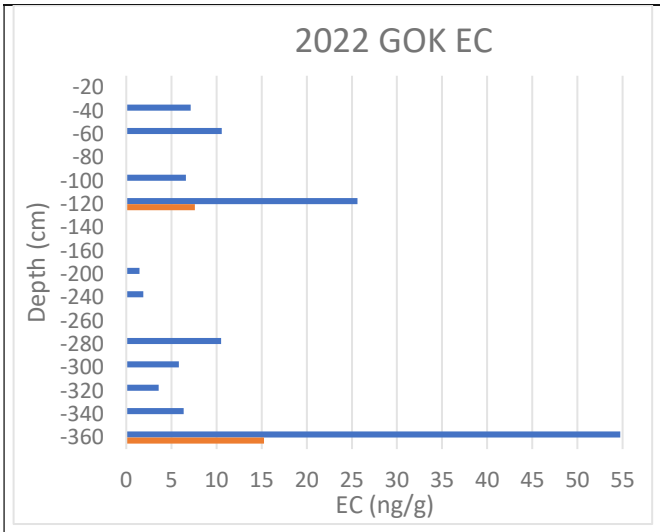


*Figure 27: Depth profile 2022 GOK EC*

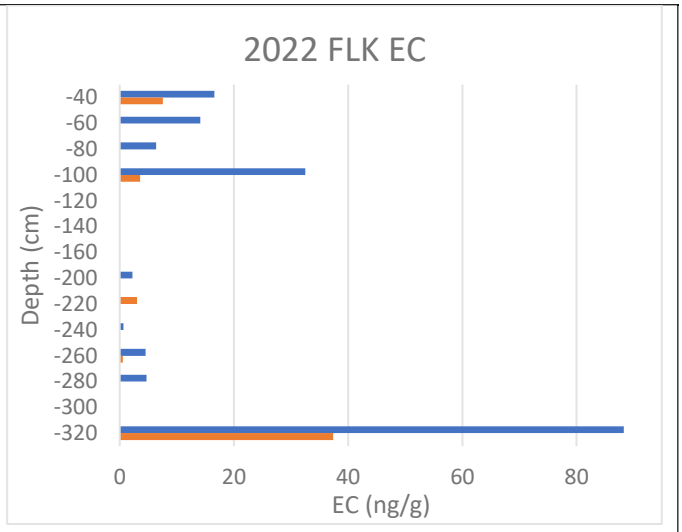


*Figure 28: Depth profile 2022 FLK EC*

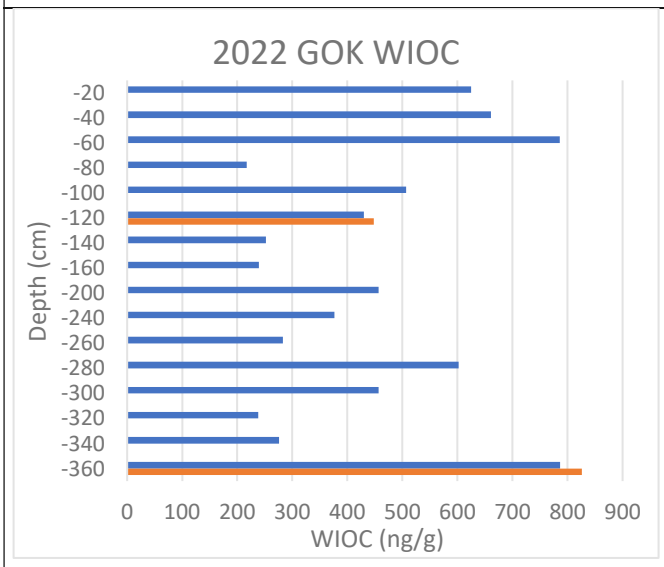


*Figure 29: Depth profile 2022 GOK WIOC*

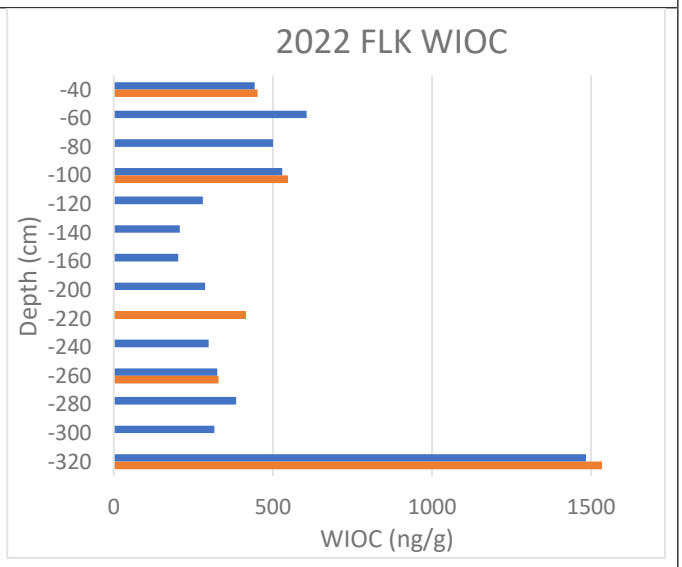


*Figure 30: Depth profile 2022 FLK WIOC*

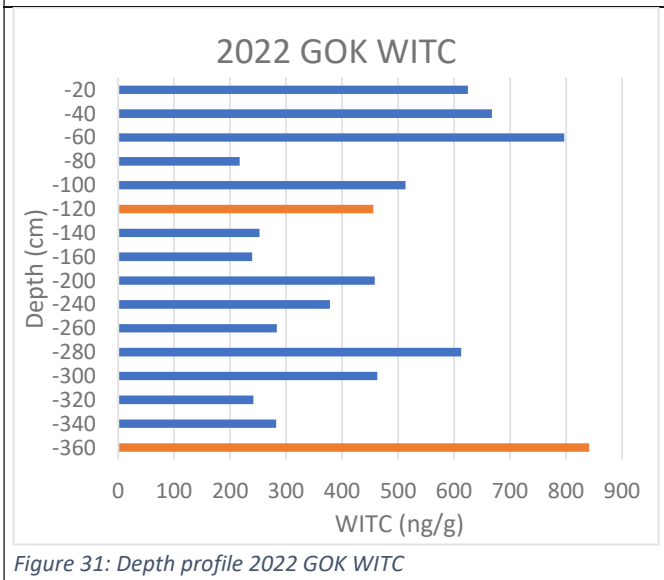


*Figure 31: Depth profile 2022 GOK WITC*

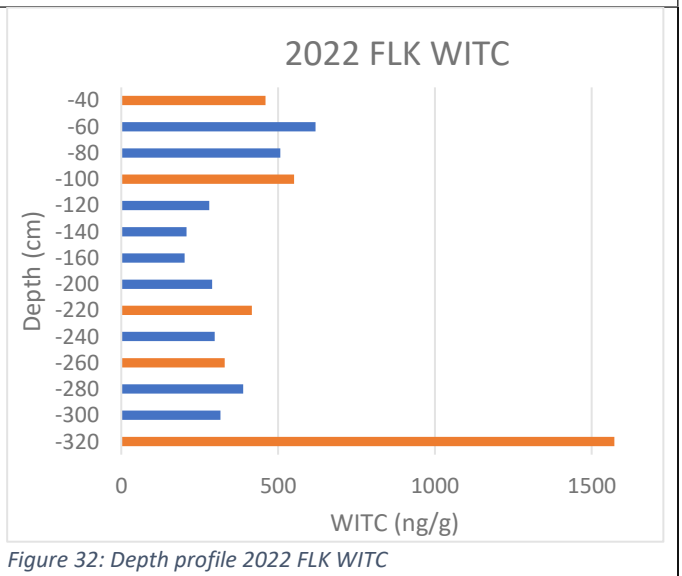


*Figure 32: Depth profile 2022 FLK WITC*

Every sample series contained at least one sample with visual MD in it. The most MD horizons occurred in 2018 GOK, namely 4. The sample year with the most mineral dust samples is 2019, with seven samples that contained mineral dust. It is important to note, that in this case samples are called MD samples, when the reddish or brownish coloration of the filters was visually perceptible.

Not every TOA measurement could be corrected. Some samples showed a transmission increase in the cooling phase, but the corrected transmission signal still couldn't reach the highest signal of the first 250 seconds. Therefore, no correction could be performed. Samples that showed these issues are: (2018) GOK 22, (2019) GOK 14, 15 and 16. Even if the transmission signal in the oxidizing phase was corrected, the value was not high enough to match the highest signal in the first 250 seconds of the measurement. Another reason to not to correct the TOA measurement is, that no correction was needed. In some cases ((2018) GOK 8 and 19, (2021) GOK 11 and GOK 23+24), there was a coloration of the filter, but no increase of the transmission signal in the cooling phase took place.

In 2017, 2021 and 2022 samples from both glaciers were taken and this allowed us to compare them with each other. In 2017 mineral dust samples were found at the deepest two points of the GOK and the second last of the FLK glacier. This points to a MD event at the start of the accumulation period which is visible at both glaciers. Most samples contained less than 10 ng EC/g, only one sample at GOK at -120 cm exceeded these values and was almost at 20 ng/g. Although the maximum value was found at GOK, the samples taken at FLK showed generally slightly higher concentrations for EC, but also WIOC. This is especially visible for snow samples in a depth of 200 cm and below. The samples with the highest WIOC and WITC values, were both taken at the FLK in 2017. In 2022 at both glaciers, the samples from the deepest position, contained most EC and WIOC and there were more mineral dust samples from FLK, five, than from GOK, two. Most GOK samples contained less than 11 ng/g EC, only two samples at -120 and -360 cm, exceeded this value and were 25.62 and 54.74 ng/g EC. At FLK 2022 the EC values were generally higher than at GOK 2022 and most samples contained less than 17 ng/g EC, only two samples at -100 and -320 cm at FLK contained 32.50 and 88.29 ng/g EC. Interestingly, the samples from the bottom of both snow pits contained most EC and WIOC. The 2021 samples were contaminated with hammer debris; this led to unreliable carbon values. Due to an increase in the transmission during the TOA, it is still possible to determine whether mineral dust is in the sample or not. Between -100 and -220 cm there are four GOK samples with a red coloration, but only three of them showed a transmission increase in the cooling phase during the TOA. At the deepest positions, both glaciers contained a mineral dust sample.

Except for 2020, there is no seasonal trend of the carbon values visible in the depth profiles. A slight trend is also visible in 2022 FLK when the highest value at -300 cm is not displayed. The trend of

elevated concentrations during spring time, which is visible for the inorganic ions nitrate, ammonium and sulfate arises from the better mixing of the atmosphere in springtime. [24] One possibility why it is not seen in every year's samples is that the values of EC and WIOC are not only driven by an increase of the mixing layer height, but by other transport processes as well.

As WIOC values are much higher than EC data, EC/WIOC ratios and EC/WITC ratios are quite similar. Overall EC/WITC ratios range between 0.007 and 0.017. The mean is 0.014 and the median is 0.015.

### 3.1.1 Comparison of corrected and not corrected carbon values

To obtain an overview of the impact of the split point correction on WIOC and EC concentrations, the corrected and not corrected values as well as the percentage increases are summarized in the following Table 5.

*Table 5: Corrected and not corrected EC and WIOC values*

| Sample name | EC not cor. (ng/g) | EC cor. (ng/g) | Increase (%) | WIOC not cor. (ng/g) | WIOC cor. (ng/g) | Decrease (%) |
|---|---|---|---|---|---|---|
| (2017) GOK 15 | 3.71 | 6.99 | 88 | 239 | 237 | 1 |
| (2017) GOK 16 | 4.17 | 6.47 | 55 | 200 | 198 | 1 |
| (2017) FLK 18 | 5.61 | 8.86 | 58 | 168 | 164 | 2 |
| (2017) FLK 20 | 107 | 185 | 73 | 4183 | 4106 | 2 |
| (2018) GOK 1 | 12.7 | 24.3 | 92 | 1280 | 1268 | 1 |
| (2018) GOK 20 | 8.86 | 13.1 | 48 | 459 | 454 | 1 |
| (2019) GOK 1 | 35.0 | 46.0 | 32 | 927 | 881 | 5 |
| (2019) GOK 7 | 24.9 | 34.2 | 38 | 2398 | 2364 | 1 |
| (2019) GOK 8 | 9.02 | 11.5 | 27 | 944 | 933 | 1 |
| (2020) GOK 9 | 7.95 | 12.4 | 56 | 476 | 472 | 1 |
| (2021) GOK 5 | 11.6 | 21.6 | 87 | 583 | 573 | 2 |
| (2021) GOK 9 | 7.78 | 15.0 | 93 | 671 | 664 | 1 |
| (2021) GOK 10 | 0.01 | 2.38 | X | 301 | 299 | 1 |
| (2021) GOK 25* | 177 | 427 | 141 | 1889 | 1662 | 12 |
| (2021) FLK 22 | 10.4 | 22.7 | 118 | 1682 | 1671 | 1 |
| (2022) GOK 6 | 7.59 | 25.6 | 238 | 448 | 430 | 4 |
| (2022) GOK 18 | 15.3 | 54.7 | 259 | 826 | 787 | 5 |
| (2022) FLK 1 + 2 | 7.55 | 16.6 | 120 | 452 | 444 | 2 |
| (2022) FLK 5 | 3.55 | 32.5 | 815 | 548 | 530 | 3 |
| (2022) FLK 13 | 0.53 | 4.54 | 760 | 329 | 325 | 1 |
| (2022) FLK 16 | 37.4 | 88.3 | 136 | 1535 | 1484 | 3 |

*The sample (2021) GOK 25 contained stones.

It becomes very obvious that changes in the split-point mainly effects EC concentrations and that the effect can be severe. The highest relative increase in EC would occur for (2021) GOK 10. Still, this value was not calculated, as no EC was detected without correction (i.e. the transmittance signal never

reached the initial value during the analysis and thus no split point be set). As the initial value was below the limit of detection no percentage increase could be calculated.

For all MD samples the correction of the TOA led to an EC increase of at least 27%. Considering the whole data set, this percentage increase can also be up to 259%, with two samples reaching even higher up (760% and 815%). The median value is 92%, but this value definitely can not be generalized as being typical, as the effect is driven by the iron loadings of the filter which will be independent of EC concentrations. The EC increase was greater the more Fe was on the filters. Above of an Fe loading of 20 µg/filter the increase was mostly at least 100%. Just one filter, which contained a lot more Fe than the others, showed different behavior. This could be an indication that above of a certain Fe value, the correction cannot be applied, similar to the findings by Kau et al. [17]

Based on absolute concentrations the corrections led to an increase of BC concentration ranging from no effect up to 78 ng/g ((2017) FLK 20).

No correlation between EC concentrations and percentage increase could be found. The increase was mostly related to the position of the automatic split point. If the not corrected split point was at the very end of the thermogram, the correction led to a very large EC increase.

Due to the high OC values, the correction of the split point results in a little change of the OC concentrations in percentage terms. The sample with the highest decrease is (2021) GOK 25, with 12% which is a lot lower than the largest effects seen for EC. Apart from this maximum value of 12%, changes observed for OC are in the range of 1 to 5%.

### 3.1.2 Comparison of the obtained WIOC and EC values

Table 6 summarizes the WIOC and EC concentrations determined within this thesis. Note that in 2021 some gross errors which occurred during sampling (abrasion from the hammer) led to non-reliable values. The data of the two profiles sampled in 2021 has to be interpreted cautiously and is actually just listed for completeness. In one of the samples from SBK FLK 2017 an insect was found and removed before the filtration. Though the values were still very high and therefore not included in the calculations of the median and mean. Both maximum values are shown for completeness in parentheses.

*Table 6: Minimum, maximum, median and mean values of WIOC and EC*

| | SBK GOK 2017 | SBK FLK 2017 | SBK GOK 2018 | SBK GOK 2019 | SBK GOK 2020 | SBK GOK 2021 | SBK FLK 2021 | SBK GOK 2022 | SBK FLK 2022 |
|---|---|---|---|---|---|---|---|---|---|
| **EC (ng/g)** | | | | | | | | | |
| **Minimum** | 0.07 | 0.07 | 0.07 | 0.15 | 0.22 | 0.07* | 0.07* | 0.07 | 0.07 |
| **Maximum** | 19.7 | 9.12 (184.6) | 24.4 | 54.3 | 26.3 | 427* | 33.6* | 54.7 | 88.3 |
| **Median** | 2.79 | 5.19 | 2.4 | 4.6 | 3.64 | 2.71* | 6.34* | 4.71 | 3.76 |
| **Mean** | 4.13 | 4.38 | 5.3 | 12.6 | 6.48 | 26.3* | 6.94* | 8.40 | 12.4 |
| **WIOC (ng/g)** | | | | | | | | | |
| **Minimum** | 132 | 40 | 138 | 297 | 193 | 299* | 309* | 217 | 202 |
| **Maximum** | 556 | 774 (4106) | 1268 | 2364 | 1789 | 3311* | 1671* | 787 | 1484 |
| **Median** | 233 | 329 | 323 | 907 | 370 | 567* | 600* | 443 | 355 |
| **Mean** | 268 | 401 | 357 | 979 | 558 | 743* | 771* | 450 | 449 |

*Data obtained in 2021 was contaminated during sampling and is not included in further evaluations.

According to the median value, the sample series with the highest EC content is SBK FLK 2017, while the lowest is SBK GOK 2018. Overall the EC medians ranges between 2.42 and 5.19 ng/g. In 2017 the median is 2.4 ng/g higher at the FLK than at the GOK. While in 2022 the difference between both glaciers is only 0.95 ng/g. Obviously the differences between the two sites are comparable to the changes determined at a single site during the five year period. For WIOC the medians range is between 233 and 907 ng/g. The highest value is found for SBK GOK 2019 and the lowest for SBK GOK 2017. Again, the median WIOC values between the two glaciers in one year differ more in 2017 (96 ng/g) and less in 2022 (88 ng/g). Thus for WIOC the year to year variability at one site is higher than the differences between the two sites, observed within one year.

According to the mean value, the sample series with the highest EC content is SBK GOK 2019 with 12.64 ng/g. While the lowest EC mean value, 4.13 ng/g, belongs to SBK GOK 17. Mean EC values are only slightly different between both glaciers in 2017, but in 2022 the mean EC values differ almost 4 ng/g. Still, the interannual variability can be slightly higher. For WIOC median values range between 268 and 979 ng/g. The difference between GOK and FLK is the biggest in 2017 with 133 ng/g and the

lowest in 2022 with only 1 ng/g. As it was already noticed for the median values, for WIOC the interannual variability is higher than the spatial differences observed with one year.

For completeness a comparison of minimum and maximum values is given as well. Note that the differences of maximum values are more difficult to interpret, as these values can be influenced accidentally.

Most of the profiles showed at least one sample with an EC concentration below the limit of detection. Thus, minimum concentrations reach down to this value, i.e. 0.07 ng/g. In every year, when both glaciers were investigated, these minimum EC values were the same. Regarding WIOC all values were above the LOD. The lowest WIOC value was measured at FLK in the year 2017. Evaluating the minimum values of all years with sampling at FLK and GOK, the minimum values differ only slightly in 2021 and 2022 (10 and 15 ng/g, respectively) while a larger difference was obtained in 2017 (92 ng/g).

The samples series that contained the sample with the highest EC value is SBK FLK 22, additionally the GOK samples from the same year show the second highest EC content. Disregarding the data from 2021 (abrasion from sampling equipment), the sample with the highest WIOC content occurred in 2019, whereby the median and mean were higher than in all the other years as well. In terms of the maximum EC value from both glaciers, 2022 showed the biggest difference, though the mean values differed not as much from each other. Note that the maximum values are difficult to interpret and the median and mean show a better overlook.

To compare the obtained values with other regions, values from other sample locations are shown in the Table 7. SV stands for Svalbard, which is an archipelago in the arctic ocean. The values are taken from Zdanowicz et al. (2021). [16] H stands for Himalaya and the source of these values is Chaman Gul et al. (2018). [4] The values for 2003/2004 Schauinsland (SIL) and Sonnblick (SBK) are taken from Mário Cerqueira et al. (2009). [20] Jonas Svensson et al. (2018) provides comparative EC values for the Finnish Arctic. [21]

*Table 7: Summary of WIOC and EC data taken from literature*

| | SV Spring 2016 [16] | H Gulkin Oct 2016 [4] | H S1-Sost Dec 15 / Jan 16 [4] | SIL Feb 03 / Aug 04 [20] | SBK Mar 03/ Jul 04 [20] | Finnish Arctic [21] | |
|---|---|---|---|---|---|---|---|
| | | | | | | Pallas 2015 | Sodankylä 2013/14 |
| **Elevation (m a.s.l.)** | 102 - 1193 | 2741 - 3319 | 2873 - 3092 | 1205 | 3106 | 450 | 179 |
| **Sample type** | All layers | Surface | Surface | All layers | All layers | Surface | |
| **EC (ng/g)** | | | | | | | |
| **Minimum** | < 1.0 | 125 | 482 | < 0.1 | < 0.1 | 6.2 | |
| **Maximum** | 22.7 | 1028 | 5957 | 192 | 12 | 102 | |
| **Median** | 1.9 | / | / | / | / | 31 | 13.1 |
| **Mean** | 2.9 | 451 | 2506 | 28 | 5.2 | 40 | 23.7 |
| **WIOC (ng/g)** | | | | | | | |
| **Minimum** | 12 | 266 | 378 | 9.6 | 33 | / | |
| **Maximum** | 550 | 3574 | 2934 | 1400 | 785 | / | |
| **Median** | 49 | / | / | / | / | / | |
| **Mean** | 88 | 1276 | 1039 | 205 | 145 | / | |

As already mentioned, the maximum value is difficult to interpret, so the mean and median value are used for the comparison.

Only two out of seven (nine) sample series from SBK 2017 – 2022 fell below the mean EC value of SBK 2003/2004 and both were in 2017 (GOK and FLK). The WIOC mean value is exceeded by the samples from 2017-2022 by a lot in every case. The same study also investigated samples from SIL 2003/2004, and the EC mean value, 28 ng/g, is a lot higher than highest value for the samples from SBK. Note, that at SIL the samples were taken at a lower altitude and there is a city called Freiburg, not far from it. Both facts lead to higher EC values at SIL. Interestingly, the WIOC mean values from SBK 2017-2022 are higher in every sample series than from SIL 2003/2004.

There are also more recent values, but unfortunately only from other regions than the Austrian Alps.

The samples from the Himalaya were taken at about the same altitude, but generally the carbon values in the snow are a lot higher in the Himalaya than in the Alps. They exceeded the WIOC and especially the EC maximum values of the samples analyzed for this work by a lot. This was expected, as regions with high emission densities can be found in the vicinity. Also keep in mind that the samples are surface samples and are not taken from all layers.

The Svalbard samples were not taken at a comparable altitude, but due to the remote location of the archipelago and the sample type, it was interesting to compare them to the samples analyzed for this

thesis. Both, median and mean of EC and especially for WIOC, are in all cases higher for the SBK samples, than for the Svalbard samples.

In recent years, snow samples were also taken in the Finnish Arctic. They are surface snow samples taken from a lot lower altitude. The median and mean of EC from the Finnish Arctic exceed the SBK 2017-2022 values in every case.

The following Table 8 is taken from Tuzet et al. (2020) and contains typical BC contents of snow samples from different regions, but no time periods are given. [2]

*Table 8: Typical BC content of snow samples from different regions [2]*

| Sample region | Typical BC content (ng/g) |
|---|---|
| Antarctic Plateau | 0.2 – 0.6 |
| Arctic | 8 – 60 |
| Greenland | 0.8 – 4.5 |
| China | 20 – 2000 |
| North America (including melt) | 5 – 70 |
| French Alps (including melt) | 0 – 80 |
| Swiss Alps (including melt) | 0 - 50 |

Even if the obtained median and mean EC values from 2017-2022 match the typical BC content of the French (0-80 ng/g) and Swiss Alps (0-50) very well, it is important to note, that the maximum EC value of a single snow sample may exceed the values given in Table 8. SBK FLK 2017 contained a sample with an EC value of 185 ng/g and SBK FLK 2022 with 88.3 ng/g. It is noteworthy that there was an insect in the mentioned SBK FLK 2017 sample and the second highest EC value of this sample series was only 8,84 ng/g. As excepted the analyzed SBK samples exceeded the comparative values from Greenland and the Antarctic Plateau and were also a lot lower than in China.

### 3.1.3 Correlations between EC fractions and the positioning of the OC/EC split

If no MD was present, the split point was usually set in EC3 or EC4. The numbering of the EC fractions refers to the different temperature levels in the oxidizing phase.

Out of 338 sample measurements, 35 split points were positioned automatically in the range of EC3, 269 in the range of EC4 and 33 in between EC3 and EC4. It was checked if there is a correlation between the size of the different EC fractions, especially EC3 and EC4, and the positioning of the automatic split point. For the 35 samples with an automatic split point set in the range of EC3, the EC3 was in 30 out of those 35 cases bigger than EC4. But there is probably no correlation between the size of EC3 and the positioning of the automatic split point in EC3, because the split point was positioned mostly in the range of EC4, even though the EC3 fractions was bigger. This leads to the conclusion that there is no correlation between the position of the automatic split point and the size of the EC3 and EC4 fraction.

Three thermograms are shown exemplarily in Figure 33, Figure 34 and Figure 35. The figures are screenshots from the calculation software of the TOA (Calc415), therefore no axis labels are shown. The split point is the vertical blue line in the right half of the thermogram.

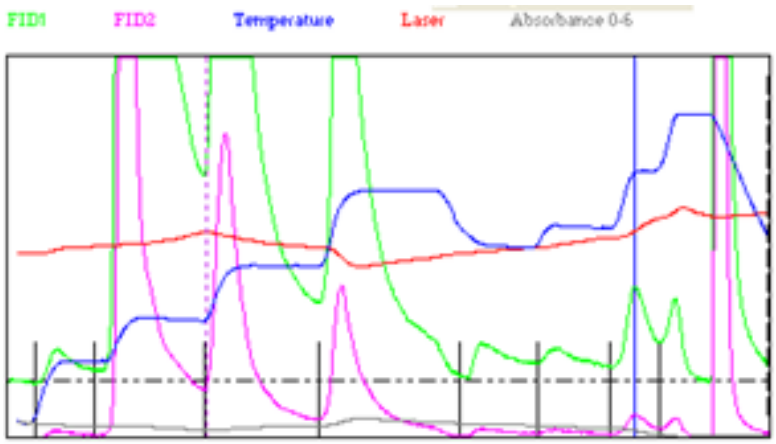


*Figure 33: Example of a thermogram with the split point in EC3*

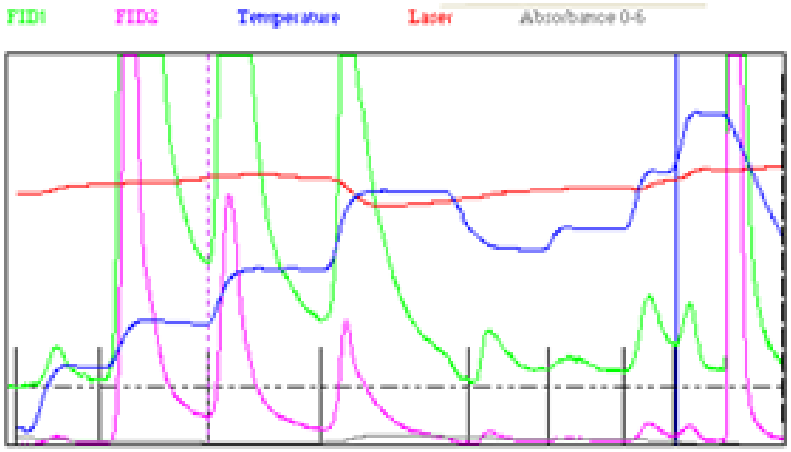


*Figure 34: Example of a thermogram with the split point between EC3 and EC4*

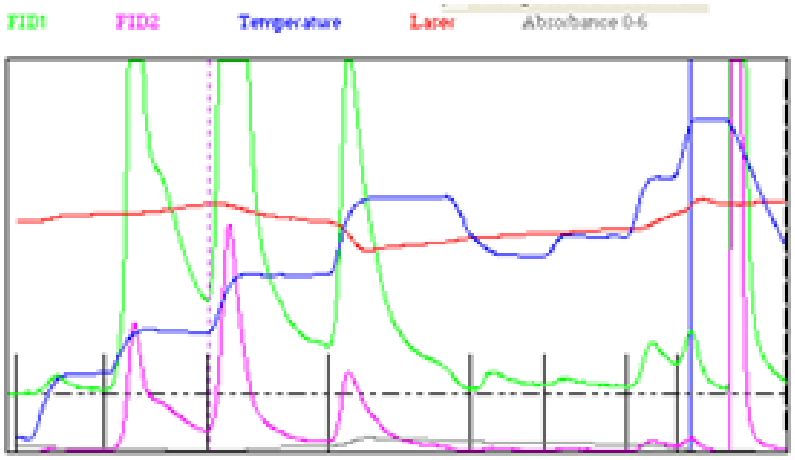


*Figure 35: Example of a thermogram with the split point in EC4*

## 3.2 Determination of mineral dust

### 3.2.1 Comparison of 10 cm and 20 cm increments

$NH_4^+$ and $Ca^{2+}$ are best suited for the comparison of 10 cm and 20 cm increments, because most results are above the LOD. The following Figure 36 to Figure 53 show the obtained values.

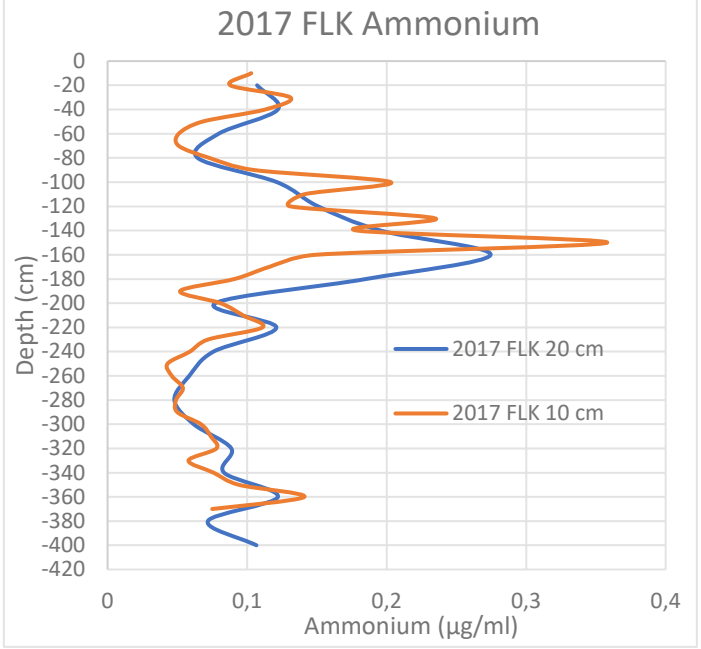


*Figure 36: 2017 FLK Ammonium concentrations*

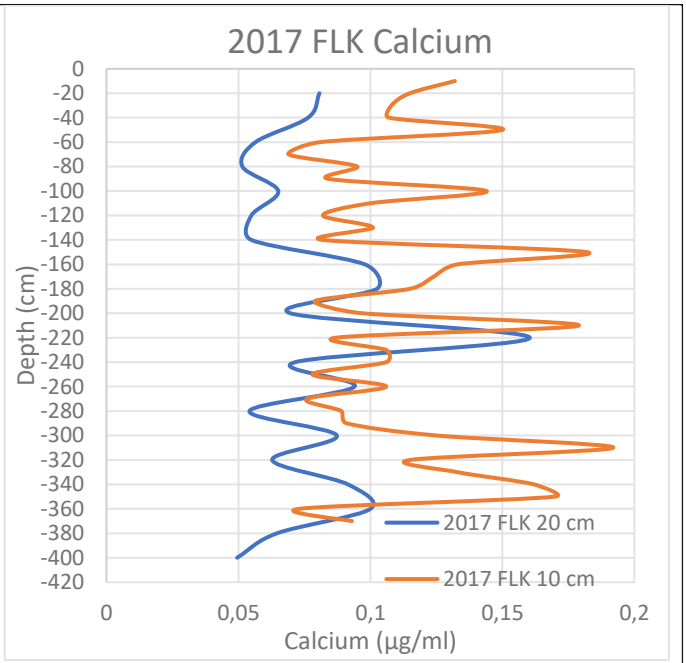


*Figure 37: 2017 FLK Calcium concentrations*

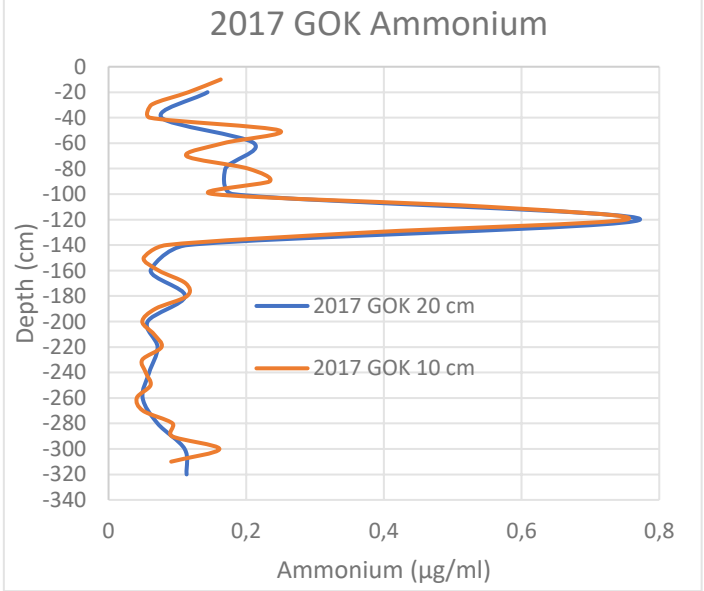


*Figure 38: 2017 GOK Ammonium concentrations*

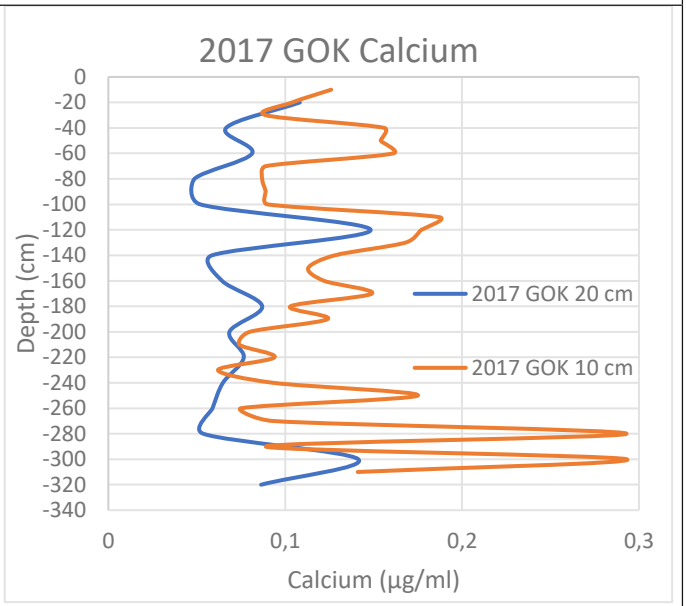


*Figure 39: 2017 FLK Calcium concentrations*

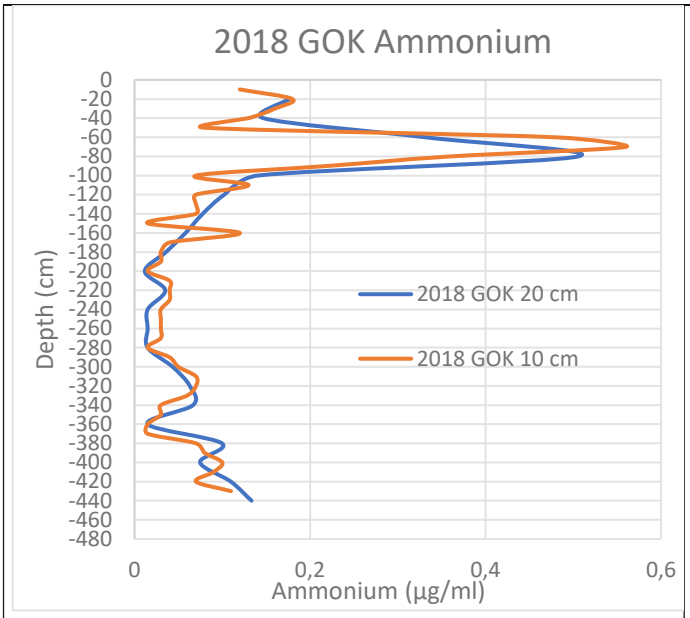


*Figure 40: 2018 GOK Ammonium concentrations*

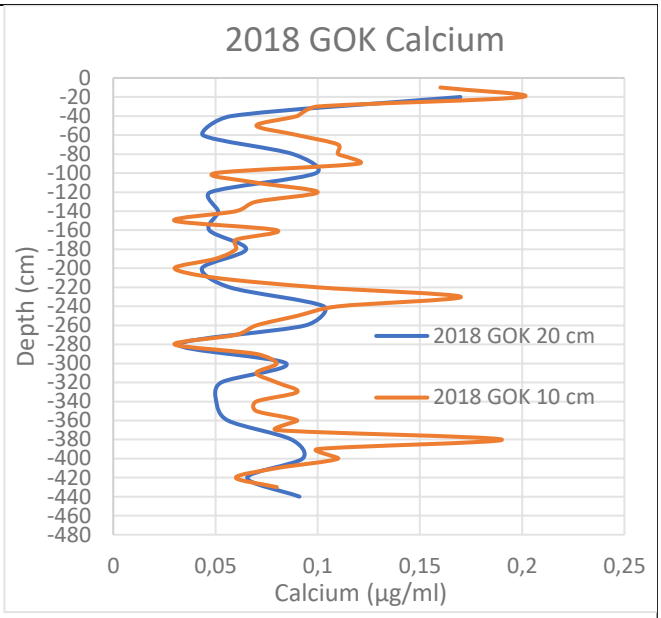


*Figure 41: 2018 GOK Calcium concentrations*

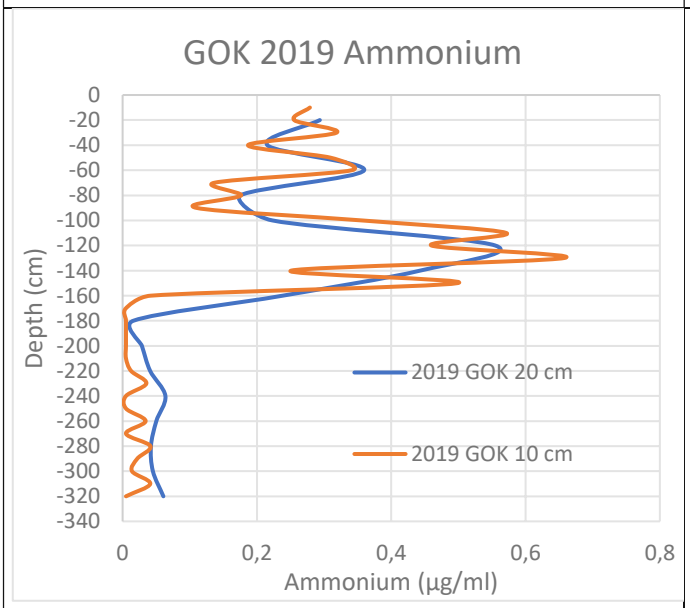


*Figure 42: 2019 GOK Ammonium concentrations*

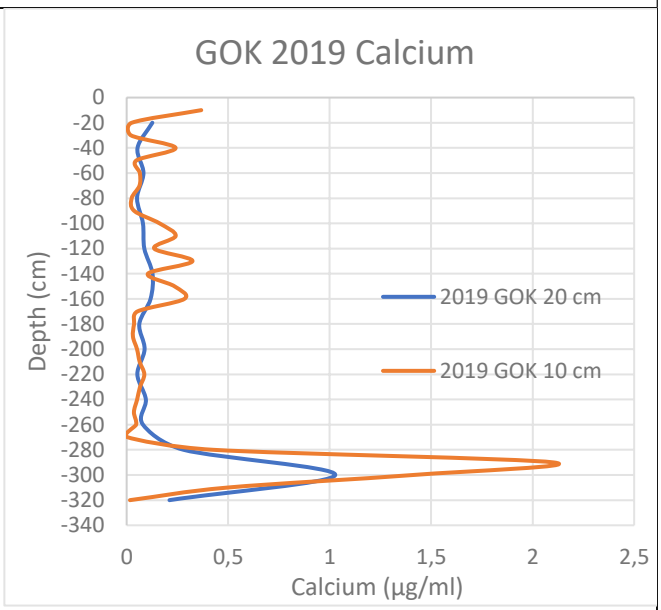


*Figure 43:2019 GOK Calcium concentrations*

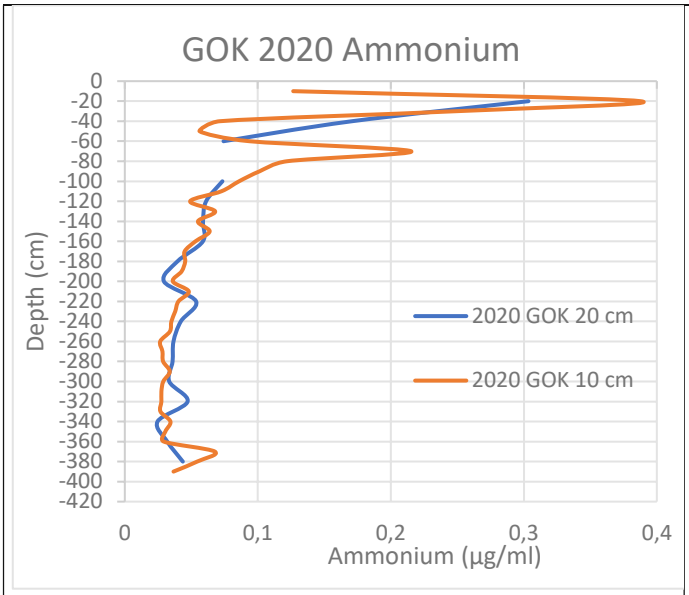


*Figure 44: 2020 GOK Ammonium concentrations*

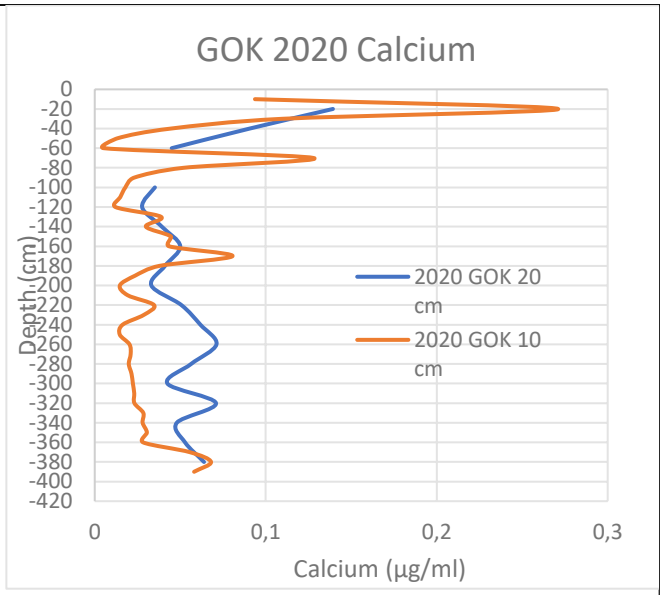


*Figure 45: 2020 GOK Calcium concentrations*

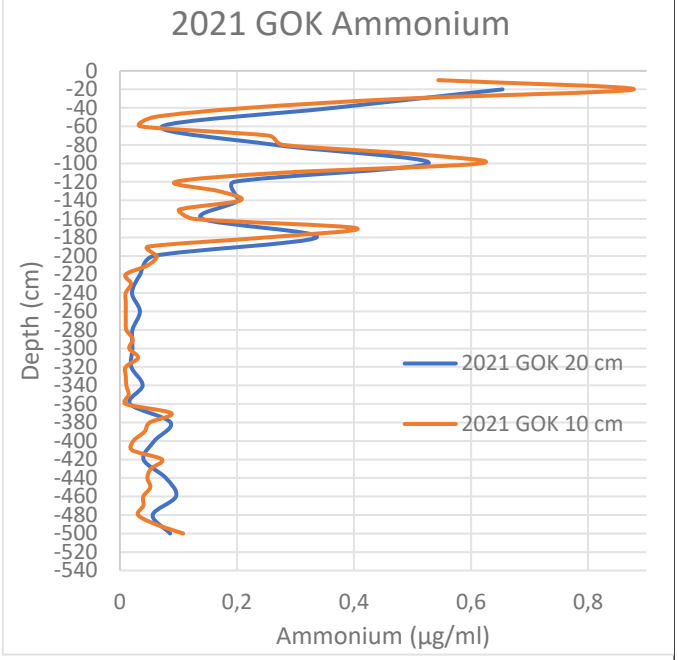


*Figure 46: 2021 GOK Ammonium concentrations*

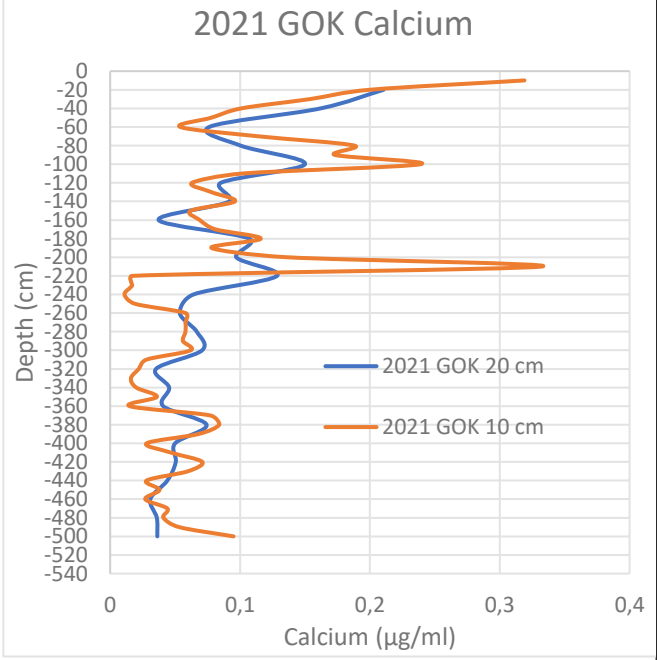


*Figure 47: 2021 GOK Calcium concentrations*

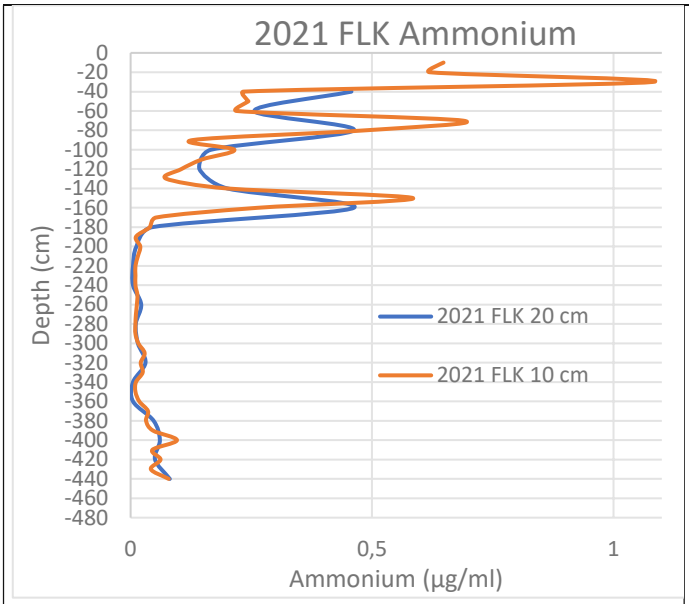


*Figure 48: 2021 FLK Ammonium concentrations*

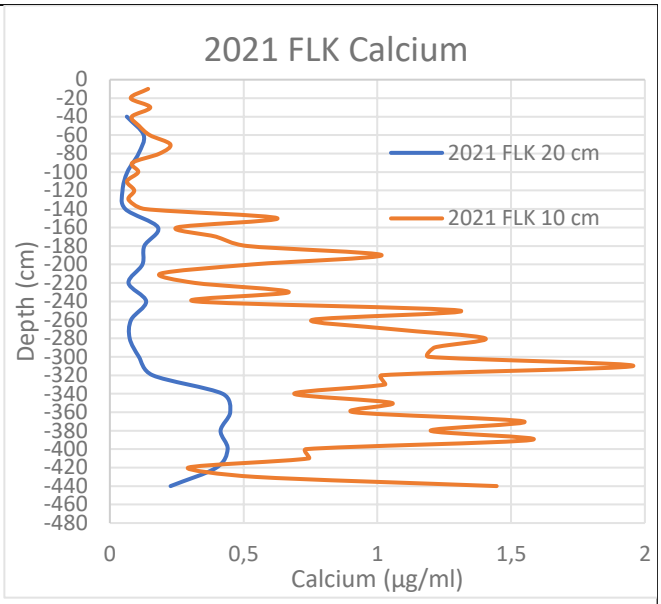


*Figure 49: 2021 FLK Calcium concentrations*

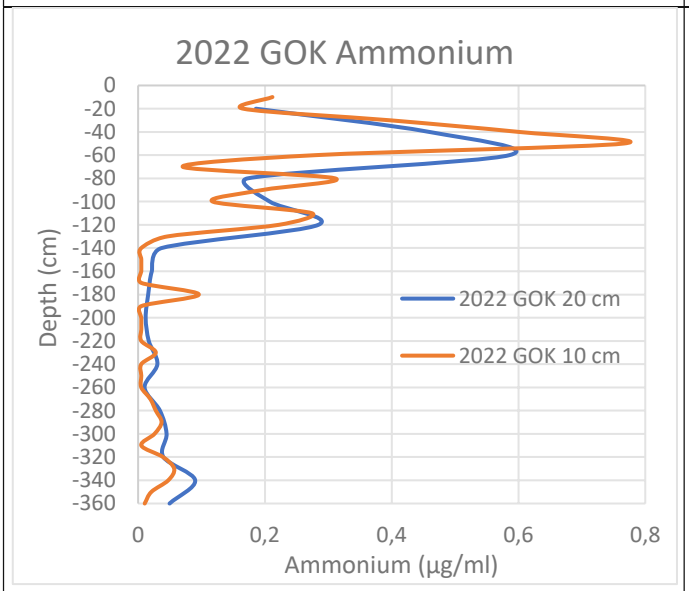


*Figure 50: 2022 GOK Ammonium concentrations*

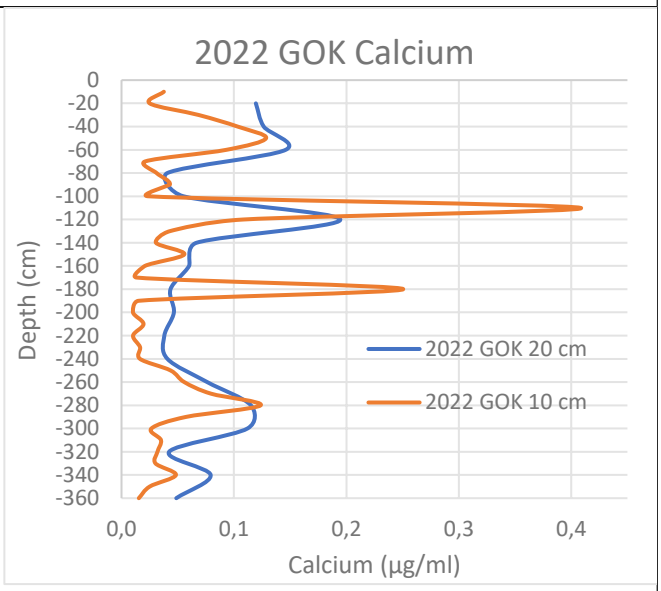


*Figure 51: 2022 GOK Calcium concentrations*

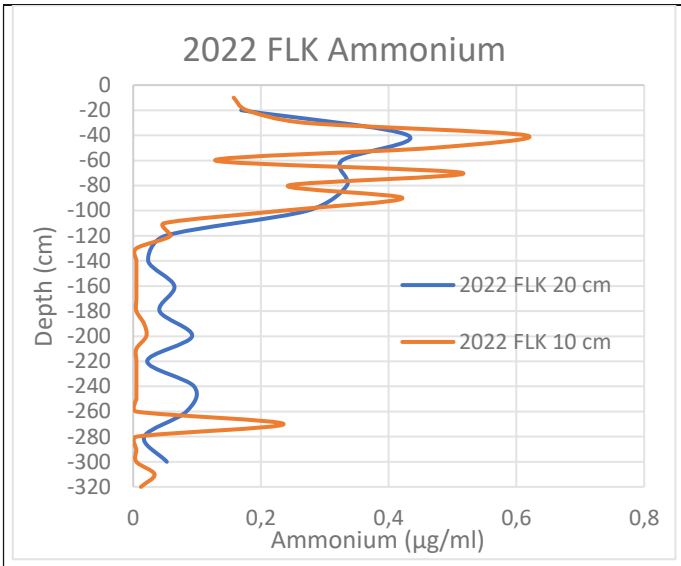


*Figure 52: 2022 FLK Ammonium concentrations*

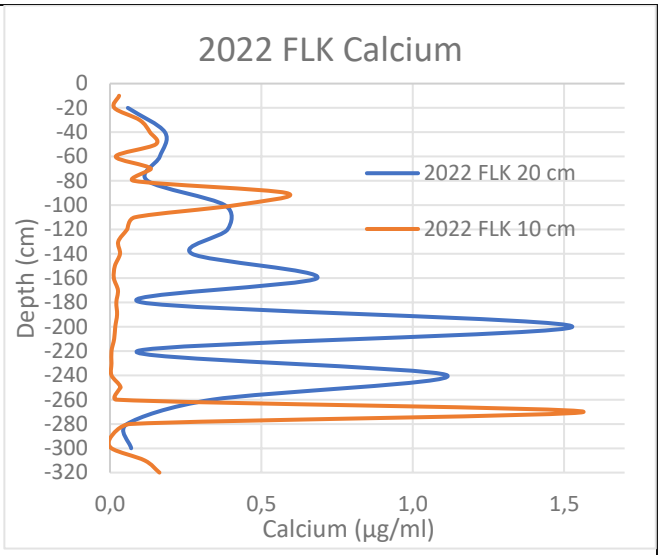


*Figure 53: 2022 GOK Calcium concentrations*

The obtained values show that especially ammonium shows a very good correlation. The concentrations obtained for the 10 cm and the 20 cm profiles are almost identical. As expected, larger variations of the concentration values are determined for the 10 cm profiles. This is due to the fact, that the 20 cm increments already present averaging. Single deposition events might lead to thin layers in the snow pit representing rather polluted or clean conditions. Taking samples in a vertical resolution of 10 cm can account for this fact better, than larger increments.

The results obtained for calcium are more difficult to interpret. Very good agreement and similar results, as discussed for ammonium, were obtained in 2018, 2019, 2020 (GOK) and overall, also in 2020. The marked differences found in 2021 can be attributed to problems during sampling, which led to contamination of part of the samples with debris of the sampling equipment (mainly the plastic hammer), which influenced the calcium concentrations markedly and rather randomly. Another phenomenon is found in 2017, when at least some of the overall features can be determined in both profiles, but overall concentrations are consistently lower for the 20 cm samples. No reason for this effect can be given presently.

### 3.2.2 Comparison of water-insoluble and water-soluble Calcium

This chapter deals with the comparison of the concentrations of water-soluble (WS) calcium, measured with the cation chromatography system, and the concentration of calcium contained in the water-insoluble (WIS) particles, measured with the ICP-OES after the micro-wave digestion. Note that the sample for the analysis via ion chromatography was taken right before the filtration. Sometimes two different samples were filtrated onto one filter to get a higher filter loading. To obtain a correct intercomparison, the respective concentrations of water-soluble calcium were multiplied with the amount of snow filtrated, then added together and divided by the sum of the sample weights of both snow samples. No comparison will be given for magnesium, as out of forty samples only eight samples are above the limit of detection for WS Mg. For the WIS Mg, it is a little bit different. Out of forty samples, twelve were above the LOD.

The obtained values are provided in the following Table 9. The used LODs are shown in chapter 2.4.1 and 3.2.4.

*Table 9: Comparison of water-insoluble and water-soluble Calcium and Magnesium*

| Sample name | Cation - chromatography | | ICP - OES | |
|---|---|---|---|---|
| | Calcium (µg/ml) | Magnesium (µg/ml) | Calcium (µg/g) | Magnesium (µg/g) |
| (2017) GOK 15 | 0.14 | <LOD | 0.04 | 0.04 |
| (2017) GOK 16 | 0.09 | <LOD | <LOD | <LOD |
| (2017) FLK 18 | 0.10 | <LOD | 0.01 | 0.02 |
| (2017) FLK 20 | 0.05 | <LOD | 0.32 | 0.70 |
| (2018) GOK1 | 0.17 | 0.02 | 0.07 | 0.11 |
| (2018) GOK2 | 0.06 | <LOD | <LOD | <LOD |
| (2018) GOK3 | 0.04 | <LOD | <LOD | <LOD |
| (2018) GOK4 | 0.09 | <LOD | <LOD | <LOD |
| (2018) GOK5 | 0.10 | <LOD | <LOD | <LOD |
| (2018) GOK6 | 0.05 | <LOD | <LOD | <LOD |
| (2018) GOK7 | 0.05 | 0,01 | <LOD | <LOD |
| (2018) GOK8 | 0.05 | <LOD | <LOD | <LOD |
| (2018) GOK9 | 0.07 | <LOD | <LOD | <LOD |
| (2018) GOK10 | 0.04 | <LOD | <LOD | <LOD |
| (2018) GOK11 | 0.06 | 0,01 | 0.01 | <LOD |
| (2018) GOK12 | 0.10 | <LOD | 0.01 | 0.02 |
| (2018) GOK13 | 0.09 | <LOD | <LOD | <LOD |
| (2018) GOK14 | 0.03 | <LOD | <LOD | <LOD |
| (2018) GOK15 | 0.08 | <LOD | <LOD | <LOD |
| (2018) GOK16 | 0.05 | <LOD | <LOD | <LOD |
| (2018) GOK17 | 0.05 | <LOD | <LOD | <LOD |
| (2018) GOK18 | 0.06 | <LOD | <LOD | <LOD |
| (2018) GOK19 | 0.09 | <LOD | 0.02 | 0.01 |
| (2018) GOK20 | 0.09 | <LOD | 0.02 | 0.02 |
| (2018) GOK21 | 0.07 | <LOD | <LOD | <LOD |
| (2018) GOK22 | 0.09 | <LOD | 0.19 | 0.12 |
| (2021) GOK5 | 0.15 | 0.02 | <LOD | <LOD |
| (2021) GOK9 | 0.11 | <LOD | <LOD | <LOD |
| (2021) GOK10 | 0.10 | <LOD | <LOD | <LOD |
| (2021) GOK11 | 0.13 | <LOD | 0.01 | <LOD |
| (2021) GOK23+24 | 0.04 | <LOD | <LOD | <LOD |
| (2021) GOK25 | 0.04 | <LOD | 0.13 | 0.12 |
| (2021) FLK22 | 0.23 | <LOD | 0.20 | <LOD |
| (2022) GOK6 | 0.20 | 0.02 | 0.08 | <LOD |
| (2022) GOK18 | 0.05 | <LOD | 0.05 | 0.08 |
| (2022) FLK1+2 | 0.14 | 0.01 | 0.01 | <LOD |
| (2022) FLK5 | 0.38 | 0.02 | 0.27 | 0.05 |
| (2022) FLK11 | 1.53 | 0.04 | 0.21 | <LOD |
| (2022) FLK13 | 1.11 | <LOD | 0.27 | <LOD |
| (2022) FLK16 | 0.07 | <LOD | 0.06 | 0.13 |

Only samples with values above the LOD are shown in the following Table 10 and Figure 54. Some samples are marked orange, because of the visible coloration of the filter. In this case µg/g is compared to µg/ml, as this was the way as results were reported for the two methods, and the error of the density of water at room temperature is neglected.

*Table 10: Calcium comparison of water-insoluble and water-insoluble Calcium above the LOD*

| Sample name | Cation - chromatography | ICP - OES |
|---|---|---|
| | Calcium (µg/ml) | Calcium (µg/g) |
| (2017) GOK 15 | 0.14 | 0.04 |
| (2017) FLK 18 | 0.10 | 0.01 |
| (2017) FLK 20 | 0.05 | 0.32 |
| (2018) GOK1 | 0.17 | 0.07 |
| (2018) GOK11 | 0.06 | 0.01 |
| (2018) GOK12 | 0.10 | 0.01 |
| (2018) GOK19 | 0.09 | 0.02 |
| (2018) GOK20 | 0.09 | 0.02 |
| (2018) GOK22 | 0.09 | 0.19 |
| (2021) GOK11 | 0.13 | 0.01 |
| (2021) GOK25 | 0.04 | 0.13 |
| (2021) FLK22 | 0.23 | 0.20 |
| (2022) GOK6 | 0.20 | 0.08 |
| (2022) GOK18 | 0.05 | 0.05 |
| (2022) FLK1+2 | 0.14 | 0.01 |
| (2022) FLK5 | 0.38 | 0.27 |
| (2022) FLK11 | 1.53 | 0.21 |
| (2022) FLK13 | 1.11 | 0.27 |
| (2022) FLK16 | 0.07 | 0.06 |

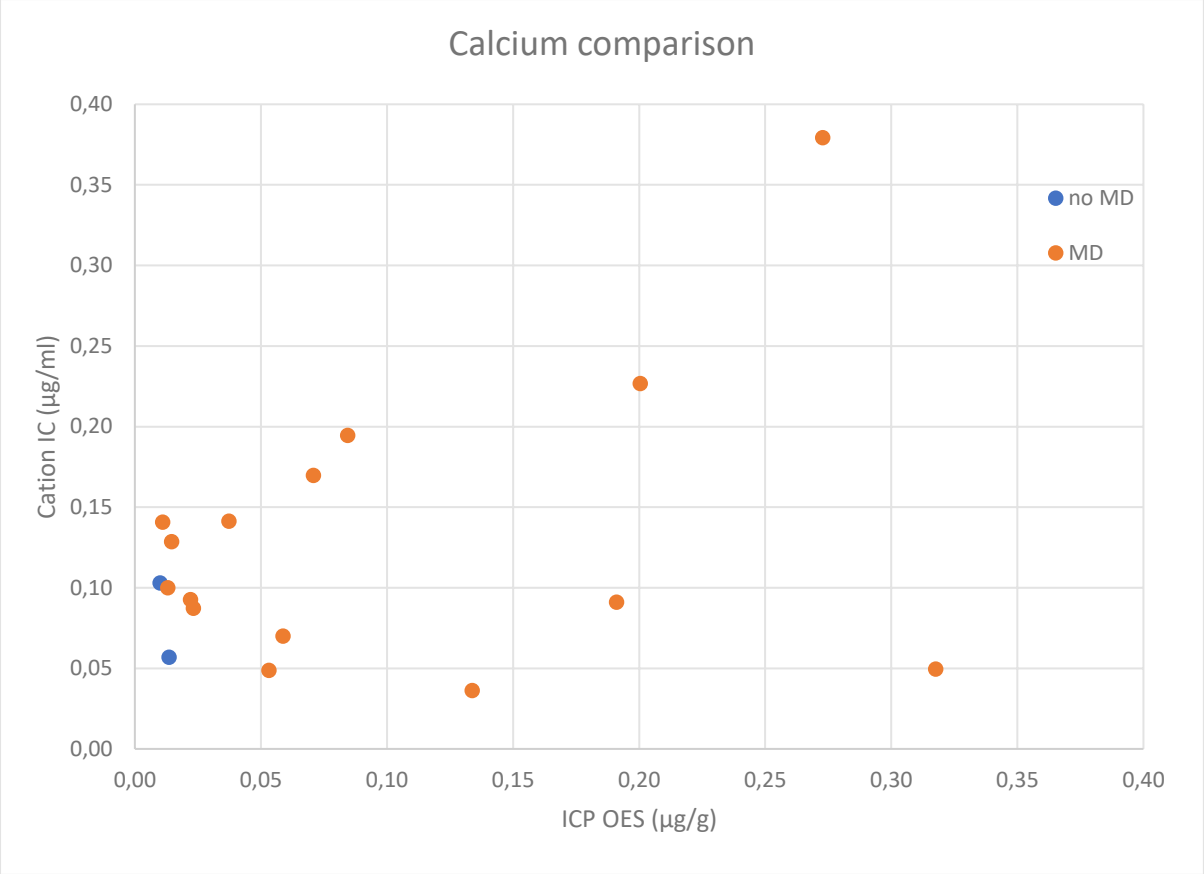


*Figure 54: Calcium comparison*

Just three out of nineteen samples have a higher WIS $Ca^{2+}$ value than WS $Ca^{2+}$ concentrations. Disregarding these three samples a weak linkage between WIS $Ca^{2+}$ values and WS $Ca^{2+}$ concentrations can be found in Figure 54.

Note that (2022) FLK11 and FLK13 are not displayed in this figure, due to their high value.

### 3.2.3 Gravimetric Analysis

During the filtration, parts of the filters were worn away, which led to a lower sampled filter weight than expected. To correct this error, a number of filters was loaded with demineralized water, i.e. with samples containing no insoluble material. Determining the resulting 'load' allowed to correct for possible losses of filter material. The following values in Table 11 were used to obtain an average loss and its' standard deviation (SD), which was necessary to evaluate the possible variation of the expected loss.

*Table 11: Blank values of the gravimetric analysis*

| **Name** | **Original filter weight (mg)** | **Sampled filter weight (mg)** | **Difference (mg)** |
|---|---|---|---|
| Blank 1 | 39.7 | 39.5 | -0.15 |
| Blank 2 | 39.8 | 39.0 | -0.81 |
| Blank 3 | 39.0 | 38.9 | -0.17 |
| Blank 4 | 38.8 | 38.5 | -0.33 |
| Blank 5 | 38.8 | 38.5 | -0.26 |
| Blank 6 | 39.1 | 38.8 | -0.36 |
| Blank 7 | 39.1 | 38.9 | -0.25 |
| Blank 8 | 39.0 | 38.7 | -0.31 |
| | **Blank average (mg)** | **SD (mg)** | **3 * SD (mg)** |
| Blank average | -0.29 | 0.18 | 0.53 |

The blank average represents the average loss and was added to the sampled filter weight of the loaded filters. If the difference between loaded and unloaded filters remains below 3 * SD, the samples were not taken into consideration for the determination of the mass of insoluble particles, which will be further used for a mass balance. Seventeen out of forty filters showed mass loading which were above 3 * SD and could be evaluated further. The obtained values, which mainly refers to filters where a possible influence of mineral dust was also obvious by visual inspection (amount, color and structure of the residues on the quartz filters), are shown in Table 12 and if they are below the already mentioned value, they are marked red.

*Table 12: Corrected sample weight*

| Sample name | Weight (mg) | Sample name | Weight (mg) |
|---|---|---|---|
| (2018) GOK 1 | 1.58 | (2021) GOK 25 | 13.1 |
| (2018) GOK 2 | 0.53 | (2021) FLK 22 | 1.64 |
| (2018) GOK 3 | 0.53 | (2022) GOK 6 | 0.77 |
| (2018) GOK 4 | 0.53 | (2022) GOK 18 | 3.38 |
| (2018) GOK 5 | 0.53 | (2022) FLK 1 + 2 | 0.75 |
| (2018) GOK 6 | 0.53 | (2022) FLK 5 | 1.77 |
| (2018) GOK 7 | 0.53 | (2022) FLK 11 | 0.94 |
| (2018) GOK 8 | 0.53 | (2022) FLK 13 | 0.63 |
| (2018) GOK 9 | 0.53 | (2022) FLK 16 | 3.63 |
| (2018) GOK 10 | 0.53 | | |
| (2018) GOK 11 | 0.54 | | |
| (2018) GOK 12 | 0.53 | | |
| (2018) GOK 13 | 0.53 | | |
| (2018) GOK 14 | 0.53 | | |
| (2018) GOK 15 | 0.53 | | |
| (2018) GOK 16 | 0.53 | | |
| (2018) GOK 17 | 0.53 | | |
| (2018) GOK 18 | 0.53 | | |
| (2018) GOK 19 | 0.53 | | |
| (2018) GOK 20 | 0.80 | | |
| (2018) GOK 21 | 0.53 | | |
| (2018) GOK 22 | 3.86 | | |
| (2017) GOK 15 | 0.53 | | |
| (2017) GOK 16 | 0.53 | | |
| (2017) FLK 18 | 0.53 | | |
| (2017) FLK 20 | 3.79 | | |
| (2021) GOK 5 | 0.57 | | |
| (2021) GOK 9 | 0.53 | | |
| (2021) GOK 10 | 0.53 | | |
| (2021) GOK 11 | 0.61 | | |
| (2021) GOK 23 + 24 | 0.67 | | |

Out of 40 samples, 17 are above 3 * SD, which is slightly less than half of the filters.

### 3.2.4 Elemental analysis

The obtained averages of the blank values and standard deviations are shown in the Table 13. The average was used for the blank correction and SD was used as the LOD. Only one value was obtained for Al, therefore no standard deviation could be determined.

*Table 13: ICP-OES blank values*

| Element | Average (µg/filter) | SD (µg/filter) | 3SD (µg/filter) |
|---|---|---|---|
| **Ca** | 7.99 | 1.88 | 5.64 |
| **Mg** | 15.0 | 2.07 | 6.21 |
| **K** | 7.12 | 2.84 | 8.52 |
| **Al** | 5.10 | - | - |
| **P** | 9.44 | 0.89 | 2.67 |
| **Ti** | 0.42 | 0.04 | 0.12 |
| **Cr** | 0.92 | 0.09 | 0.27 |
| **Mn** | 0.27 | 0.27 | 0.81 |
| **Fe** | 2.03 | 0.90 | 2.70 |
| **Co** | 0.74 | 0.07 | 0.21 |
| **Sr** | 0.21 | 0.32 | 0.96 |
| **Ni** | 1.59 | 0.76 | 2.28 |
| **Pb** | 4.36 | 2.80 | 8.40 |

Co, Ni, Cr, Pb and P were below the LOD and therefore are not mentioned in the following Table 14, which contains the end results (µg/g snow). Every filter that had an orange or red coloration is mentioned in the following table. Additionally, the whole (2018) GOK profile is shown. Samples that show a red or orange coloration are marked orange.

*Table 14: Results of the elemental analysis*

| Sample name | Mg (µg/g) | K (µg/g) | Fe (µg/g) | Mn (µg/g) | Sr (µg/g) | Ca (µg/g) | Ti (µg/g) | Al (µg/g) | Si (µg/g) |
|---|---|---|---|---|---|---|---|---|---|
| (2018) GOK1 | 1,05E-01 | 1,1E-01 | 2,7E-01 | <LOD | <LOD | 7,1E-02 | 3,0E-02 | 9,1E-01 | 2,3E+00 |
| (2018) GOK2 | <LOD | <LOD | 1,3E-02 | <LOD | <LOD | <LOD | 2,9E-03 | 6,9E-02 | 1,7E-01 |
| (2018) GOK3 | <LOD | <LOD | 5,0E-03 | <LOD | <LOD | <LOD | 2,1E-03 | 5,5E-02 | 1,4E-01 |
| (2018) GOK4 | <LOD | <LOD | 1,4E-02 | <LOD | <LOD | <LOD | 2,1E-03 | 7,0E-02 | 1,7E-01 |
| (2018) GOK5 | <LOD | <LOD | 7,0E-03 | <LOD | <LOD | <LOD | <LOD | 4,6E-02 | 1,2E-01 |
| (2018) GOK6 | <LOD | <LOD | 1,1E-02 | <LOD | <LOD | <LOD | 4,5E-03 | 7,0E-02 | 1,7E-01 |
| (2018) GOK7 | <LOD | <LOD | 1,1E-02 | <LOD | <LOD | <LOD | <LOD | 1,1E-01 | 2,7E-01 |
| (2018) GOK8 | <LOD | <LOD | <LOD | <LOD | <LOD | <LOD | <LOD | 8,6E-02 | 2,1E-01 |
| (2018) GOK9 | <LOD | <LOD | 8,8E-03 | <LOD | <LOD | <LOD | 3,0E-03 | 9,9E-02 | 2,5E-01 |
| (2018) GOK10 | <LOD | <LOD | <LOD | <LOD | <LOD | <LOD | 3,6E-03 | 4,9E-02 | 1,2E-01 |
| (2018) GOK11 | <LOD | <LOD | 2,4E-02 | <LOD | <LOD | 1,4E-02 | 3,6E-03 | 1,0E-01 | 2,5E-01 |
| (2018) GOK12 | 2,0E-02 | <LOD | 5,8E-02 | <LOD | <LOD | 1,0E-02 | 7,8E-03 | 2,0E-01 | 5,0E-01 |
| (2018) GOK13 | <LOD | <LOD | 9,4E-03 | <LOD | <LOD | <LOD | 2,7E-03 | 7,2E-02 | 1,8E-01 |
| (2018) GOK14 | <LOD | <LOD | 6,2E-03 | <LOD | <LOD | <LOD | 2,9E-03 | 6,6E-02 | 1,6E-01 |
| (2018) GOK15 | <LOD | <LOD | 7,2E-03 | <LOD | <LOD | <LOD | 2,8E-03 | 9,6E-02 | 2,4E-01 |

*Table 14 continued*

| Sample name | Mg (µg/g) | K (µg/g) | Fe (µg/g) | Mn (µg/g) | Sr (µg/g) | Ca (µg/g) | Ti (µg/g) | Al (µg/g) | Si (µg/g) |
|---|---|---|---|---|---|---|---|---|---|
| (2018) GOK16 | <LOD | <LOD | 4,5E-03 | <LOD | <LOD | <LOD | 3,2E-03 | 6,2E-02 | 1,5E-01 |
| (2018) GOK17 | <LOD | <LOD | 4,3E-03 | <LOD | <LOD | <LOD | <LOD | 4,0E-02 | 9,9E-02 |
| (2018) GOK18 | <LOD | <LOD | 1,9E-02 | <LOD | <LOD | <LOD | 2,6E-03 | 6,9E-02 | 1,7E-01 |
| (2018) GOK19 | 1,1E-02 | <LOD | 5,1E-02 | <LOD | <LOD | 2,3E-02 | 7,0E-03 | 1,9E-01 | 4,7E-01 |
| (2018) GOK20 | 2,0E-02 | <LOD | 6,9E-02 | <LOD | <LOD | 2,2E-02 | 6,3E-03 | 2,2E-01 | 5,4E-01 |
| (2018) GOK21 | <LOD | <LOD | 2,9E-02 | <LOD | <LOD | <LOD | 3,9E-03 | 9,1E-02 | 2,3E-01 |
| (2018) GOK22 | 1,1E-01 | 5,7E-01 | 4,0E-01 | <LOD | 5,7E-03 | 1,9E-01 | 5,5E-02 | 2,9E+00 | 7,3E+00 |
| (2017) GOK 15 | 4,0E-02 | <LOD | 1,0E-01 | <LOD | <LOD | 3,7E-02 | 1,5E-02 | 3,7E-01 | 9,3E-01 |
| (2017) GOK 16 | <LOD | <LOD | 4,8E-02 | <LOD | <LOD | <LOD | 7,0E-03 | 2,0E-01 | 5,1E-01 |
| (2017) FLK 18 | 2,2E-02 | <LOD | 5,9E-02 | <LOD | <LOD | 1,3E-02 | 8,0E-03 | 2,4E-01 | 5,9E-01 |
| (2017) FLK 20 | 7,0E-01 | 1,1E+00 | 2,1E+00 | 1,0E-02 | <LOD | 3,2E-01 | 1,9E-01 | 6,7E+00 | 1,7E+01 |
| (2021) GOK 5 | <LOD | <LOD | 6,3E-02 | <LOD | <LOD | <LOD | 9,4E-03 | 2,1E-01 | 5,1E-01 |
| (2021) GOK 9 | <LOD | <LOD | 5,1E-02 | <LOD | <LOD | <LOD | 8,5E-03 | 2,5E-01 | 6,1E-01 |
| (2021) GOK 10 | <LOD | <LOD | 3,8E-02 | <LOD | <LOD | <LOD | 7,2E-03 | 1,8E-01 | 4,6E-01 |
| (2021) GOK 11 | <LOD | <LOD | 5,7E-02 | <LOD | <LOD | 1,5E-02 | 8,4E-03 | 3,1E-01 | 7,7E-01 |

*Table 14 continued*

| Sample name | Mg (µg/g) | K (µg/g) | Fe (µg/g) | Mn (µg/g) | Sr (µg/g) | Ca (µg/g) | Ti (µg/g) | Al (µg/g) | Si (µg/g) |
|---|---|---|---|---|---|---|---|---|---|
| (2021) GOK 23+24 | <LOD | <LOD | 3,7E-02 | <LOD | <LOD | <LOD | 5,0E-03 | 1,5E-01 | 3,7E-01 |
| (2021) GOK 25 | 1,2E-01 | 5,1E-01 | 6,8E-01 | <LOD | <LOD | 1,3E-01 | 7,1E-02 | 2,4E+00 | 6,0E+00 |
| (2021) FLK 22 | <LOD | 6,3E-02 | 1,8E-01 | <LOD | <LOD | 2,0E-01 | 1,7E-02 | 5,1E-01 | 1,3E+00 |
| (2022) GOK 6 | <LOD | 8,9E-02 | 1,8E-01 | <LOD | <LOD | 8,4E-02 | 1,7E-02 | 5,5E-01 | 1,4E+00 |
| (2022) GOK 18 | 8,3E-02 | 3,4E-01 | 4,6E-01 | <LOD | <LOD | 5,3E-02 | 5,0E-02 | 1,5E+00 | 3,7E+00 |
| (2022) FLK 1+2 | <LOD | <LOD | 5,8E-02 | <LOD | <LOD | 1,1E-02 | 8,1E-03 | 1,9E-01 | 4,8E-01 |
| (2022) FLK 5 | 5,3E-02 | 1,2E-01 | 2,9E-01 | <LOD | <LOD | 2,7E-01 | 3,1E-02 | 8,5E-01 | 2,1E+00 |
| (2022) FLK 11 | <LOD | <LOD | 4,6E-02 | <LOD | <LOD | 2,1E-01 | 5,6E-03 | 3,8E-01 | 9,5E-01 |
| (2022) FLK 13 | <LOD | <LOD | 3,4E-02 | <LOD | <LOD | 2,7E-01 | 3,7E-03 | 1,5E-01 | 3,8E-01 |
| (2022) FLK 16 | 1,3E-01 | 4,1E-01 | 7,1E-01 | <LOD | <LOD | 5,9E-02 | 7,1E-02 | 2,1E+00 | 5,3E+00 |

### 3.2.5 Evaluation of the presence of mineral dust

The following Table 15 to Table 20 show which samples match the mentioned criteria. Due to the incident with the hammer in 2021, no information about (2021) FLK is shown. The tables contain the results of (2021) GOK, because only few samples were visually contaminated. Nevertheless, the results have to be interpreted cautiously.

After showing in chapter 3.2.1 that the samples show a very good correlation between the 10 cm and 20 cm increments, the pH and $Ca^{2+}$ values of the 10 cm samples can be used for this evaluation. It is important to note that both mentioned criteria must be fulfilled. If there is an X in the VIS column, it means that there is a reddish or yellowish color of the filter. The TM column refers to the increase of the transmission signal in the cooling phase of the TOA, so if there is a transmission increase, an X is in the corresponding cell. Additionally, note that the samples from 2019 and 2020 couldn't be analyzed with ICP-OES, due to a contaminated HBF4-solution. Therefore, no Fe value is shown for these samples.

*Table 15: FLK and GOK 2017 mineral dust criteria and Fe loadings (More explanations about VIS and TM are given in the text)*

| FLK 2017 | | | | | | GOK 2017 | | | | |
|---|---|---|---|---|---|---|---|---|---|---|
| VIS | TM | pH | $Ca^{2+}$ (µev/l) | Fe (µg/filter) | Depth (cm) | VIS | TM | pH | $Ca^{2+}$ (µev/l) | Fe (µg/filter) |
| | | | | | -20 | | | | | |
| | | | | | -40 | | | | | |
| | | - / 5.63 | | | -60 | | | | | |
| | | | | | -80 | | | | | |
| | | | | | -100 | | | | | |
| | | | | | -120 | | | | | |
| | | | | | -140 | | | | | |
| | | | | | -160 | | | | | |
| | | | | | -180 | | | | | |
| | | | | | -200 | | | | | |
| | | | | | -220 | | | | | |
| | | | | | -240 | | | | | |
| | | | | | -260 | | | | | |
| | | | | | -280 | | | - / 5.84 | - / 14.6 | |
| | | | | | -300 | X | X | | - / 14.6 | 17.8 |
| | | | | | -320 | X | X | | | 7.38 |
| | | 5.62 / - | | | -340 | | | | | |
| X | X | - / 5.76 | | 11.3 | -360 | | | | | |
| | | | | | -380 | | | | | |
| X | X | | | 163 | -400 | | | | | |

*Table 16: GOK 2018 mineral dust criteria and Fe loadings*

| GOK 2018 | | | | | |
|---|---|---|---|---|---|
| **VIS** | **TM** | **pH** | **$Ca^{2+}$ (µev/l)** | **Fe (µg/filter)** | **Depth (cm)** |
| X | X | 5.76 / 5.77 | | 50.8 | -20 |
| | | 5.61 / 5.61 | | | -40 |
| | | - / 5.64 | | | -60 |
| | | 5.73 / - | | | -80 |
| | | | | | -100 |
| | | | | | -120 |
| | | | | | -140 |
| X | | | | <LOD | -160 |
| | | | | | -180 |
| | | | | | -200 |
| | | | | | -220 |
| | | 5.62 / - | | | -240 |
| | | | | | -260 |
| | | | | | -280 |
| | | | | | -300 |
| | | | | | -320 |
| | | | | | -340 |
| | | | | | -360 |
| X | | - / 5.76 | | 13.7 | -380 |
| X | X | 5.62 / - | | 15.8 | -400 |
| | | | | | -420 |
| X | X | 5.62 / - | | 52.5 | -440 |

*Table 17: GOK 2019 mineral dust criteria and Fe loadings*

| GOK 2019 | | | | | |
|---|---|---|---|---|---|
| **VIS** | **TM** | **pH** | **$Ca^{2+}$ (µev/l)** | **Fe (µg/filter)** | **Depth (cm)** |
| X | X | | 18.3 / - | | -20 |
| | | | - / 12.0 | | -40 |
| | | - / 5.62 | | | -60 |
| | | | | | -80 |
| | | | | | -100 |
| | | | | | -120 |
| X | X | 5.61 / 5.66 | 16.2 / - | | -140 |
| X | X | - / 5.71 | 11.8 / 14.2 | | -160 |
| | | 5.61 / - | | | -180 |
| | | | | | -200 |
| | | | | | -220 |
| | | | | | -240 |
| | | | | | -260 |
| X | X | 5.63 / 6.16 | - / 21.3 | | -280 |
| X | X | 6.76 / 6.68 | 105 / 70.4 | | -300 |
| X | X | 6.28 / 5.76 | 24.8 / - | | -320 |

*Table 18: GOK 2020 mineral dust criteria and Fe loadings*

| GOK 2020 | | | | | |
|---|---|---|---|---|---|
| **VIS** | **TM** | **pH** | **$Ca^{2+}$ (µev/l)** | **Fe (µg/filters)** | **Depth (cm)** |
| | | - / 5.80 | - / 13.5 | | -20 |
| | | 5.82 / 5.71 | | | -40 |
| | | 5.62 / 5.64 | | | -60 |
| | | 5.70 / 5.70 | | | -80 |
| | | 5.65 / - | | | -100 |
| | | | | | -120 |
| | | - / 5.61 | | | -140 |
| | | 5.64 / - | | | -160 |
| X | X | - / 5.64 | | | -180 |
| | | | | | -200 |
| | | | | | -220 |
| | | | | | -240 |
| | | | | | -260 |
| | | | | | -280 |
| | | | | | -300 |
| | | | | | -320 |
| | | | | | -360 |
| | | | | | -400 |

*Table 19: GOK 2021 mineral dust criteria and Fe loadings*

| GOK 2021 | | | | | |
|---|---|---|---|---|---|
| **VIS** | **TM** | **pH** | **$Ca^{2+}$ (µev/l)** | **Fe (µg/filter)** | **Depth (cm)** |
| | | 5.79 / - | 15.9 / - | | -20 |
| | | | | | -40 |
| | | | | | -60 |
| | | - / 5.73 | | | -80 |
| X | X | - / 5.64 | - / 11.9 | 10.3 | -100 |
| | | | | | -120 |
| | | | | | -140 |
| | | | | | -160 |
| X | X | | | 9.43 | -180 |
| X | X | - / 5.74 | | 7.70 | -200 |
| X | | 5.92 / - | 16.6 / - | 11.1 | -220 |
| | | | | | -240 |
| | | | | | -260 |
| | | | | | -280 |
| | | | | | -300 |
| | | | | | -320 |
| | | | | | -340 |
| | | | | | -360 |
| | | | | | -380 |
| | | | | | -400 |
| | | | | | -420 |
| | | | | | -440 |
| X | | | | 16.7 | -460 |
| | | | | | -480 |
| X | X | | | 138 | -500 |

*Table 20: FLK and GOK 2022 mineral dust criteria and Fe loadings*

| FLK 2022 | | | | | | GOK 2022 | | | | |
|---|---|---|---|---|---|---|---|---|---|---|
| **VIS** | **TM** | **pH** | **$Ca^{2+}$ (µev/l)** | **Fe (µg/filter)** | **Depth (cm)** | **VIS** | **TM** | **pH** | **$Ca^{2+}$ (µev/l)** | **Fe (µg/filter)** |
| X | X | | | 13.0 | -20 | | | | | |
| | | 5.86 / 5.75 | | | -40 | | | 5.66 /5.70 | | |
| | | 5.71 / - | | | -60 | | | 5.67 / 5.62 | | |
| | | 5.77 / - | | | -80 | | | | | |
| X | X | 6.24 / 6.26 | 29.1 / 20.7 | 53.0 | -100 | | | | | |
| | | - / 5.61 | | | -120 | X | X | 6.10 / 5.68 | 20.4 / - | 31.5 |
| | | - / 5.63 | | | -140 | | | 5.62 / - | | |
| | | | | | -160 | | | | | |
| | | | | | -180 | | | - / 5.73 | - / 12.5 | |
| | | | | | -200 | | | | | |
| X | X | | | 10.3 | -220 | | | - / 5.72 | | |
| | | | | | -240 | | | | | |
| X | X | | | 7.39 | -260 | | | - / 5.62 | | |
| | | 6.45 / - | 78.1 / - | | -280 | | | | | |
| | | | | | -300 | | | | | |
| X | X | 5.86 / 5.87 | | 126 | -320 | | | | | |
| | | | | | -340 | | | | | |
| | | | | | -360 | X | X | | | 98.0 |

Most samples, twenty-five out of twenty-nine, that show a visible reddish or brownish coloration, also show the noticeable increase in the transmission in the cooling phase at the end of the TOA. Less agreement is found when the coloration of the filter is compared with the pH and $Ca^{2+}$ concentrations. Out of twenty-nine colored filters, only nine match the required pH and $Ca^{2+}$ values. One possible explanation would be, that the required pH and $Ca^{2+}$ values were identified based on 10 cm increments. The increments evaluated here are 20 cm and thus a dilution of dust layers can take place. On the other hand, there are also five samples that match the pH and $Ca^{2+}$ criteria, but no coloration was found. It could be that it indicated the presence of MD, but the iron content is not high enough to lead to issues during the placement of the OC/EC split. Interestingly, some samples with a rather low Fe loading (7.39 and 7.38 µg/filter) show a transmission increase in the cooling phase, but some with a higher content (11.1, 13.7 and 16.7 µg/filter) don't. Only one colored sample contained less Fe than the LOD and also showed no noticeable transmission increase. Keep in mind, that there are no Fe values for the samples from 2019 and 2020, due to the contaminated $HBF_4$-solution.

### 3.2.6 Mass balance

Every sample that showed a visible coloration and / or a transmission increase in the cooling phase is further described in this chapter. The Si values were obtained by calculating the Al values as described in chapter 1.1. Equation 1 is used to calculate the mineral dust content of these samples, except (2021) GOK5 and (2021) GOK23+24, because the calcium value is below the LOD. After that, the WITC values from chapter 3.1 and the obtained MD values are compared with the sample weight. The gathered data is shown in Table 21 and Table 22.

*Table 21: Mass balance percentages*

| Sample name | MD fraction (%) | WITC fraction (%) | WITC+MD fraction (%) |
|---|---|---|---|
| (2021) GOK 11 | 90 | 17 | 107 |
| (2021) GOK 25 | 35 | 3 | 38 |
| (2021) FLK 22 | 66 | 22 | 88 |
| (2022) GOK 6 | 120 | 10 | 130 |
| (2022) GOK 18 | 87 | 5 | 92 |
| (2022) FLK 1+2 | 53 | 14 | 67 |
| (2022) FLK 5 | 88 | 6 | 94 |
| (2022) FLK 11 | 89 | 10 | 99 |
| (2022) FLK 13 | 64 | 12 | 76 |
| (2022) FLK 16 | 96 | 8 | 104 |
| (2018) GOK 1 | 102 | 15 | 117 |
| (2018) GOK 11 | 39 | 18 | 57 |
| (2018) GOK 20 | 59 | 14 | 73 |
| (2018) GOK 22 | 89 | 1 | 90 |
| (2017) FLK 20 | 130 | 9 | 139 |

*Table 22: Mass balance values in mg*

| Sample name | Sample weight (mg) | Mineral dust (mg) | WITC (mg) | Remaining sample weight (mg) |
|---|---|---|---|---|
| (2021) GOK 11 | 0.61 | 0.55 | 0.10 | -0.04 |
| (2021) GOK 25 | 13.1 | 4.52 | 0.42 | 8.19 |
| (2021) FLK 22 | 1.64 | 1.07 | 0.36 | 0.21 |
| (2022) GOK 6 | 0.77 | 0.92 | 0.08 | -0.23 |
| (2022) GOK 18 | 3.38 | 2.95 | 0.18 | 0.25 |
| (2022) FLK 1+2 | 0.75 | 0.40 | 0.10 | 0.25 |
| (2022) FLK 5 | 1.77 | 1.55 | 0.10 | 0.12 |
| (2022) FLK 11 | 0.93 | 0.83 | 0.09 | 0.01 |
| (2022) FLK 13 | 0.62 | 0.40 | 0.07 | 0.16 |
| (2022) FLK 16 | 3.63 | 3.50 | 0.28 | -0.15 |
| (2018) GOK 1 | 1.58 | 1.60 | 0.24 | -0.27 |
| (2018) GOK 11 | 0.53 | 0.21 | 0.10 | 0.23 |
| (2018) GOK 20 | 0.80 | 0.47 | 0.11 | 0.22 |
| (2018) GOK 22 | 3.86 | 3.42 | 0.04 | 0.39 |
| (2017) FLK 20 | 3.79 | 4.91 | 0.34 | -1.46 |

All mass balance values are shown in Figure 55, except (2021) GOK 25, because its' values are a lot higher than the others so it can't be displayed properly.

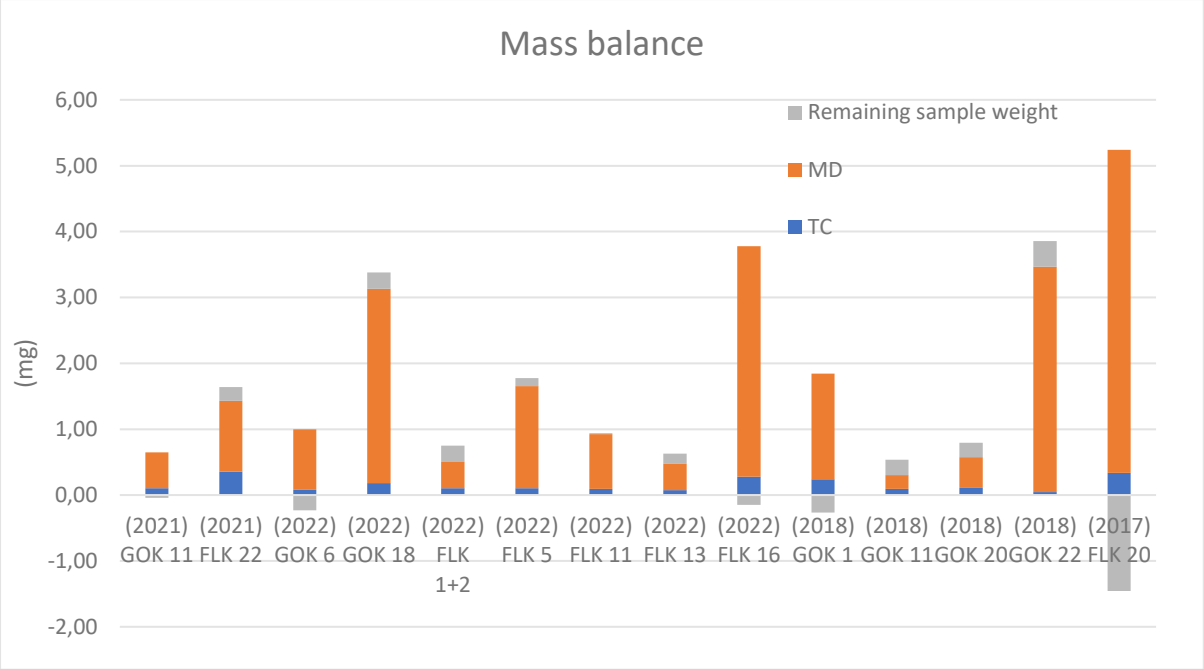


*Figure 55: Mass balance*

The sum of the mass of WITC and mass of MD of five out of fifteen samples is higher than the actual sample weight. There are a few reasons why this could happen. One of the main reasons is that there is a high potential error in the gravimetrical analysis. Additionally, there is a potential error in the elemental and thermal-optical analysis.

There is also probably biological material in the samples and there is a way to correct this error. Usually, the WITC is converted to organic matter (OM). This is achieved by multiplying the WITC value with a factor accounting for heteroatoms, with 1.5 being a factor commonly applied [15]. This is a possibility to find out what the unaccounted sample weight could consist of.

# 4. Conclusion

Every sample from the investigated years, except of GOK and FLK 2017, contained more EC and WIOC than samples from 2003/2004 from the same location. Another sample location from the same time period, is located in Germany at the SIL. Regarding the mean value, the EC was higher than in every SBK sample series, but for the WIOC it was the other way around. The samples, analyzed for this thesis, were also compared to other regions and more recent values. These regions were Himalaya, Finnish Arctic, Svalbard (Arctic Ocean). As expected, the EC and WIOC values of the samples from the Himalaya exceeded the values from the SBK 2017-2022. In all cases, the EC and WIOC values from the Svalbard samples were below the ones from SBK 2017-2022. Samples from the Finnish Arctic exceeded the EC and WIOC values from SBK 2017-2022 in every case. Additionally, the typical BC content of the Antarctic Plateau, North America, French Alps, Greenland and Swiss Alps was compared with the SBK samples from 2017-2022. As expected, the BC values from China are in a lot higher range than the ones from the analyzed SBK samples. The typical BC content of the samples from the French and Swiss Alps matches the SBK values well. Due to the remote location of Greenland and the Antarctic Plateau, it is not surprising that the SBK values are higher than theirs.

The method used for the correction of the TOA split point of the samples from 2017-2020 worked for most measurements, but not for all. Therefore, the second method, using the transmission signal from an additional measurement, should be used. This led to a split point correction of every mineral dust sample from 2021 and 2022. Due to the correction, the EC and WIOC values were more realistic and the EC increased by at least 27%.

Additionally, there is no correlation between the content of the different EC fractions and the positioning of the automatic split point.

There was at least one sample in every snow profile with visual MD in it. Out of the six years of sampling, only in three years, 2017, 2021 and 2022, both glaciers were investigated. The comparison between the FLK and GOK show that in 2017 both MD horizons are at or near the deepest sampling positions. Interestingly, in 2022 there are five MD horizons at the FLK and only two at the GOK, but both are at matching depths. No comparison was done for 2021, due to problems and contaminations during sampling

Different criteria have been defined to identify the presence of MD. Most samples, twenty-five out of twenty-nine, that showed a visual reddish or brownish coloration of the filter, also showed a transmission signal increase in the cooling phase, which led to the conclusion that the automatic EC/OC split point is at the wrong position. The main reason for that, is the hematite and therefore the Fe in the sample. Interestingly, some samples with a rather low Fe content, 7.38 and 7.39 µg/filter,

showed the increase in the cooling phase, but some samples with a higher content, 11.1, 13.7 and 16.7 µg/filter, didn't. Note, that for the samples from 2019 and 2020 no elemental analysis could be performed, due to the contaminated $HBF_4$-solution. Several discrepancies have been found in regard to identifying the presence of MD, via certain pH and $Ca^{2+}$ content. The calcium and especially the ammonium values show a very good correlation, this enabled the usage of data obtained for the 10 cm increments. This allowed us to use another way to determine whether there is mineral dust in the sample or not. After evaluating the obtained data, we concluded that using the pH and calcium content of the sample is not a good way for this determination, because only nine out of twenty-nine colored samples match this criterion. When it is used additionally to other methods, it can be helpful, but it should not be used on its own. Furthermore, a red coloration of the filter does not always indicate that there will be issues during the positioning of the split point. In some cases, the iron content is not high enough to lead to this kind of issues.

Initially, the comparison of water-soluble (WS) and water-insoluble (WIS) magnesium and calcium should have been performed. But WS and WIS magnesium was mostly below the LOD, so only calcium was compared. While all WS calcium values were above the LOD, only 19 out of 40 WIS calcium values were above the LOD. Three out of nine-teen samples have a higher WIS calcium value and there is some relationship between WS and WIS calcium.

The obtained mass balances of the mineral dust samples were below 100% for most samples. One possibility to correct these values would be to multiply the TC value with a factor to gather the organic matter (OM) content. Another one is to use other equations for the calculation of the MD content. Note that five out of fifteen samples were above 100%, these methods would lead to an even further overestimation.

# 5. Appendix

## 5.1 Obtained TOA values

*Table 23: Depth profile 2017 EC values*

| GOK 2017 | | | | FLK 2017 | | |
|---|---|---|---|---|---|---|
| **Sample name** | **not cor. EC (ng/g)** | **EC (ng/g)** | **Depth (cm)** | **not cor. EC (ng/g)** | **EC (ng/g)** | **Sample name** |
| GOK 1 | / | 1.84 | -20 | / | 0.03 | FLK 1 |
| GOK 2 | / | 1.45 | -40 | / | 0.02 | FLK 2 |
| GOK 3 | / | 5.40 | -60 | / | 0.01 | FLK 3 |
| GOK 4 | / | 0.02 | -80 | / | 0.01 | FLK 4 |
| GOK 5 | / | 0.01 | -100 | / | 9.02 | FLK 5 |
| GOK 6 | / | 19.7 | -120 | / | 6.67 | FLK 6 |
| GOK 7 | / | 3.75 | -140 | / | 0.01 | FLK 7 |
| GOK 8 | / | 0.01 | -160 | / | 6.93 | FLK 8 |
| GOK 9 | / | 4.96 | -180 | / | 4.72 | FLK 9 |
| GOK 10 | / | 0.01 | -200 | / | 2.25 | FLK 10 |
| GOK 11 | / | 9.04 | -220 | / | 6.89 | FLK 11 |
| GOK 12 | / | 6.42 | -240 | / | 9.12 | FLK 12 |
| GOK 13 | / | 0.03 | -260 | / | 6.39 | FLK 13 |
| GOK 14 | / | 0.02 | -280 | / | 5.91 | FLK 14 |
| GOK 15 | 3.71 | 6.99 | -300 | / | 2.48 | FLK 15 |
| GOK 16 | 4.17 | 6.47 | -320 | / | 6.64 | FLK 16 |
| | | | -340 | / | 2.17 | FLK 17 |
| | | | -360 | 5.61 | 8.86 | FLK 18 |
| | | | -380 | / | 5.19 | FLK 19 |
| | | | -400 | 107 | 185 | FLK 20 |

*Table 24: Depth profile 2017 WIOC values*

| GOK 2017 | | | | FLK 2017 | | |
|---|---|---|---|---|---|---|
| **Sample name** | **not cor. WIOC (ng/g)** | **WIOC (ng/g)** | **Depth (cm)** | **not cor. WIOC (ng/g)** | **WIOC (ng/g)** | **Sample name** |
| GOK 1 | / | 495 | -20 | / | 476 | FLK 1 |
| GOK 2 | / | 556 | -40 | / | 555 | FLK 2 |
| GOK 3 | / | 327 | -60 | / | 253 | FLK 3 |
| GOK 4 | / | 165 | -80 | / | 252 | FLK 4 |
| GOK 5 | / | 144 | -100 | / | 329 | FLK 5 |
| GOK 6 | / | 507 | -120 | / | 254 | FLK 6 |
| GOK 7 | / | 265 | -140 | / | 39.8 | FLK 7 |
| GOK 8 | / | 214 | -160 | / | 321 | FLK 8 |
| GOK 9 | / | 248 | -180 | / | 295 | FLK 9 |
| GOK 10 | / | 177 | -200 | / | 402 | FLK 10 |
| GOK 11 | / | 132 | -220 | / | 774 | FLK 11 |
| GOK 12 | / | 230 | -240 | / | 650 | FLK 12 |
| GOK 13 | / | 146 | -260 | / | 709 | FLK 13 |
| GOK 14 | / | 248 | -280 | / | 563 | FLK 14 |

*Table 24 continued*

| GOK 2017 | | | | FLK 2017 | | |
|---|---|---|---|---|---|---|
| **Sample name** | **not cor. WIOC (ng/g)** | **WIOC (ng/g)** | **Depth (cm)** | **not cor. WIOC (ng/g)** | **WIOC (ng/g)** | **Sample name** |
| GOK 15 | 239 | 237 | -300 | / | 569 | FLK 15 |
| GOK 16 | 200 | 198 | -320 | / | 284 | FLK 16 |
| | | | -340 | / | 518 | FLK 17 |
| | | | -360 | 168 | 164 | FLK 18 |
| | | | -380 | / | 216 | FLK 19 |
| | | | -400 | 4183 | 4106 | FLK 20 |

*Table 25: Depth profile 2017 WITC values*

| GOK 2017 | | | FLK 2017 | |
|---|---|---|---|---|
| **Sample name** | **WITC (ng/g)** | **Depth (cm)** | **WITC (ng/g)** | **Sample name** |
| GOK 1 | 497 | -20 | 476 | FLK 1 |
| GOK 2 | 558 | -40 | 555 | FLK 2 |
| GOK 3 | 333 | -60 | 253 | FLK 3 |
| GOK 4 | 165 | -80 | 252 | FLK 4 |
| GOK 5 | 144 | -100 | 338 | FLK 5 |
| GOK 6 | 527 | -120 | 261 | FLK 6 |
| GOK 7 | 269 | -140 | 39.8 | FLK 7 |
| GOK 8 | 214 | -160 | 328 | FLK 8 |
| GOK 9 | 253 | -180 | 300 | FLK 9 |
| GOK 10 | 177 | -200 | 404 | FLK 10 |
| GOK 11 | 141 | -220 | 781 | FLK 11 |
| GOK 12 | 236 | -240 | 659 | FLK 12 |
| GOK 13 | 146 | -260 | 715 | FLK 13 |
| GOK 14 | 248 | -280 | 569 | FLK 14 |
| GOK 15 | 244 | -300 | 572 | FLK 15 |
| GOK 16 | 204 | -320 | 291 | FLK 16 |
| | | -340 | 521 | FLK 17 |
| | | -360 | 173 | FLK 18 |
| | | -380 | 221 | FLK 19 |
| | | -400 | 4290 | FLK 20 |

*Table 26: Depth profile 2018 EC values*

| GOK 2018 | | | |
|---|---|---|---|
| **Sample name** | **not cor. EC (ng/g)** | **EC (ng/g)** | **Depth (cm)** |
| GOK 1 | 12.7 | 24.3 | -20 |
| GOK 2 | / | 0.70 | -40 |
| GOK 3 | / | 10.8 | -60 |
| GOK 4 | / | 24.4 | -80 |
| GOK 5 | / | 10.9 | -100 |
| GOK 6 | / | 3.40 | -120 |
| GOK 7 | / | 7.64 | -140 |
| GOK 8 | / | 0.50 | -160 |
| GOK 9 | / | 0.01 | -180 |
| GOK 10 | / | 0.53 | -200 |
| GOK 11 | / | 2.90 | -220 |
| GOK 12 | / | 0.01 | -240 |
| GOK 13 | / | 0.01 | -260 |
| GOK 14 | / | 2.53 | -280 |
| GOK 15 | / | 4.71 | -300 |
| GOK 16 | / | 6.39 | -320 |
| GOK 17 | / | 0.00 | -340 |
| GOK 18 | / | 0.93 | -360 |
| GOK 19 | / | 1.55 | -380 |
| GOK 20 | 8.86 | 13.1 | -400 |
| GOK 21 | / | 2.31 | -420 |
| GOK 22 | / | 0.05 | -440 |

*Table 27: Depth profile 2018 WIOC values*

| GOK 2018 | | | |
|---|---|---|---|
| **Sample name** | **not cor. WIOC (ng/g)** | **WIOC (ng/g)** | **Depth (cm)** |
| GOK 1 | 1280 | 1268 | -20 |
| GOK 2 | / | 411 | -40 |
| GOK 3 | / | 266 | -60 |
| GOK 4 | / | 225 | -80 |
| GOK 5 | / | 250 | -100 |
| GOK 6 | / | 241 | -120 |
| GOK 7 | / | 138 | -140 |
| GOK 8 | / | 178 | -160 |
| GOK 9 | / | 399 | -180 |
| GOK 10 | / | 399 | -200 |
| GOK 11 | / | 425 | -220 |
| GOK 12 | / | 261 | -240 |
| GOK 13 | / | 493 | -260 |
| GOK 14 | / | 416 | -280 |
| GOK 15 | / | 318 | -300 |
| GOK 16 | / | 265 | -320 |
| GOK 17 | / | 159 | -340 |
| GOK 18 | / | 327 | -360 |
| GOK 19 | / | 371 | -380 |
| GOK 20 | 459 | 454 | -400 |
| GOK 21 | / | 274 | -420 |
| GOK 22 | / | 334 | -440 |

*Table 28: Depth profile 2018 WITC values*

| GOK 2018 | | |
|---|---|---|
| **Sample name** | **WITC (ng/g)** | **Depth (cm)** |
| GOK 1 | 1293 | -20 |
| GOK 2 | 411 | -40 |
| GOK 3 | 277 | -60 |
| GOK 4 | 250 | -80 |
| GOK 5 | 260 | -100 |
| GOK 6 | 245 | -120 |
| GOK 7 | 146 | -140 |
| GOK 8 | 178 | -160 |
| GOK 9 | 399 | -180 |
| GOK 10 | 399 | -200 |
| GOK 11 | 428 | -220 |
| GOK 12 | 261 | -240 |
| GOK 13 | 493 | -260 |
| GOK 14 | 419 | -280 |
| GOK 15 | 323 | -300 |
| GOK 16 | 271 | -320 |
| GOK 17 | 159 | -340 |
| GOK 18 | 328 | -360 |
| GOK 19 | 373 | -380 |
| GOK 20 | 468 | -400 |
| GOK 21 | 276 | -420 |
| GOK 22 | 334 | -440 |

*Table 29: Depth profile 2019 EC values*

| GOK 2019 | | | |
|---|---|---|---|
| **Sample name** | **not cor. EC (ng/g)** | **EC (ng/g)** | **Depth (cm)** |
| (2019) GOK1 | 35.0 | 46.0 | -20 |
| (2019) GOK2 | / | 11.9 | -40 |
| (2019) GOK3 | / | 8.41 | -60 |
| (2019) GOK4 | / | 4.39 | -80 |
| (2019) GOK5 | / | 10.3 | -100 |
| (2019) GOK6 | / | 54.3 | -120 |
| (2019) GOK7 | 24.9 | 34.2 | -140 |
| (2019) GOK8 | 9.02 | 11.5 | -160 |
| (2019) GOK9 | / | 2.20 | -180 |
| (2019) GOK10 | / | 4.15 | -200 |
| (2019) GOK11 | / | 4.62 | -220 |
| (2019) GOK12 | / | 4.59 | -240 |
| (2019) GOK13 | / | 3.94 | -260 |
| (2019) GOK14 | / | 0.15 | -280 |
| (2019) GOK15 | / | 0.16 | -300 |
| (2019) GOK16 | / | 1.44 | -320 |

*Table 30: Depth profile 2019 WIOC values*

| GOK 2019 | | | |
|---|---|---|---|
| **Sample name** | **not cor. WIOC (ng/g)** | **WIOC (ng/g)** | **Depth (cm)** |
| (2019) GOK1 | 927 | 881 | -20 |
| (2019) GOK2 | / | 375 | -40 |
| (2019) GOK3 | / | 534 | -60 |
| (2019) GOK4 | / | 297 | -80 |
| (2019) GOK5 | / | 790 | -100 |
| (2019) GOK6 | / | 858 | -120 |
| (2019) GOK7 | 2398 | 2364 | -140 |
| (2019) GOK8 | 944 | 933 | -160 |
| (2019) GOK9 | / | 1631 | -180 |
| (2019) GOK10 | / | 1787 | -200 |
| (2019) GOK11 | / | 532 | -220 |
| (2019) GOK12 | / | 1130 | -240 |
| (2019) GOK13 | / | 993 | -260 |
| (2019) GOK14 | / | 1047 | -280 |
| (2019) GOK15 | / | 433 | -300 |
| (2019) GOK16 | / | 1076 | -320 |

*Table 31: Depth profile 2019 WITC values*

| GOK 2019 | | |
|---|---|---|
| **Sample name** | **WITC (ng/g)** | **Depth (cm)** |
| (2019) GOK1 | 927 | -20 |
| (2019) GOK2 | 387 | -40 |
| (2019) GOK3 | 543 | -60 |
| (2019) GOK4 | 302 | -80 |
| (2019) GOK5 | 800 | -100 |
| (2019) GOK6 | 912 | -120 |
| (2019) GOK7 | 2398 | -140 |
| (2019) GOK8 | 944 | -160 |
| (2019) GOK9 | 1633 | -180 |
| (2019) GOK10 | 1791 | -200 |
| (2019) GOK11 | 537 | -220 |
| (2019) GOK12 | 1134 | -240 |
| (2019) GOK13 | 997 | -260 |
| (2019) GOK14 | 1047 | -280 |
| (2019) GOK15 | 433 | -300 |
| (2019) GOK16 | 1078 | -320 |

*Table 32: Depth profile 2020 EC values*

| GOK 2020 | | | |
|---|---|---|---|
| **Sample name** | **not cor. EC (ng/g)** | **EC (ng/g)** | **Depth (cm)** |
| GOK1 | / | 26.3 | -20 |
| GOK2 | / | 3.64 | -40 |
| GOK3 | / | 0.22 | -60 |
| GOK5 | / | 16.0 | -100 |
| GOK6 | / | 9.52 | -120 |
| GOK7 | / | 8.47 | -140 |
| GOK8 | / | 10.8 | -160 |
| GOK9 | 7.95 | 12.4 | -180 |
| GOK10 | / | 5.61 | -200 |
| GOK11 | / | 4.53 | -220 |
| GOK12 | / | 3.48 | -240 |
| GOK13 | / | 0.66 | -260 |
| GOK14 | / | 1.32 | -280 |
| GOK15 | / | 1.51 | -300 |
| GOK16 | / | 1.11 | -320 |
| GOK17+18 | / | 2.70 | -360 |
| GOK19+20 | / | 1.94 | -400 |

*Table 33: Depth profile 2020 WIOC values*

| GOK 2020 | | | |
|---|---|---|---|
| **Sample name** | **not cor. WIOC (ng/g)** | **WIOC (ng/g)** | **Depth (cm)** |
| GOK1 | / | 1789 | -20 |
| GOK2 | / | 1034 | -40 |
| GOK3 | / | 1553 | -60 |
| GOK5 | / | 220 | -100 |
| GOK6 | / | 385 | -120 |
| GOK7 | / | 520 | -140 |
| GOK8 | / | 731 | -160 |
| GOK9 | 476 | 472 | -180 |
| GOK10 | / | 370 | -200 |
| GOK11 | / | 551 | -220 |
| GOK12 | / | 274 | -240 |
| GOK13 | / | 252 | -260 |
| GOK14 | / | 235 | -280 |
| GOK15 | / | 193 | -300 |
| GOK16 | / | 352 | -320 |
| GOK17+18 | / | 298 | -360 |
| GOK19+20 | / | 255 | -400 |

*Table 34: Depth profile 2020 WITC values*

| GOK 2020 | | |
|---|---|---|
| **Sample name** | **WITC (ng/g)** | **Depth (cm)** |
| GOK1 | 1815 | -20 |
| GOK2 | 1038 | -40 |
| GOK3 | 1553 | -60 |
| GOK5 | 236 | -100 |
| GOK6 | 395 | -120 |
| GOK7 | 528 | -140 |
| GOK8 | 742 | -160 |
| GOK9 | 484 | -180 |
| GOK10 | 375 | -200 |
| GOK11 | 555 | -220 |
| GOK12 | 278 | -240 |
| GOK13 | 252 | -260 |
| GOK14 | 236 | -280 |
| GOK15 | 195 | -300 |
| GOK16 | 353 | -320 |
| GOK17+18 | 301 | -360 |
| GOK19+20 | 257 | -400 |

*Table 35: Depth profile 2021 EC values*

| GOK 2021 | | | | FLK 2021 | | | |
|---|---|---|---|---|---|---|---|
| **Sample name** | **not cor. EC (ng/g)** | **EC (ng/g)** | **Depth (cm)** | **not cor. EC (ng/g)** | **EC (ng/g)** | **Sample name** | **Depth (cm)** |
| GOK 1 | / | 32.5 | -20 | / | 11.3 | FLK 2 | -40 |
| GOK 2 | / | 13.9 | -40 | / | 5.99 | FLK 3 | -60 |
| GOK 3 + 4 | / | 7.55 | -80 | / | 7.86 | FLK 4 | -80 |
| GOK 5 | 11.6 | 21.6 | -100 | / | 6.68 | FLK 5 | -100 |
| GOK 6 + 7 | / | 5.16 | -140 | / | 0.01 | FLK 6 | -120 |
| GOK 8 | / | 0.02 | -160 | / | 0.02 | FLK 7 | -140 |
| GOK 9 | 7.78 | 15.0 | -180 | / | 9.01 | FLK 8 | -160 |
| GOK 10 | 0.01 | 2.38 | -200 | / | 0.01 | FLK 9 | -180 |
| GOK 11 | / | 0.01 | -220 | / | 2.07 | FLK 10 | -220 |
| GOK 12 + 13 | / | 2.51 | -260 | / | 1.15 | FLK 11+12 | -240 |
| GOK 14 | / | 1.42 | -280 | / | 0.52 | FLK 13 | -260 |
| GOK 15 | / | 0.02 | -300 | / | 0.01 | FLK 14 | -280 |
| GOK 16 | / | 0.02 | -320 | / | 2.69 | FLK 15 | -300 |
| GOK 17 | / | 1.87 | -340 | / | 2.66 | FLK 16 | -320 |
| GOK 18 | / | 2.15 | -360 | / | 6.74 | FLK 17 | -340 |
| GOK 19 | / | 2.71 | -380 | / | 6.89 | FLK 18 | -360 |
| GOK 20 | / | 1.50 | -400 | / | 11.9 | FLK 19 | -380 |
| GOK 21 | / | 2.91 | -420 | / | 7.00 | FLK 20 | -400 |
| GOK 22 | / | 5.47 | -440 | / | 33.6 | FLK 21 | -420 |
| GOK 23 + 24 | / | 7.60 | -480 | 10.4 | 22.7 | FLK 22 | -440 |
| GOK 25 | 177 | 427 | -500 | | | | |

*Table 36: Depth profile 2021 WIOC values*

| GOK 2021 | | | | FLK 2021 | | | |
|---|---|---|---|---|---|---|---|
| **Sample name** | **not cor. WIOC (ng/g)** | **WIOC (ng/g)** | **Depth (cm)** | **not cor. WIOC (ng/g)** | **WIOC (ng/g)** | **Sample name** | **Depth (cm)** |
| GOK 1 | / | 3311 | -20 | / | 872 | FLK 2 | -40 |
| GOK 2 | / | 734 | -40 | / | 534 | FLK 3 | -60 |
| GOK 3+4 | / | 463 | -80 | / | 678 | FLK 4 | -80 |
| GOK 5 | 583 | 573 | -100 | / | 938 | FLK 5 | -100 |
| GOK 6+7 | / | 494 | -140 | / | 460 | FLK 6 | -120 |
| GOK 8 | / | 350 | -160 | / | 448 | FLK 7 | -140 |
| GOK 9 | 671 | 664 | -180 | / | 665 | FLK 8 | -160 |
| GOK 10 | 301 | 299 | -200 | / | 309 | FLK 9 | -180 |
| GOK 11 | / | 529 | -220 | / | 376 | FLK 10 | -220 |
| GOK 12+13 | / | 355 | -260 | / | 402 | FLK 11+12 | -240 |
| GOK 14 | / | 475 | -280 | / | 407 | FLK 13 | -260 |
| GOK 15 | / | 710 | -300 | / | 349 | FLK 14 | -280 |
| GOK 16 | / | 465 | -320 | / | 357 | FLK 15 | -300 |
| GOK 17 | / | 888 | -340 | / | 359 | FLK 16 | -320 |
| GOK 18 | / | 781 | -360 | / | 1021 | FLK 17 | -340 |
| GOK 19 | / | 567 | -380 | / | 1201 | FLK 18 | -360 |
| GOK 20 | / | 719 | -400 | / | 1629 | FLK 19 | -380 |
| GOK 21 | / | 698 | -420 | / | 1162 | FLK 20 | -400 |
| GOK 22 | / | 415 | -440 | / | 1575 | FLK 21 | -420 |
| GOK 23+24 | / | 453 | -480 | 1682 | 1671 | FLK 22 | -440 |
| GOK 25 | 1889 | 1662 | -500 | | | | |

*Table 37: Depth profile 2021 WITC values*

| GOK 2021 | | | FLK 2021 | | |
|---|---|---|---|---|---|
| **Sample name** | **WITC (ng/g)** | **Depth (cm)** | **WITC (ng/g)** | **Sample name** | **Depth (cm)** |
| GOK 1 | 3343 | -20 | 884 | FLK 2 | -40 |
| GOK 2 | 747 | -40 | 540 | FLK 3 | -60 |
| GOK 3 + 4 | 470 | -80 | 686 | FLK 4 | -80 |
| GOK 5 | 594 | -100 | 944 | FLK 5 | -100 |
| GOK 6 + 7 | 499 | -140 | 460 | FLK 6 | -120 |
| GOK 8 | 350 | -160 | 448 | FLK 7 | -140 |
| GOK 9 | 679 | -180 | 674 | FLK 8 | -160 |
| GOK 10 | 301 | -200 | 309 | FLK 9 | -180 |
| GOK 11 | 529 | -220 | 378 | FLK 10 | -220 |
| GOK 12+13 | 357 | -260 | 403 | FLK 11+12 | -240 |
| GOK 14 | 476 | -280 | 407 | FLK 13 | -260 |
| GOK 15 | 710 | -300 | 349 | FLK 14 | -280 |
| GOK 16 | 465 | -320 | 360 | FLK 15 | -300 |
| GOK 17 | 890 | -340 | 362 | FLK 16 | -320 |
| GOK 18 | 783 | -360 | 1027 | FLK 17 | -340 |
| GOK 19 | 570 | -380 | 1208 | FLK 18 | -360 |
| GOK 20 | 720 | -400 | 1640 | FLK 19 | -380 |
| GOK 21 | 701 | -420 | 1169 | FLK 20 | -400 |
| GOK 22 | 421 | -440 | 1609 | FLK 21 | -420 |
| GOK 23+24 | 460 | -480 | 1692 | FLK 22 | -440 |
| GOK 25 | 2067 | -500 | | | |

*Table 38: Depth profile 2022 EC values*

| GOK 2022 | | | | FLK 2022 | | | |
|---|---|---|---|---|---|---|---|
| **Sample name** | **not cor. EC (ng/g)** | **EC (ng/g)** | **Depth (cm)** | **not cor. EC (ng/g)** | **EC (ng/g)** | **Sample name** | **Depth (cm)** |
| GOK 1 | / | 0.02 | -20 | 7.55 | 16.6 | FLK 1 + 2 | -40 |
| GOK 2 | / | 7.15 | -40 | / | 14.1 | FLK 3 | -60 |
| GOK 3 | / | 10.6 | -60 | / | 6.40 | FLK 4 | -80 |
| GOK 4 | / | 0.02 | -80 | 3.55 | 32.5 | FLK 5 | -100 |
| GOK 5 | / | 6.59 | -100 | / | 0.04 | FLK 6 | -120 |
| GOK 6 | 7.59 | 25.6 | -120 | / | 0.03 | FLK 7 | -140 |
| GOK 7 | / | 0.01 | -140 | / | 0.01 | FLK 8 | -160 |
| GOK 8 | / | 0.01 | -160 | / | 2.25 | FLK 10 | -200 |
| GOK 9+10 | / | 1.47 | -200 | / | 2.98 | FLK 11 | -220 |
| GOK 11+12 | / | 1.89 | -240 | / | 0.67 | FLK 12 | -240 |
| GOK 13 | / | 0.02 | -260 | 0.53 | 4.54 | FLK 13 | -260 |
| GOK 14 | / | 10.5 | -280 | / | 4.70 | FLK 14 | -280 |
| GOK 15 | / | 5.81 | -300 | / | 0.02 | FLK 15 | -300 |
| GOK 16 | / | 3.60 | -320 | 37.4 | 88.3 | FLK 16 | -320 |
| GOK 17 | / | 6.35 | -340 | | | | |
| GOK 18 | 15.3 | 54.7 | -360 | | | | |

*Table 39: Depth profile 2022 WIOC values*

| GOK 2022 | | | | FLK 2022 | | | |
|---|---|---|---|---|---|---|---|
| **Sample name** | **not cor. WIOC (ng/g)** | **WIOC (ng/g)** | **Depth (cm)** | **not cor. WIOC (ng/g)** | **WIOC (ng/g)** | **Sample name** | **Depth (cm)** |
| GOK 1 | / | 625 | -20 | 452.44 | 443 | FLK 1 + 2 | -40 |
| GOK 2 | / | 661 | -40 | / | 606 | FLK 3 | -60 |
| GOK 3 | / | 786 | -60 | / | 500 | FLK 4 | -80 |
| GOK 4 | / | 217 | -80 | 547.50 | 529 | FLK 5 | -100 |
| GOK 5 | / | 507 | -100 | / | 280 | FLK 6 | -120 |
| GOK 6 | 448 | 430 | -120 | / | 208 | FLK 7 | -140 |
| GOK 7 | / | 252 | -140 | / | 202 | FLK 8 | -160 |
| GOK 8 | / | 239 | -160 | / | 287 | FLK 10 | -200 |
| GOK 9+10 | / | 457 | -200 | / | 413 | FLK 11 | -220 |
| GOK 11+12 | / | 376 | -240 | / | 298 | FLK 12 | -240 |
| GOK 13 | / | 283 | -260 | 329 | 325 | FLK 13 | -260 |
| GOK 14 | / | 602 | -280 | / | 384 | FLK 14 | -280 |
| GOK 15 | / | 457 | -300 | / | 317 | FLK 15 | -300 |
| GOK 16 | / | 238 | -320 | 1535 | 1484 | FLK 16 | -320 |
| GOK 17 | / | 276 | -340 | | | | |
| GOK 18 | 826 | 787 | -360 | | | | |

*Table 40: Depth profile 2022 WITC values*

| GOK 2022 | | | FLK 2022 | | |
|---|---|---|---|---|---|
| **Sample name** | **WITC (ng/g)** | **Depth (cm)** | **WITC (ng/g)** | **Sample name** | **Depth (cm)** |
| GOK 1 | 625 | -20 | 460 | FLK 1 + 2 | -40 |
| GOK 2 | 668 | -40 | 620 | FLK 3 | -60 |
| GOK 3 | 797 | -60 | 507 | FLK 4 | -80 |
| GOK 4 | 217 | -80 | 551 | FLK 5 | -100 |
| GOK 5 | 513 | -100 | 280 | FLK 6 | -120 |
| GOK 6 | 456 | -120 | 208 | FLK 7 | -140 |
| GOK 7 | 252 | -140 | 202 | FLK 8 | -160 |
| GOK 8 | 239 | -160 | 290 | FLK 10 | -200 |
| GOK 9+10 | 458 | -200 | 416 | FLK 11 | -220 |
| GOK 11+12 | 378 | -240 | 298 | FLK 12 | -240 |
| GOK 13 | 283 | -260 | 330 | FLK 13 | -260 |
| GOK 14 | 613 | -280 | 389 | FLK 14 | -280 |
| GOK 15 | 463 | -300 | 317 | FLK 15 | -300 |
| GOK 16 | 242 | -320 | 1572 | FLK 16 | -320 |
| GOK 17 | 282 | -340 | | | |
| GOK 18 | 841 | -360 | | | |

## 5.2 Used ammonium and calcium values

*Table 41: Used 20 cm 2017 profile ammonium and calcium values*

| 2017 20 cm | | | |
|---|---|---|---|
| **Sample name** | **$NH_4^+$ (µg/ml)** | **$Ca^{2+}$ (µg/ml)** | **Depth (cm)** |
| FLK 1 | 0.11 | 0.08 | -20 |
| FLK 2 | 0.12 | 0.08 | -40 |
| FLK 3 | 0.08 | 0.06 | -60 |
| FLK 4 | 0.07 | 0.05 | -80 |
| FLK 5 | 0.12 | 0.07 | -100 |
| FLK 6 | 0.15 | 0.06 | -120 |
| FLK 7 | 0.20 | 0.06 | -140 |
| FLK 8 | 0.28 | 0.10 | -160 |
| FLK 9 | 0.19 | 0.10 | -180 |
| FLK 10 | 0.08 | 0.07 | -200 |
| FLK 11 | 0.12 | 0.16 | -220 |
| FLK 12 | 0.08 | 0.07 | -240 |
| FLK 13 | 0.06 | 0.09 | -260 |
| FLK 14 | 0.05 | 0.05 | -280 |
| FLK 15 | 0.06 | 0.09 | -300 |
| FLK 16 | 0.09 | 0.06 | -320 |
| FLK 17 | 0.08 | 0.09 | -340 |
| FLK 18 | 0.12 | 0.10 | -360 |
| FLK 19 | 0.08 | 0.07 | -380 |
| FLK 20 | 0.11 | 0.05 | -400 |
| **Sample name** | **$NH_4^+$ (µg/ml)** | **$Ca^{2+}$ (µg/ml)** | **Depth (cm)** |
| GOK 1 | 0.14 | 0.11 | -20 |
| GOK 2 | 0.07 | 0.07 | -40 |
| GOK 3 | 0.21 | 0.08 | -60 |
| GOK 4 | 0.17 | 0.05 | -80 |
| GOK 5 | 0.18 | 0.05 | -100 |
| GOK 6 | 0.77 | 0.15 | -120 |
| GOK 7 | 0.12 | 0.06 | -140 |
| GOK 8 | 0.06 | 0.06 | -160 |
| GOK 9 | 0.11 | 0.09 | -180 |
| GOK 10 | 0.06 | 0.07 | -200 |
| GOK 11 | 0.07 | 0.08 | -220 |
| GOK 12 | 0.06 | 0.07 | -240 |
| GOK 13 | 0.05 | 0.06 | -260 |
| GOK 14 | 0.07 | 0.05 | -280 |
| GOK 15 | 0.11 | 0.14 | -300 |
| GOK 16 | 0.11 | 0.09 | -320 |

*Table 42: Used 10 cm 2017 profile ammonium and calcium values*

| 2017 FLK 10 cm | | | | 2017 GOK 10 cm | | |
|---|---|---|---|---|---|---|
| **Sample name** | **$NH_4^+$ (µg/ml)** | **$Ca^{2+}$ (µg/ml)** | **Depth (cm)** | **Sample name** | **$NH_4^+$ (µg/ml)** | **$Ca^{2+}$ (µg/ml)** |
| FLK 1 | 0.10 | 0.13 | -10 | GOK 1 | 0.16 | 0.13 |
| FLK 2 | 0.09 | 0.12 | -20 | GOK 2 | 0.12 | 0.10 |
| FLK 3 | 0.13 | 0.11 | -30 | GOK 3 | 0.06 | 0.09 |
| FLK 4 | 0.11 | 0.11 | -40 | GOK 4 | 0.06 | 0.16 |
| FLK 5 | 0.07 | 0.15 | -50 | GOK 5 | 0.25 | 0.15 |
| FLK 6 | 0.05 | 0.08 | -60 | GOK 6 | 0.17 | 0.16 |
| FLK 7 | 0.05 | 0.07 | -70 | GOK 7 | 0.11 | 0.09 |
| FLK 8 | 0.07 | 0.10 | -80 | GOK 8 | 0.20 | 0.09 |
| FLK 9 | 0.12 | 0.08 | -90 | GOK 9 | 0.23 | 0.09 |
| FLK 10 | 0.20 | 0.14 | -100 | GOK 10 | 0.15 | 0.09 |
| FLK 11 | 0.14 | 0.10 | -110 | GOK 11 | 0.55 | 0.19 |
| FLK 12 | 0.13 | 0.08 | -120 | GOK 12 | 0.75 | 0.18 |
| FLK 13 | 0.24 | 0.10 | -130 | GOK 13 | 0.38 | 0.17 |
| FLK 14 | 0.18 | 0.08 | -140 | GOK 14 | 0.08 | 0.13 |
| FLK 15 | 0.36 | 0.18 | -150 | GOK 15 | 0.05 | 0.11 |
| FLK 16 | 0.15 | 0.13 | -160 | GOK 16 | 0.07 | 0.12 |
| FLK 17 | 0.12 | 0.12 | -170 | GOK 17 | 0.11 | 0.15 |
| FLK 18 | 0.09 | 0.12 | -180 | GOK 18 | 0.11 | 0.10 |
| FLK 19 | 0.05 | 0.08 | -190 | GOK 19 | 0.07 | 0.12 |
| FLK 20 | 0.08 | 0.10 | -200 | GOK 20 | 0.05 | 0.08 |
| FLK 21 | 0.10 | 0.18 | -210 | GOK 21 | 0.07 | 0.07 |
| FLK 22 | 0.11 | 0.09 | -220 | GOK 22 | 0.08 | 0.09 |
| FLK 23 | 0.07 | 0.11 | -230 | GOK 23 | 0.05 | 0.06 |
| FLK 24 | 0.06 | 0.11 | -240 | GOK 24 | 0.05 | 0.09 |
| FLK 25 | 0.04 | 0.08 | -250 | GOK 25 | 0.06 | 0.18 |
| FLK 26 | 0.05 | 0.11 | -260 | GOK 26 | 0.04 | 0.08 |
| FLK 27 | 0.05 | 0.08 | -270 | GOK 27 | 0.05 | 0.09 |
| FLK 28 | 0.05 | 0.09 | -280 | GOK 28 | 0.09 | 0.29 |
| FLK 29 | 0.05 | 0.09 | -290 | GOK 29 | 0.09 | 0.09 |
| FLK 30 | 0.07 | 0.13 | -300 | GOK 30 | 0.16 | 0.29 |
| FLK 31 | 0.07 | 0.19 | -310 | GOK 31 | 0.09 | 0.14 |
| FLK 32 | 0.08 | 0.12 | -320 | | | |
| FLK 33 | 0.06 | 0.13 | -330 | | | |
| FLK 34 | 0.08 | 0.16 | -340 | | | |
| FLK 35 | 0.09 | 0.17 | -350 | | | |
| FLK 36 | 0.14 | 0.07 | -360 | | | |
| FLK 37 | 0.08 | 0.09 | -370 | | | |
| FLK 38 | / | / | -380 | | | |
| FLK 39 | 0.11 | 0.09 | -390 | | | |

*Table 43: Used 2018 GOK ammonium and calcium values*

| 2018 GOK 20 cm | | | | 2018 GOK 10 cm | | | |
|---|---|---|---|---|---|---|---|
| **Sample** | **$NH_4^+$ (µg/ml)** | **$Ca^{2+}$ (µg/ml)** | **Depth (cm)** | **Sample** | **$NH_4^+$ (µg/ml)** | **$Ca^{2+}$ (µg/ml)** | **Depth (cm)** |
| GOK 1 | 0.18 | 0.17 | -20 | GOK 1 | 0.12 | 0.16 | -10 |
| GOK 2 | 0.15 | 0.06 | -40 | GOK 2 | 0.18 | 0.20 | -20 |
| GOK 3 | 0.33 | 0.04 | -60 | GOK 3 | 0.16 | 0.10 | -30 |
| GOK 4 | 0.51 | 0.09 | -80 | GOK 4 | 0.13 | 0.09 | -40 |
| GOK 5 | 0.14 | 0.10 | -100 | GOK 5 | 0.08 | 0.07 | -50 |
| GOK 6 | 0.10 | 0.05 | -120 | GOK 6 | 0.48 | 0.09 | -60 |
| GOK 7 | 0.08 | 0.05 | -140 | GOK 7 | 0.56 | 0.11 | -70 |
| GOK 8 | 0.06 | 0.05 | -160 | GOK 8 | 0.36 | 0.11 | -80 |
| GOK 9 | 0.04 | 0.07 | -180 | GOK 9 | 0.22 | 0.12 | -90 |
| GOK 10 | 0.01 | 0.04 | -200 | GOK 10 | 0.07 | 0.05 | -100 |
| GOK 11 | 0.04 | 0.06 | -220 | GOK 11 | 0.13 | 0.07 | -110 |
| GOK 12 | 0.02 | 0.10 | -240 | GOK 12 | 0.07 | 0.10 | -120 |
| GOK 13 | 0.02 | 0.10 | -260 | GOK 13 | 0.07 | 0.07 | -130 |
| GOK 14 | 0.02 | 0.03 | -280 | GOK 14 | 0.07 | 0.06 | -140 |
| GOK 15 | 0.04 | 0.09 | -300 | GOK 15 | 0.02 | 0.03 | -150 |
| GOK 16 | 0.06 | 0.05 | -320 | GOK 16 | 0.12 | 0.08 | -160 |
| GOK 17 | 0.07 | 0.05 | -340 | GOK 17 | 0.04 | 0.06 | -170 |
| GOK 18 | 0.02 | 0.06 | -360 | GOK 18 | 0.03 | 0.06 | -180 |
| GOK 19 | 0.10 | 0.09 | -380 | GOK 19 | 0.03 | 0.05 | -190 |
| GOK 20 | 0.08 | 0.09 | -400 | GOK 20 | 0.02 | 0.03 | -200 |
| GOK 21 | 0.11 | 0.07 | -420 | GOK 21 | 0.04 | 0.05 | -210 |
| GOK 22 | 0.13 | 0.09 | -440 | GOK 22 | 0.04 | 0.10 | -220 |
| | | | | GOK 23 | 0.04 | 0.17 | -230 |
| | | | | GOK 24 | 0.03 | 0.11 | -240 |
| | | | | GOK 25 | 0.03 | 0.09 | -250 |
| | | | | GOK 26 | 0.03 | 0.07 | -260 |
| | | | | GOK 27 | 0.03 | 0.06 | -270 |
| | | | | GOK 28 | 0.02 | 0.03 | -280 |
| | | | | GOK 29 | 0.04 | 0.07 | -290 |
| | | | | GOK 30 | 0.05 | 0.08 | -300 |
| | | | | GOK 31 | 0.07 | 0.07 | -310 |
| | | | | GOK 32 | 0.07 | 0.08 | -320 |
| | | | | GOK 33 | 0.06 | 0.09 | -330 |
| | | | | GOK 34 | 0.03 | 0.07 | -340 |
| | | | | GOK 35 | 0.03 | 0.07 | -350 |
| | | | | GOK 36 | 0.02 | 0.09 | -360 |
| | | | | GOK 37 | 0.02 | 0.08 | -370 |
| | | | | GOK 38 | 0.07 | 0.19 | -380 |
| | | | | GOK 39 | 0.08 | 0.10 | -390 |
| | | | | GOK 40 | 0.10 | 0.11 | -400 |
| | | | | GOK 41 | 0.09 | 0.08 | -410 |
| | | | | GOK 42 | 0.07 | 0.06 | -420 |
| | | | | GOK 43 | 0.11 | 0.08 | -430 |

*Table 44: Used 2019 GOK ammonium and calcium values*

| 2019 GOK 20 cm | | | | 2019 GOK 10 cm | | | |
|---|---|---|---|---|---|---|---|
| **Sample name** | **$NH_4^+$ (µg/ml)** | **$Ca^{2+}$ (µg/ml)** | **Depth (cm)** | **Sample name** | **$NH_4^+$ (µg/ml)** | **$Ca^{2+}$ (µg/ml)** | **Depth (cm)** |
| GOK 1 | 0.29 | 0.13 | -20 | GOK 1 | 0.28 | 0.37 | -10 |
| GOK 2 | 0.22 | 0.05 | -40 | GOK 2 | 0.26 | 0.03 | -20 |
| GOK 3 | 0.36 | 0.09 | -60 | GOK 3 | 0.32 | 0.02 | -30 |
| GOK 4 | 0.18 | 0.05 | -80 | GOK 4 | 0.19 | 0.24 | -40 |
| GOK 5 | 0.22 | 0.08 | -100 | GOK 5 | 0.31 | 0.05 | -50 |
| GOK 6 | 0.56 | 0.09 | -120 | GOK 6 | 0.34 | 0.07 | -60 |
| GOK 7 | 0.44 | 0.13 | -140 | GOK 7 | 0.14 | 0.06 | -70 |
| GOK 8 | 0.24 | 0.12 | -160 | GOK 8 | 0.18 | 0.03 | -80 |
| GOK 9 | 0.02 | 0.06 | -180 | GOK 9 | 0.11 | 0.04 | -90 |
| GOK 10 | 0.03 | 0.09 | -200 | GOK 10 | 0.36 | 0.16 | -100 |
| GOK 11 | 0.04 | 0.05 | -220 | GOK 11 | 0.57 | 0.24 | -110 |
| GOK 12 | 0.06 | 0.10 | -240 | GOK 12 | 0.46 | 0.136 | -120 |
| GOK 13 | 0.05 | 0.08 | -260 | GOK 13 | 0.66 | 0.32 | -130 |
| GOK 14 | 0.04 | 0.28 | -280 | GOK 14 | 0.25 | 0.11 | -140 |
| GOK 15 | 0.05 | 1.03 | -300 | GOK 15 | 0.50 | 0.24 | -150 |
| GOK 16 | 0.06 | 0.21 | -320 | GOK 16 | 0.04 | 0.29 | -160 |
| | | | | GOK 17 | <LOD | 0.05 | -170 |
| | | | | GOK 18 | <LOD | 0.04 | -180 |
| | | | | GOK 19 | <LOD | 0.03 | -190 |
| | | | | GOK 20 | <LOD | 0.05 | -200 |
| | | | | GOK 21 | <LOD | 0.06 | -210 |
| | | | | GOK 22 | 0.01 | 0.09 | -220 |
| | | | | GOK 23 | 0.04 | 0.07 | -230 |
| | | | | GOK 24 | <LOD | 0.05 | -240 |
| | | | | GOK 25 | <LOD | 0.04 | -250 |
| | | | | GOK 26 | 0.03 | 0.05 | -260 |
| | | | | GOK 27 | <LOD | <LOD | -270 |
| | | | | GOK 28 | 0.04 | 0.43 | -280 |
| | | | | GOK 29 | 0.02 | 2.10 | -290 |
| | | | | GOK 30 | 0.01 | 1.41 | -300 |
| | | | | GOK 31 | 0.04 | 0.50 | -310 |
| | | | | GOK 32 | <LOD | 0.02 | -320 |

*Table 45: Used 2020 GOK ammonium and calcium values*

| 2020 GOK 20 cm | | | | 2020 GOK 10 cm | | | |
|---|---|---|---|---|---|---|---|
| **Sample name** | **$NH_4^+$ (µg/ml)** | **$Ca^{2+}$ (µg/ml)** | **Depth (cm)** | **Sample name** | **$NH_4^+$ (µg/ml)** | **$Ca^{2+}$ (µg/ml)** | **Depth (cm)** |
| GOK 1 | 0.31 | 0.14 | -20 | GOK 1 | 0.13 | 0.09 | -10 |
| GOK 2 | 0.17 | 0.09 | -40 | GOK 2 | 0.39 | 0.27 | -20 |
| GOK 3 | 0.07 | 0.05 | -60 | GOK 3 | 0.25 | 0.11 | -30 |
| GOK 4 | / | / | -80 | GOK 4 | 0.07 | 0.05 | -40 |
| GOK 5 | 0.07 | 0.04 | -100 | GOK 5 | 0.06 | 0.01 | -50 |
| GOK 6 | 0.06 | 0.03 | -120 | GOK 6 | 0.09 | 0.01 | -60 |
| GOK 7 | 0.06 | 0.04 | -140 | GOK 7 | 0.22 | 0.13 | -70 |
| GOK 8 | 0.06 | 0.05 | -160 | GOK 8 | 0.12 | 0.05 | -80 |
| GOK 9 | 0.04 | 0.04 | -180 | GOK 9 | 0.10 | 0.02 | -90 |
| GOK 10 | 0.03 | 0.03 | -200 | GOK 10 | 0.09 | 0.02 | -100 |
| GOK 11 | 0.05 | 0.05 | -220 | GOK 11 | 0.07 | 0.02 | -110 |
| GOK 12 | 0.04 | 0.06 | -240 | GOK 12 | 0.05 | 0.01 | -120 |
| GOK 13 | 0.04 | 0.07 | -260 | GOK 13 | 0.07 | 0.04 | -130 |
| GOK 14 | 0.04 | 0.06 | -280 | GOK 14 | 0.06 | 0.03 | -140 |
| GOK 15 | 0.03 | 0.04 | -300 | GOK 15 | 0.06 | 0.05 | -150 |
| GOK 16 | 0.05 | 0.07 | -320 | GOK 16 | 0.05 | 0.04 | -160 |
| GOK 17 | 0.02 | 0.05 | -340 | GOK 17 | 0.05 | 0.08 | -170 |
| GOK 18 | 0.03 | 0.05 | -360 | GOK 18 | 0.05 | 0.04 | -180 |
| GOK 19 | 0.04 | 0.06 | -380 | GOK 19 | 0.04 | 0.02 | -190 |
| | | | | GOK 20 | 0.04 | 0.02 | -200 |
| | | | | GOK 21 | 0.05 | 0.02 | -210 |
| | | | | GOK 22 | 0.04 | 0.04 | -220 |
| | | | | GOK 23 | 0.04 | 0.03 | -230 |
| | | | | GOK 24 | 0.04 | 0.02 | -240 |
| | | | | GOK 25 | 0.03 | 0.02 | -250 |
| | | | | GOK 26 | 0.07 | 0.02 | -260 |
| | | | | GOK 27 | 0.03 | 0.02 | -270 |
| | | | | GOK 28 | 0.03 | 0.02 | -280 |
| | | | | GOK 29 | 0.04 | 0.02 | -290 |
| | | | | GOK 30 | 0.03 | 0.02 | -300 |
| | | | | GOK 31 | 0.03 | 0.02 | -310 |
| | | | | GOK 32 | 0.03 | 0.02 | -320 |
| | | | | GOK 33 | 0.03 | 0.03 | -330 |
| | | | | GOK 34 | 0.03 | 0.03 | -340 |
| | | | | GOK 35 | 0.03 | 0.03 | -350 |
| | | | | GOK 36 | 0.03 | 0.03 | -360 |
| | | | | GOK 37 | 0.07 | 0.06 | -370 |
| | | | | GOK 38 | 0.05 | 0.07 | -380 |
| | | | | GOK 39 | 0.04 | 0.06 | -390 |

*Table 46: Used 2021 GOK 20 cm ammonium and calcium values*

| 2021 GOK 20 cm | | | | 2021 FLK 20 cm | | | |
|---|---|---|---|---|---|---|---|
| **Sample name** | **$NH_4^+$ (µg/ml)** | **$Ca^{2+}$ (µg/ml)** | **Depth (cm)** | **Sample name** | **$NH_4^+$ (µg/ml)** | **$Ca^{2+}$ (µg/ml)** | **Depth (cm)** |
| GOK 1 | 0.65 | 0.21 | -20 | FLK 2 | 0.46 | 0.06 | -40 |
| GOK 2 | 0.37 | 0.16 | -40 | FLK 3 | 0.26 | 0.13 | -60 |
| GOK 3 | 0.07 | 0.08 | -60 | FLK 4 | 0.46 | 0.11 | -80 |
| GOK 4 | 0.27 | 0.10 | -80 | FLK 5 | 0.17 | 0.07 | -100 |
| GOK 5 | 0.53 | 0.15 | -100 | FLK 6 | 0.14 | 0.05 | -120 |
| GOK 6 | 0.20 | 0.09 | -120 | FLK 7 | 0.20 | 0.06 | -140 |
| GOK 7 | 0.20 | 0.09 | -140 | FLK 8 | 0.46 | 0.18 | -160 |
| GOK 8 | 0.14 | 0.04 | -160 | FLK 9 | 0.04 | 0.13 | -180 |
| GOK 9 | 0.34 | 0.11 | -180 | FLK 10 | 0.01 | 0.12 | -200 |
| GOK 10 | 0.06 | 0.10 | -200 | FLK 11 | <LOD | 0.07 | -220 |
| GOK 11 | 0.04 | 0.13 | -220 | FLK 12 | <LOD | 0.14 | -240 |
| GOK 12 | 0.02 | 0.06 | -240 | FLK 13 | 0.02 | 0.08 | -260 |
| GOK 13 | 0.03 | 0.05 | -260 | FLK 14 | 0.01 | 0.07 | -280 |
| GOK 14 | 0.02 | 0.07 | -280 | FLK 15 | 0.01 | 0.11 | -300 |
| GOK 15 | 0.02 | 0.07 | -300 | FLK 16 | 0.03 | 0.16 | -320 |
| GOK 16 | 0.02 | 0.04 | -320 | FLK 17 | <LOD | 0.42 | -340 |
| GOK 17 | 0.04 | 0.05 | -340 | FLK 18 | <LOD | 0.45 | -360 |
| GOK 18 | 0.02 | 0.04 | -360 | FLK 19 | 0.05 | 0.41 | -380 |
| GOK 19 | 0.09 | 0.07 | -380 | FLK 20 | 0.06 | 0.44 | -400 |
| GOK 20 | 0.06 | 0.05 | -400 | FLK 21 | 0.05 | 0.40 | -420 |
| GOK 21 | 0.04 | 0.05 | -420 | FLK 22 | 0.08 | 0.23 | -440 |
| GOK 22 | 0.08 | 0.04 | -440 | | | | |
| GOK 23 | 0.10 | 0.03 | -460 | | | | |
| GOK 24 | 0.06 | 0.04 | -480 | | | | |
| GOK 25 | 0.09 | 0.04 | -500 | | | | |

*Table 47: Used 2021 10 cm ammonium and calcium values*

| 2021 GOK 10 cm | | | | 2021 FLK 10 cm | | |
|---|---|---|---|---|---|---|
| **Sample name** | **$NH_4^+$ (µg/ml)** | **$Ca^{2+}$ (µg/ml)** | **Depth (cm)** | **Sample name** | **$NH_4^+$ (µg/ml)** | **$Ca^{2+}$ (µg/ml)** |
| GOK 1 | 0.54 | 0.32 | -10 | FLK 1 | 0.65 | 0.14 |
| GOK 2 | 0.88 | 0.20 | -20 | FLK 2 | 0.62 | 0.08 |
| GOK 3 | 0.49 | 0.15 | -30 | FLK 3 | 1.08 | 0.15 |
| GOK 4 | 0.22 | 0.10 | -40 | FLK 4 | 0.23 | 0.08 |
| GOK 5 | 0.06 | 0.08 | -50 | FLK 5 | 0.24 | 0.11 |
| GOK 6 | 0.04 | 0.05 | -60 | FLK 6 | 0.22 | 0.15 |
| GOK 7 | 0.25 | 0.11 | -70 | FLK 7 | 0.69 | 0.23 |
| GOK 8 | 0.28 | 0.19 | -80 | FLK 8 | 0.49 | 0.19 |
| GOK 9 | 0.51 | 0.17 | -90 | FLK 9 | 0.13 | 0.08 |
| GOK 10 | 0.62 | 0.24 | -100 | FLK 10 | 0.22 | 0.11 |
| GOK 11 | 0.28 | 0.10 | -110 | FLK 11 | 0.15 | 0.06 |
| GOK 12 | 0.10 | 0.06 | -120 | FLK 12 | 0.11 | 0.09 |
| GOK 13 | 0.17 | 0.08 | -130 | FLK 13 | 0.07 | 0.07 |
| GOK 14 | 0.21 | 0.10 | -140 | FLK 14 | 0.20 | 0.13 |
| GOK 15 | 0.10 | 0.06 | -150 | FLK 15 | 0.59 | 0.63 |
| GOK 16 | 0.13 | 0.07 | -160 | FLK 16 | 0.26 | 0.25 |
| GOK 17 | 0.40 | 0.08 | -170 | FLK 17 | 0.05 | 0.40 |
| GOK 18 | 0.25 | 0.12 | -180 | FLK 18 | 0.04 | 0.51 |
| GOK 19 | 0.05 | 0.08 | -190 | FLK 19 | 0.01 | 1.02 |
| GOK 20 | 0.06 | 0.14 | -200 | FLK 20 | 0.02 | 0.53 |
| GOK 21 | 0.05 | 0.33 | -210 | FLK 21 | 0.02 | 0.19 |
| GOK 22 | 0.01 | 0.02 | -220 | FLK 22 | 0.01 | 0.32 |
| GOK 23 | 0.02 | 0.02 | -230 | FLK 23 | 0.01 | 0.67 |
| GOK 24 | 0.01 | 0.01 | -240 | FLK 24 | 0.01 | 0.32 |
| GOK 25 | 0.01 | 0.02 | -250 | FLK 25 | 0.01 | 1.31 |
| GOK 26 | 0.01 | 0.06 | -260 | FLK 26 | 0.01 | 0.76 |
| GOK 27 | 0.01 | 0.06 | -270 | FLK 27 | 0.01 | 1.05 |
| GOK 28 | 0.01 | 0.06 | -280 | FLK 28 | 0.01 | 1.40 |
| GOK 29 | 0.02 | 0.06 | -290 | FLK 29 | 0.01 | 1.21 |
| GOK 30 | 0.02 | 0.06 | -300 | FLK 30 | 0.02 | 1.19 |
| GOK 31 | 0.03 | 0.03 | -310 | FLK 31 | 0.03 | 1.96 |
| GOK 32 | 0.01 | 0.02 | -320 | FLK 32 | 0.02 | 1.016 |
| GOK 33 | 0.01 | 0.02 | -330 | FLK 33 | 0.03 | 1.029 |
| GOK 34 | 0.01 | 0.02 | -340 | FLK 34 | 0.01 | 0.689 |
| GOK 35 | 0.02 | 0.04 | -350 | FLK 35 | 0.01 | 1.055 |
| GOK 36 | 0.01 | 0.02 | -360 | FLK 36 | 0.02 | 0.912 |
| GOK 37 | 0.09 | 0.08 | -370 | FLK 37 | 0.04 | 1.547 |
| GOK 38 | 0.05 | 0.08 | -380 | FLK 38 | 0.03 | 1.199 |
| GOK 39 | 0.04 | 0.07 | -390 | FLK 39 | 0.05 | 1.576 |
| GOK 40 | 0.02 | 0.03 | -400 | FLK 40 | 0.10 | 0.733 |
| GOK 41 | 0.02 | 0.05 | -410 | FLK 41 | 0.05 | 0.744 |
| GOK 42 | 0.07 | 0.07 | -420 | FLK 42 | 0.06 | 0.293 |

*Table 47 continued*

| 2021 GOK 10 cm | | | | 2021 FLK 10 cm | | |
|---|---|---|---|---|---|---|
| **Sample name** | **$NH_4^+$ (µg/ml)** | **$Ca^{2+}$ (µg/ml)** | **Depth (cm)** | **Sample name** | **$NH_4^+$ (µg/ml)** | **$Ca^{2+}$ (µg/ml)** |
| GOK 43 | 0.05 | 0.06 | -430 | FLK 43 | 0.04 | 0.54 |
| GOK 44 | 0.05 | 0.03 | -440 | FLK 44 | 0.08 | 1.45 |
| GOK 45 | 0.05 | 0.04 | -450 | | | |
| GOK 46 | 0.04 | 0.03 | -460 | | | |
| GOK 47 | 0.04 | 0.04 | -470 | | | |
| GOK 48 | 0.03 | 0.04 | -480 | | | |
| GOK 49 | 0.06 | 0.05 | -490 | | | |
| GOK 50 | 0.11 | 0.10 | -500 | | | |

*Table 48: Used 2022 20 cm ammonium and calcium values*

| 2022 20 cm | | | |
|---|---|---|---|
| **Sample name** | **$NH_4^+$ (µg/ml)** | **$Ca^{2+}$ (µg/ml)** | **Depth (cm)** |
| GOK 1 | 0.19 | 0.12 | -20 |
| GOK 2 | 0.46 | 0.13 | -40 |
| GOK 3 | 0.59 | 0.15 | -60 |
| GOK 4 | 0.17 | 0.04 | -80 |
| GOK 5 | 0.21 | 0.06 | -100 |
| GOK 6 | 0.28 | 0.20 | -120 |
| GOK 7 | 0.04 | 0.07 | -140 |
| GOK 8 | 0.02 | 0.06 | -160 |
| GOK 9 | 0.02 | 0.04 | -180 |
| GOK 10 | 0.01 | 0.05 | -200 |
| GOK 11 | 0.02 | 0.04 | -220 |
| GOK 12 | 0.03 | 0.04 | -240 |
| GOK 13 | 0.01 | 0.08 | -260 |
| GOK 14 | 0.03 | 0.12 | -280 |
| GOK 15 | 0.05 | 0.11 | -300 |
| GOK 16 | 0.04 | 0.04 | -320 |
| GOK 17 | 0.09 | 0.08 | -340 |
| GOK 18 | 0.05 | 0.05 | -360 |
| **Sample name** | **$NH_4^+$ (µg/ml)** | **$Ca^{2+}$ (µg/ml)** | **Depth (cm)** |
| FLK 1 | 0.17 | 0.06 | -20 |
| FLK 2 | 0.43 | 0.18 | -40 |
| FLK 3 | 0.33 | 0.17 | -60 |
| FLK 4 | 0.34 | 0.12 | -80 |
| FLK 5 | 0.27 | 0.38 | -100 |
| FLK 6 | 0.05 | 0.39 | -120 |
| FLK 7 | 0.02 | 0.27 | -140 |
| FLK 8 | 0.06 | 0.69 | -160 |
| FLK 9 | 0.04 | 0.11 | -180 |
| FLK 10 | 0.09 | 1.52 | -200 |

*Table 48 continued*

| 2022 20 cm | | | |
|---|---|---|---|
| **Sample name** | **$NH_4^+$ (µg/ml)** | **$Ca^{2+}$ (µg/ml)** | **Depth (cm)** |
| FLK 11 | 0.02 | 0.09 | -220 |
| FLK 12 | 0.10 | 1.11 | -240 |
| FLK 13 | 0.08 | 0.34 | -260 |
| FLK 14 | 0.02 | 0.06 | -280 |
| FLK 15 | 0.05 | 0.07 | -300 |

*Table 49: Used 2022 10 cm ammonium and calcium values*

| 2022 GOK 10 cm | | | | 2022 FLK 10 cm | | |
|---|---|---|---|---|---|---|
| **Sample name** | **$NH_4^+$ (µg/ml)** | **$Ca^{2+}$ (µg/ml)** | **Depth (cm)** | **Sample name** | **$NH_4^+$ (µg/ml)** | **$Ca^{2+}$ (µg/ml)** |
| GOK 1 | 0.21 | 0.04 | -10 | FLK 1 | 0.16 | 0.03 |
| GOK 2 | 0.17 | 0.03 | -20 | FLK 2 | 0.18 | 0.02 |
| GOK 3 | 0.40 | 0.07 | -30 | FLK 3 | 0.27 | 0.10 |
| GOK 4 | 0.60 | 0.10 | -40 | FLK 4 | 0.62 | 0.13 |
| GOK 5 | 0.77 | 0.13 | -50 | FLK 5 | 0.47 | 0.15 |
| GOK 6 | 0.28 | 0.09 | -60 | FLK 6 | 0.13 | 0.02 |
| GOK 7 | 0.07 | 0.02 | -70 | FLK 7 | 0.52 | 0.14 |
| GOK 8 | 0.31 | 0.03 | -80 | FLK 8 | 0.24 | 0.08 |
| GOK 9 | 0.20 | 0.04 | -90 | FLK 9 | 0.42 | 0.59 |
| GOK 10 | 0.12 | 0.02 | -100 | FLK 10 | 0.23 | 0.42 |
| GOK 11 | 0.27 | 0.41 | -110 | FLK 11 | 0.05 | 0.08 |
| GOK 12 | 0.22 | 0.11 | -120 | FLK 12 | 0.06 | 0.06 |
| GOK 13 | 0.05 | 0.04 | -130 | FLK 13 | <LOD | 0.03 |
| GOK 14 | <LOD | 0.03 | -140 | FLK 14 | <LOD | 0.03 |
| GOK 15 | <LOD | 0.06 | -150 | FLK 15 | <LOD | 0.02 |
| GOK 16 | <LOD | 0.02 | -160 | FLK 16 | <LOD | 0.01 |
| GOK 17 | <LOD | 0.01 | -170 | FLK 17 | <LOD | 0.03 |
| GOK 18 | 0.10 | 0.25 | -180 | FLK 18 | <LOD | 0.02 |
| GOK 19 | <LOD | 0.02 | -190 | FLK 19 | 0.02 | 0.02 |
| GOK 20 | <LOD | 0.01 | -200 | FLK 20 | 0.02 | 0.02 |
| GOK 21 | <LOD | 0.02 | -210 | FLK 21 | <LOD | 0.01 |
| GOK 22 | <LOD | 0.01 | -220 | FLK 22 | <LOD | <LOD |
| GOK 23 | 0.03 | 0.02 | -230 | FLK 23 | <LOD | <LOD |
| GOK 24 | <LOD | 0.02 | -240 | FLK 24 | <LOD | <LOD |
| GOK 25 | <LOD | 0.04 | -250 | FLK 25 | <LOD | 0.04 |
| GOK 26 | <LOD | 0.06 | -260 | FLK 26 | <LOD | 0.02 |
| GOK 27 | 0.02 | 0.08 | -270 | FLK 27 | 0.24 | 1.57 |
| GOK 28 | 0.03 | 0.12 | -280 | FLK 28 | <LOD | 0.07 |
| GOK 29 | 0.04 | 0.06 | -290 | FLK 29 | <LOD | <LOD |
| GOK 30 | 0.03 | 0.03 | -300 | FLK 30 | <LOD | <LOD |
| GOK 31 | <LOD | 0.04 | -310 | FLK 31 | 0.03 | 0.12 |
| GOK 32 | 0.04 | 0.03 | -320 | FLK 32 | 0.01 | 0.16 |

*Table 49 continued*

| 2022 GOK 10 cm | | | | 2022 FLK 10 cm | | |
|---|---|---|---|---|---|---|
| **Sample name** | **$NH_4^+$ (µg/ml)** | **$Ca^{2+}$ (µg/ml)** | **Depth (cm)** | **Sample name** | **$NH_4^+$ (µg/ml)** | **$Ca^{2+}$ (µg/ml)** |
| GOK 33 | 0.06 | 0.03 | -330 | | | |
| GOK 34 | 0.05 | 0.05 | -340 | | | |
| GOK 35 | 0.02 | 0.03 | -350 | | | |
| GOK 36 | 0.01 | 0.02 | -360 | | | |

## 5.3 Used pH and Ca2+ values

*Table 50: Used 2017 pH and Calcium values*

| 2017 FLK | | | 2017 GOK | |
|---|---|---|---|---|
| **pH** | **$Ca^{2+}$ (µev/L)** | **Depth (cm)** | **pH** | **$Ca^{2+}$ (µev/L)** |
| 5.25 | 6.59 | -10 | 5.26 | 6.29 |
| 5.27 | 5.74 | -20 | 5.15 | 5.19 |
| 5.12 | 5.39 | -30 | 5.19 | 4.44 |
| 5.15 | 5.34 | -40 | 5.33 | 7.78 |
| 5.42 | 7.49 | -50 | 5.60 | 7.68 |
| 5.63 | 4.04 | -60 | 5.22 | 8.03 |
| 5.43 | 3.44 | -70 | 5.09 | 4.44 |
| 5.44 | 4.74 | -80 | 5.48 | 4.34 |
| 5.75 | 4.19 | -90 | 5.44 | 4.44 |
| 5.17 | 7.19 | -100 | 5.29 | 4.49 |
| 5.38 | 4.99 | -110 | 5.47 | 9.33 |
| 5.51 | 4.09 | -120 | 5.48 | 8.83 |
| 5.63 | 5.04 | -130 | 5.60 | 8.38 |
| 5.50 | 4.09 | -140 | 5.35 | 6.39 |
| 5.78 | 9.08 | -150 | 5.28 | 5.64 |
| 5.51 | 6.64 | -160 | 5.01 | 6.09 |
| 5.40 | 6.19 | -170 | 5.09 | 7.44 |
| 5.30 | 5.74 | -180 | 5.36 | 5.14 |
| 5.28 | 3.94 | -190 | 5.27 | 6.19 |
| 5.07 | 4.84 | -200 | 5.10 | 3.99 |
| 5.37 | 8.93 | -210 | 5.24 | 3.69 |
| 5.48 | 4.34 | -220 | 5.10 | 4.69 |
| 5.33 | 5.29 | -230 | 5.18 | 3.09 |
| 5.30 | 5.29 | -240 | 5.27 | 4.64 |

| 2017 FLK | | | 2017 GOK | |
|---|---|---|---|---|
| pH | $Ca^{2+}$ (µev/L) | Depth (cm) | pH | $Ca^{2+}$ (µev/L) |
| 5.35 | 3.89 | -250 | 5.29 | 8.73 |
| 5.4 | 5.29 | -260 | 5.26 | 3.74 |
| 5.23 | 3.79 | -270 | 5.38 | 4.64 |
| 5.39 | 4.44 | -280 | 5.84 | 14.6 |
| 5.3 | 4.54 | -290 | 5.14 | 4.44 |
| 5.47 | 6.24 | -300 | 5.36 | 14.6 |
| 5.56 | 9.58 | -310 | 5.07 | 7.04 |
| 5.38 | 5.74 | -320 | | |
| 5.62 | 6.64 | -330 | | |
| 5.53 | 8.08 | -340 | | |
| 5.58 | 8.48 | -350 | | |
| 5.76 | 3.64 | -360 | | |
| 5.33 | 4.64 | -370 | | |
| - | - | -380 | | |
| 5.4 | 4.44 | -390 | | |

*Table 51: Used 2018 pH and Calcium values*

| 2018 GOK | | | | | |
|---|---|---|---|---|---|
| **pH** | **$Ca^{2+}$ (µev/L)** | **depth (cm)** | **pH** | **$Ca^{2+}$ (µev/L)** | **depth (cm)** |
| 5.76 | 7.77 | -10 | 5.36 | 3.45 | -310 |
| 5.77 | 10.0 | -20 | 5.19 | 4.15 | -320 |
| 5.61 | 5.15 | -30 | 5.20 | 4.57 | -330 |
| 5.61 | 4.73 | -40 | 5.20 | 3.49 | -340 |
| 5.55 | 3.43 | -50 | 5.38 | 3.48 | -350 |
| 5.64 | 4.66 | -60 | 5.54 | 4.41 | -360 |
| 5.73 | 5.49 | -70 | 5.55 | 3.91 | -370 |
| 5.48 | 5.38 | -80 | 5.76 | 9.36 | -380 |
| 5.32 | 5.94 | -90 | 5.62 | 5.21 | -390 |
| 5.39 | 2.71 | -100 | 5.56 | 5.49 | -400 |
| 5.44 | 3.45 | -110 | 5.57 | 3.97 | -410 |
| 5.48 | 4.84 | -120 | 5.58 | 2.99 | -420 |
| 4.92 | 3.28 | -130 | 5.62 | 3.91 | -430 |
| 5.21 | 3.14 | -140 | | | |
| 5.33 | 1.25 | -150 | | | |
| 5.16 | 4.17 | -160 | | | |
| 5.29 | 2.81 | -170 | | | |
| 5.27 | 3.08 | -180 | | | |
| 5.35 | 2.61 | -190 | | | |
| 5.40 | 1.25 | -200 | | | |
| 5.43 | 2.57 | -210 | | | |
| 5.43 | 5.16 | -220 | | | |
| 5.62 | 8.72 | -230 | | | |
| 5.56 | 5.31 | -240 | | | |
| 5.46 | 4.45 | -250 | | | |
| 4.81 | 3.53 | -260 | | | |
| 5.34 | 3.02 | -270 | | | |
| 5.47 | 1.25 | -280 | | | |
| 5.23 | 3.57 | -290 | | | |
| 5.15 | 3.77 | -300 | | | |

*Table 52: Used 2019 pH and calcium values*

| 2019 GOK | | | | | |
|---|---|---|---|---|---|
| pH | $Ca^{2+}$ (µev/L) | depth (cm) | pH | $Ca^{2+}$ (µev/L) | depth (cm) |
| 5.40 | 18.3 | -10 | 6.68 | 70.4 | -300 |
| 5.22 | 1.27 | -20 | 6.28 | 24.8 | -310 |
| 5.15 | 1.05 | -30 | 5.76 | 0.82 | -320 |
| 5.41 | 12.0 | -40 | | | |
| 5.40 | 2.39 | -50 | | | |
| 5.62 | 3.25 | -60 | | | |
| 5.50 | 3.16 | -70 | | | |
| 5.56 | 1.24 | -80 | | | |
| 5.31 | 1.85 | -90 | | | |
| 5.15 | 8.09 | -100 | | | |
| 5.33 | 12.1 | -110 | | | |
| 5.36 | 6.77 | -120 | | | |
| 5.61 | 16.2 | -130 | | | |
| 5.66 | 5.23 | -140 | | | |
| 5.54 | 11.8 | -150 | | | |
| 5.71 | 14.2 | -160 | | | |
| 5.61 | 2.65 | -170 | | | |
| 5.55 | 1.83 | -180 | | | |
| 5.47 | 1.55 | -190 | | | |
| 5.45 | 2.55 | -200 | | | |
| 5.48 | 3.20 | -210 | | | |
| 5.44 | 4.34 | -220 | | | |
| 5.37 | 3.29 | -230 | | | |
| 5.56 | 2.58 | -240 | | | |
| 5.58 | 1.79 | -250 | | | |
| 5.55 | 2.32 | -260 | | | |
| 5.63 | 0.36 | -270 | | | |
| 6.16 | 21.3 | -280 | | | |
| 6.76 | 105 | -290 | | | |

*Table 53: Used 2020 pH and calcium values*

| 2020 GOK | | | | | |
|---|---|---|---|---|---|
| **pH** | **$Ca^{2+}$ (µev/L)** | **depth (cm)** | **pH** | **$Ca^{2+}$ (µev/L)** | **depth (cm)** |
| 5.44 | 4.68 | -10 | 5.48 | 1.07 | -290 |
| 5.80 | 13.5 | -20 | 5.50 | 1.11 | -300 |
| 5.82 | 5.48 | -30 | 5.46 | 1.15 | -310 |
| 5.71 | 2.22 | -40 | 5.52 | 1.16 | -320 |
| 5.62 | 0.65 | -50 | 5.46 | 1.42 | -330 |
| 5.64 | 0.27 | -60 | 5.47 | 1.40 | -340 |
| 5.70 | 6.34 | -70 | 5.45 | 1.52 | -350 |
| 5.70 | 2.59 | -80 | 5.44 | 1.41 | -360 |
| 5.65 | 1.15 | -90 | 5.44 | 2.77 | -370 |
| 5.55 | 0.89 | -100 | 5.34 | 3.39 | -380 |
| 5.53 | 0.74 | -110 | 5.39 | 2.90 | -390 |
| 5.50 | 0.60 | -120 | | | |
| 5.59 | 1.94 | -130 | | | |
| 5.61 | 1.49 | -140 | | | |
| 5.64 | 2.22 | -150 | | | |
| 5.56 | 2.17 | -160 | | | |
| 5.59 | 4.02 | -170 | | | |
| 5.64 | 1.89 | -180 | | | |
| 5.57 | 1.18 | -190 | | | |
| 5.56 | 0.73 | -200 | | | |
| 5.60 | 0.96 | -210 | | | |
| 5.55 | 1.73 | -220 | | | |
| 5.59 | 1.43 | -230 | | | |
| 5.58 | 0.81 | -240 | | | |
| 5.55 | 0.73 | -250 | | | |
| 5.55 | 1.01 | -260 | | | |
| 5.54 | 1.05 | -270 | | | |
| 5.49 | 0.99 | -280 | | | |

*Table 54: Used 2021 pH and calcium values*

| 2021 GOK | | | 2021 FLK | |
|---|---|---|---|---|
| pH | $Ca^{2+}$ (µev/L) | Depth (cm) | pH | $Ca^{2+}$ (µev/L) |
| 5.79 | 15.9 | -10 | 5.50 | 7.13 |
| 5.60 | 9.98 | -20 | 5.51 | 3.89 |
| 5.54 | 7.66 | -30 | 5.42 | 7.51 |
| 5.35 | 5.04 | -40 | 5.43 | 4.07 |
| 5.34 | 3.90 | -50 | 5.58 | 5.42 |
| 5.38 | 2.70 | -60 | 5.75 | 7.44 |
| 5.54 | 5.68 | -70 | 5.83 | 11.3 |
| 5.73 | 9.36 | -80 | 5.73 | 9.27 |
| 5.55 | 8.62 | -90 | 5.47 | 4.19 |
| 5.64 | 11.9 | -100 | 5.34 | 5.26 |
| 5.51 | 5.11 | -110 | 5.34 | 3.17 |
| 5.26 | 3.12 | -120 | 5.57 | 4.54 |
| 5.26 | 3.88 | -130 | 5.55 | 3.51 |
| 5.28 | 4.80 | -140 | 5.67 | 6.53 |
| 5.42 | 3.11 | -150 | 6.17 | 31.2 |
| 5.43 | 3.43 | -160 | 5.86 | 12.5 |
| 5.52 | 4.04 | -170 | 6.05 | 19.8 |
| 5.57 | 5.77 | -180 | 6.15 | 25.5 |
| 5.55 | 3.90 | -190 | 6.35 | 50.7 |
| 5.74 | 6.80 | -200 | 6.01 | 26.6 |
| 5.92 | 16.6 | -210 | 5.79 | 9.44 |
| 5.38 | 0.84 | -220 | 5.87 | 15.8 |
| 5.24 | 0.85 | -230 | 6.19 | 33.4 |
| 5.28 | 0.52 | -240 | 5.90 | 16.0 |
| 5.43 | 0.96 | -250 | 6.51 | 65.3 |
| 5.36 | 2.88 | -260 | 6.29 | 37.8 |
| 5.36 | 2.89 | -270 | 6.12 | 52.5 |
| 5.41 | 2.88 | -280 | 6.95 | 70.0 |
| 5.41 | 2.81 | -290 | 6.37 | 60.5 |
| 5.41 | 3.09 | -300 | 6.57 | 59.4 |

*Table 54 continued*

| 2021 GOK | | | 2021 FLK | |
|---|---|---|---|---|
| pH | $Ca^{2+}$ (µev/L) | Depth (cm) | pH | $Ca^{2+}$ (µev/L) |
| 5.59 | 1.39 | -310 | 6.67 | 97.6 |
| 5.53 | 1.10 | -320 | 6.38 | 50.7 |
| 5.38 | 0.77 | -330 | 6.47 | 51.4 |
| 5.46 | 1.00 | -340 | 6.18 | 34.4 |
| 5.56 | 1.80 | -350 | 6.29 | 52.6 |
| 5.49 | 0.77 | -360 | 6.08 | 45.5 |
| 5.47 | 3.86 | -370 | 6.37 | 77.2 |
| 5.41 | 4.17 | -380 | 6.42 | 59.9 |
| 5.48 | 3.40 | -390 | 6.50 | 78.7 |
| 5.54 | 1.39 | -400 | 6.16 | 36.6 |
| 5.5 | 2.34 | -410 | 5.95 | 37.1 |
| 5.25 | 3.52 | -420 | 5.85 | 14.6 |
| 5.29 | 2.98 | -430 | 6.06 | 27.0 |
| 5.45 | 1.39 | -440 | 6.36 | 72.2 |
| 5.47 | 1.92 | -450 | | |
| 5.56 | 1.35 | -460 | | |
| 5.58 | 2.21 | -470 | | |
| 5.40 | 2.03 | -480 | | |
| 5.40 | 2.63 | -490 | | |
| 5.41 | 4.76 | -500 | | |

*Table 55: Used 2022 pH and calcium values*

| 2022 GOK | | | 2022 FLK | |
|---|---|---|---|---|
| pH | $Ca^{2+}$ (µev/L) | Depth (cm) | pH | $Ca^{2+}$ (µev/L) |
| 5.44 | 1.88 | -10 | 5.49 | 1.50 |
| 5.55 | 1.25 | -20 | 5.54 | 0.72 |
| 5.66 | 3.42 | -30 | 5.86 | 4.90 |
| 5.70 | 5.15 | -40 | 5.75 | 6.59 |
| 5.67 | 6.42 | -50 | 5.71 | 7.54 |
| 5.62 | 4.66 | -60 | 5.50 | 0.95 |
| 5.55 | 1.05 | -70 | 5.77 | 6.74 |
| 5.59 | 1.56 | -80 | 5.60 | 3.95 |
| 5.49 | 2.15 | -90 | 6.24 | 29.1 |
| 5.27 | 1.19 | -100 | 6.26 | 20.7 |
| 6.10 | 20.4 | -110 | 5.56 | 4.11 |
| 5.68 | 5.41 | -120 | 5.61 | 2.82 |
| 5.61 | 2.16 | -130 | 5.44 | 1.36 |
| 5.53 | 1.53 | -140 | 5.63 | 1.65 |
| 5.53 | 2.79 | -150 | 5.47 | 0.80 |
| 5.41 | 1.04 | -160 | 5.32 | 0.63 |
| 5.44 | 0.67 | -170 | 5.43 | 1.31 |
| 5.73 | 12.5 | -180 | 5.39 | 1.04 |
| 5.43 | 0.76 | -190 | 5.11 | 1.17 |
| 5.50 | 0.51 | -200 | 5.03 | 0.87 |
| 5.55 | 0.98 | -210 | 5.40 | 0.69 |
| 5.72 | 0.51 | -220 | 5.52 | 0.48 |
| 5.35 | 0.82 | -230 | 5.58 | 0.35 |
| 5.48 | 0.82 | -240 | 5.49 | 0.37 |
| 5.58 | 2.18 | -250 | 5.57 | 1.76 |
| 5.62 | 2.78 | -260 | 5.41 | 1.05 |
| 5.47 | 3.97 | -270 | 6.45 | 78.1 |
| 5.48 | 6.18 | -280 | 5.52 | 3.40 |
| 5.30 | 2.87 | -290 | 5.57 | 0.38 |
| 5.39 | 1.33 | -300 | 5.49 | 0.47 |

*Table 55 continued*

| 2022 GOK | | | 2022 FLK | |
|---|---|---|---|---|
| **pH** | **$Ca^{2+}$ (µev/L)** | **Depth (cm)** | **pH** | **$Ca^{2+}$ (µev/L)** |
| 5.44 | 1.75 | -310 | 5.86 | 5.71 |
| 5.46 | 1.60 | -320 | 5.87 | 8.15 |
| 5.55 | 1.51 | -330 | | |
| 5.59 | 2.42 | -340 | | |
| 5.46 | 1.25 | -350 | | |
| 5.54 | 0.77 | -360 | | |

## 5.4 Used mineral dust values

*Table 56: Mineral dust weight and sample weight*

| Sample name | MD (µg/g) | Sample weight (g) | MD (µg) |
|---|---|---|---|
| (2021) GOK 5 | 1.91 | 164 | 313 |
| (2021) GOK 11 | 2.79 | 196 | 546 |
| (2021) GOK23+24 | 1.33 | 447 | 595 |
| (2021) GOK25 | 22.2 | 204 | 4523 |
| (2021) FLK22 | 5.09 | 211 | 1075 |
| (2022) GOK6 | 5.24 | 175 | 917 |
| (2022) GOK18 | 13.8 | 214 | 2950 |
| (2022) FLK1+2 | 1.78 | 224 | 399 |
| (2022) FLK5 | 8.41 | 185 | 1553 |
| (2022) FLK11 | 3.68 | 226 | 832 |
| (2022) FLK13 | 1.83 | 219 | 401 |
| (2022) FLK16 | 19.8 | 177 | 3499 |
| (2018) GOK1 | 8.54 | 187 | 1600 |
| (2018) GOK11 | 0.93 | 222 | 207 |
| (2018) GOK12 | 1.85 | 221 | 409 |
| (2018) GOK19 | 1.78 | 267 | 474 |
| (2018) GOK20 | 2.04 | 230 | 469 |
| (2018) GOK22 | 25.9 | 132 | 3423 |
| (2017) GOK 15 | 3.48 | 176 | 611 |
| (2017) FLK 18 | 2.19 | 190 | 415 |
| (2017) FLK 20 | 62.8 | 78.2 | 4906 |

## 5.5 Sample and filter weight

*Table 57: Sample and filter weight*

| Sample name | Sample weight (g) | Filter weight (mg) | Sampled filter weight (mg) | Weight difference (mg) |
|---|---|---|---|---|
| (2017) GOK 1 | 84.2 | 39.0 | 38.9 | -0.07 |
| (2017) GOK 2 | 127 | 39.7 | 39.6 | -0.07 |
| (2017) GOK 3 | 147 | 38.7 | 38.6 | -0.12 |
| (2017) GOK 4 | 143 | 39.1 | 38.9 | -0.20 |
| (2017) GOK 5 | 135 | 39.6 | 39.4 | -0.14 |
| (2017) GOK 6 | 185 | 39.0 | 39.7 | 0.65 |
| (2017) GOK 7 | 130 | 38.7 | 38.8 | 0.11 |
| (2017) GOK 8 | 158 | 39.6 | 39.6 | 0.00 |
| (2017) GOK 9 | 183 | 39.4 | 39.4 | 0.02 |
| (2017) GOK 10 | 202 | 38.6 | 38.4 | -0.10 |
| (2017) GOK 11 | 219 | 39.3 | 39.1 | -0.21 |
| (2017) GOK 12 | 215 | 40.4 | 40.0 | -0.37 |
| (2017) GOK 13 | 183 | 38.7 | 38.4 | -0.26 |
| (2017) GOK 14 | 196 | 38.6 | 38.4 | -0.17 |
| (2017) GOK 15 | 176 | 39.2 | 39.3 | 0.23 |
| (2017) GOK 16 | 155 | 39.9 | 40.0 | 0.14 |
| (2017) FLK 1 | 82.8 | 39.3 | 39.2 | -0.05 |
| (2017) FLK 2 | 99.5 | 39.4 | 39.5 | 0.03 |
| (2017) FLK 3 | 115 | 39.4 | 39.3 | -0.05 |
| (2017) FLK 4 | 116 | 39.6 | 39.6 | -0.02 |
| (2017) FLK 5 | 149 | 37.9 | 37.9 | -0.04 |
| (2017) FLK 6 | 148 | 39.7 | 39.7 | -0.09 |
| (2017) FLK 7 | 135 | 39.2 | 39.0 | -0.08 |
| (2017) FLK 8 | 182 | 39.1 | 39.3 | 0.21 |
| (2017) FLK 9 | 218 | 39.8 | 39.7 | -0.08 |
| (2017) FLK 10 | 183 | 39.2 | 39.1 | -0.03 |
| (2017) FLK 11 | 212 | 39.3 | 39.5 | 0.17 |
| (2017) FLK 12 | 250 | 39.7 | 39.9 | 0.25 |
| (2017) FLK 13 | 243 | 39.4 | 39.8 | 0.33 |
| (2017) FLK 14 | 238 | 39.7 | 39.8 | 0.10 |
| (2017) FLK 15 | 251 | 39.2 | 39.2 | -0.01 |
| (2017) FLK 16 | 206 | 39.7 | 39.6 | -0.12 |
| (2017) FLK 17 | 185 | 39.0 | 39.0 | 0.01 |
| (2017) FLK 18 | 190 | 39.0 | 39.0 | 0.08 |
| (2017) FLK 19 | 206 | 39.9 | 39.7 | -0.20 |
| (2017) FLK 20 | 78.2 | 39.6 | 43.1 | 3.49 |
| (2018) GOK1 | 187 | 38.6 | 39.8 | 1.28 |
| (2018) GOK2 | 184 | 38.9 | 39.0 | 0.08 |
| (2018) GOK3 | 201 | 39.7 | 39.5 | -0.18 |
| (2018) GOK4 | 216 | 39.7 | 39.3 | -0.38 |
| (2018) GOK5 | 226 | 38.5 | 38.3 | -0.24 |
| (2018) GOK6 | 216 | 39.4 | 39.0 | -0.40 |

*Table 57 continued*

| Sample name | Sample weight (g) | Filter weight (mg) | Sampled filter weight (mg) | Weight difference (mg) |
|---|---|---|---|---|
| (2018) GOK7 | 192 | 39.5 | 39.4 | -0.11 |
| (2018) GOK8 | 198 | 39.4 | 39.4 | -0.03 |
| (2018) GOK9 | 203 | 39.7 | 39.6 | -0.12 |
| (2018) GOK10 | 212 | 39.6 | 39.5 | -0.15 |
| (2018) GOK11 | 222 | 39.3 | 39.5 | 0.24 |
| (2018) GOK12 | 221 | 38.6 | 38.6 | -0.02 |
| (2018) GOK13 | 221 | 39.7 | 39.7 | -0.02 |
| (2018) GOK14 | 231 | 39.6 | 39.5 | -0.09 |
| (2018) GOK15 | 221 | 39.3 | 39.1 | -0.15 |
| (2018) GOK16 | 232 | 39.8 | 39.6 | -0.27 |
| (2018) GOK17 | 240 | 39.1 | 39.0 | -0.17 |
| (2018) GOK18 | 232 | 38.6 | 38.5 | -0.10 |
| (2018) GOK19 | 267 | 38.6 | 38.8 | 0.18 |
| (2018) GOK20 | 230 | 33.9 | 34.4 | 0.50 |
| (2018) GOK21 | 265 | 36.0 | 35.9 | -0.01 |
| (2018) GOK22 | 132 | 35.8 | 39.4 | 3.56 |
| (2019) GOK1 | 458 | 36.1 | 37.4 | 1.27 |
| (2019) GOK2 | 419 | 35.0 | 36.2 | 0.22 |
| (2019) GOK3 | 574 | 36.1 | 36.7 | 0.58 |
| (2019) GOK4 | 528 | 36.1 | 36.0 | -0.10 |
| (2019) GOK5 | 621 | 36.0 | 36.7 | 0.65 |
| (2019) GOK6 | 416 | 36.1 | 37.0 | 0.91 |
| (2019) GOK7 | 410 | 35.2 | 37.5 | 2.32 |
| (2019) GOK8 | 412 | 36.1 | 37.1 | 1.01 |
| (2019) GOK9 | 440 | 35.5 | 36.6 | 1.06 |
| (2019) GOK10 | 450 | 35.5 | 37.1 | 1.61 |
| (2019) GOK11 | 468 | 36.0 | 36.5 | 0.49 |
| (2019) GOK12 | 430 | 34.7 | 36.1 | 1.38 |
| (2019) GOK13 | 424 | 35.5 | 36.2 | 0.70 |
| (2019) GOK14 | 459 | 34.7 | 37.1 | 2.44 |
| (2019) GOK15 | 448 | 34.6 | 39.3 | 4.67 |
| (2019) GOK16 | 376 | 35.8 | 36.6 | 0.79 |
| (2020) GOK1 | 86.5 | 35.1 | 35.4 | 0.28 |
| (2020) GOK2 | 114 | 34.5 | 34.5 | 0.04 |
| (2020) GOK3 | 113 | 35.7 | 35.8 | 0.09 |
| (2020) GOK4 | 216 | 35.5 | 35.5 | 0.00 |
| (2020) GOK5 | 218 | 34.3 | 34.3 | 0.02 |
| (2020) GOK6 | 249 | 34.2 | 35.7 | 1.46 |
| (2020) GOK7 | 233 | 35.4 | 35.9 | 0.50 |
| (2020) GOK8 | 246 | 35.6 | 36.1 | 0.57 |
| (2020) GOK9 | 239 | 35.1 | 35.2 | 0.11 |
| (2020) GOK10 | 247 | 36.2 | 36.2 | 0.03 |
| (2020) GOK11 | 251 | 35.5 | 35.4 | -0.12 |
| (2020) GOK12 | 252 | 35.7 | 35.6 | -0.10 |

*Table 57 continued*

| Sample name | Sample weight (g) | Filter weight (mg) | Sampled filter weight (mg) | Weight difference (mg) |
|---|---|---|---|---|
| (2020) GOK13 | 253 | 36.0 | 35.9 | -0.18 |
| (2020) GOK14 | 259 | 35.7 | 35.5 | -0.21 |
| (2020) GOK15 | 257 | 35.9 | 35.9 | -0.05 |
| (2020) GOK17+18 | 536 | 36.2 | 36.3 | 0.05 |
| (2020) GOK19+20 | 378 | 35.7 | 35.7 | -0.05 |
| (2021) GOK 1 | 109 | 39.3 | 39.7 | 0.44 |
| (2021) GOK 2 | 144 | 39.1 | 39.0 | -0.06 |
| (2021) GOK 3 | 129 | 39.4 | 39.6 | 0.20 |
| (2021) GOK 4 | 158 | / | / | / |
| (2021) GOK 5 | 164 | 39.2 | 39.5 | 0.28 |
| (2021) GOK 6 | 175 | 39.0 | 39.2 | 0.20 |
| (2021) GOK 7 | 197 | / | / | / |
| (2021) GOK 8 | 198 | 39.2 | 38.4 | -0.79 |
| (2021) GOK 9 | 186 | 39.6 | 39.7 | 0.11 |
| (2021) GOK 10 | 203 | 39.7 | 39.7 | -0.01 |
| (2021) GOK 11 | 196 | 39.5 | 39.8 | 0.31 |
| (2021) GOK 12 | 223 | 40.7 | 40.4 | -0.25 |
| (2021) GOK 13 | 227 | / | / | / |
| (2021) GOK 14 | 217 | 39.1 | 39.6 | 0.50 |
| (2021) GOK 15 | 217 | 38.9 | 39.1 | 0.16 |
| (2021) GOK 16 | 229 | 39.3 | 39.4 | 0.04 |
| (2021) GOK 17 | 230 | 38.7 | 38.9 | 0.16 |
| (2021) GOK 18 | 228 | 40.0 | 39.2 | -0.77 |
| (2021) GOK 19 | 222 | 39.1 | 39.3 | 0.16 |
| (2021) GOK 20 | 210 | 38.7 | 38.7 | 0.03 |
| (2021) GOK 21 | 200 | 38.6 | 38.7 | 0.03 |
| (2021) GOK 22 | 214 | 39.3 | 39.1 | -0.21 |
| (2021) GOK 23 | 209 | 38.7 | 39.1 | 0.37 |
| (2021) GOK 24 | 237 | / | / | / |
| (2021) GOK 25 | 204 | 39.5 | 52.3 | 12.8 |
| (2021) FLK 2 | 107 | 39.8 | 39.7 | -0.09 |
| (2021) FLK 3 | 147 | 39.1 | 39.3 | 0.14 |
| (2021) FLK 4 | 152 | 39.0 | 39.2 | 0.11 |
| (2021) FLK 5 | 172 | 39.1 | 39.2 | 0.13 |
| (2021) FLK 6 | 181 | 39.0 | 38.9 | -0.07 |
| (2021) FLK 7 | 181 | 39.7 | 39.4 | -0.25 |
| (2021) FLK 8 | 187 | 40.3 | 39.8 | -0.49 |
| (2021) FLK 9 | 185 | 39.3 | 39.4 | 0.11 |
| (2021) FLK 10 | 209 | 40.2 | 39.9 | -0.24 |
| (2021) FLK 11 | 204 | 38.6 | 38.7 | 0.16 |
| (2021) FLK 12 | 204 | / | / | / |
| (2021) FLK 13 | 225 | 39.5 | 39.4 | -0.09 |
| (2021) FLK 14 | 220 | 39.6 | 39.6 | -0.04 |
| (2021) FLK 15 | 230 | 38.6 | 38.9 | 0.23 |

*Table 57 continued*

| Sample name | Sample weight (g) | Filter weight (mg) | Sampled filter weight (mg) | Weight difference (mg) |
|---|---|---|---|---|
| (2021) FLK 16 | 235 | 39.2 | 39.2 | 0.04 |
| (2021) FLK 17 | 231 | 38.7 | 39.2 | 0.54 |
| (2021) FLK 18 | 240 | 39.1 | 40.0 | 0.86 |
| (2021) FLK 19 | 212 | 38.7 | 39.5 | 0.88 |
| (2021) FLK 20 | 202 | 39.7 | 40.2 | 0.50 |
| (2021) FLK 21 | 303 | 39.0 | 40.1 | 1.16 |
| (2021) FLK 22 | 211 | 39.4 | 40.7 | 1.35 |
| (2022) GOK 1 | 70.7 | 37.9 | 37.9 | -0.02 |
| (2022) GOK 2 | 129 | 39.7 | 39.8 | 0.09 |
| (2022) GOK 3 | 146 | 38.6 | 38.9 | 0.22 |
| (2022) GOK 4 | 175 | 39.7 | 39.3 | -0.34 |
| (2022) GOK 5 | 178 | 39.1 | 39.2 | 0.10 |
| (2022) GOK 6 | 175 | 39.0 | 39.4 | 0.47 |
| (2022) GOK 7 | 183 | 39.78 | 39.8 | -0.02 |
| (2022) GOK 8 | 203 | 38.6 | 38.7 | 0.06 |
| (2022) GOK 9 | 177 | 38.8 | 39.5 | 0.68 |
| (2022) GOK 10 | 203 | / | / | / |
| (2022) GOK 11 | 201 | 39.5 | 39.5 | -0.02 |
| (2022) GOK 12 | 220 | / | / | / |
| (2022) GOK 13 | 217 | 39.0 | 39.2 | 0.22 |
| (2022) GOK 14 | 205 | 38.23 | 38.8 | 0.58 |
| (2022) GOK 15 | 242 | 38.7 | 39.0 | 0.28 |
| (2022) GOK 16 | 221 | 38.9 | 39.0 | 0.12 |
| (2022) GOK 17 | 193 | 39.4 | 39.9 | 0.54 |
| (2022) GOK 18 | 214 | 38.9 | 42.0 | 3.08 |
| (2022) FLK 1 | 74.5 | 34.4 | 34.9 | 0.46 |
| (2022) FLK 2 | 150 | / | / | / |
| (2022) FLK 3 | 149 | 34.3 | 34.6 | 0.29 |
| (2022) FLK 4 | 188 | 35.2 | 35.5 | 0.28 |
| (2022) FLK 5 | 185 | 34.9 | 36.4 | 1.48 |
| (2022) FLK 6 | 189 | 33.6 | 33.9 | 0.25 |
| (2022) FLK 7 | 186 | 35.0 | 35.2 | 0.19 |
| (2022) FLK 8 | 203 | 34.5 | 34.7 | 0.18 |
| (2022) FLK 9 | 195 | 34.9 | 35.0 | 0.10 |
| (2022) FLK 10 | 226 | 34.1 | 34.7 | 0.64 |
| (2022) FLK 11 | 210 | 34.6 | 34.4 | -0.17 |
| (2022) FLK 12 | 219 | 35.5 | 35.8 | 0.33 |
| (2022) FLK 13 | 216 | 35.7 | 35.7 | -0.02 |
| (2022) FLK 14 | 220 | 34.7 | 34.8 | 0.11 |
| (2022) FLK 15 | 177 | 35.8 | 39.2 | 3.33 |

# 6. References


[1] Francois Tuzet, et al., *A multilayer physically based snowpack model simulating direct and indirect radiative impacts of light-absorbing impurities in snow,* The Cryosphere, 2017, 11, 2633–2653

[2] Francois Tuzet et al., *Quantification of the radiative impact of light-absorbing particles during two contrasted snow seasons at Col du Lautaret (2058 m a.s.l., French Alps),* The Cryosphere, 2020, 14, 4553–4579

[3] Skiles, S. M., Flanner, M., Cook, J. M., Dumont, M., and Painter, T. H.: *Radiative forcing by light-absorbing particles in snow*, Nature Climate Change, 8, 964–971

[4] Chaman Gul, et al., *Concentrations and source regions of light-absorbing particles in snow/ice in northern Pakistan and their impact on snow albedo,* Atmos. Chem. Phys., 2018, 18, 4981–5000

[5] Heinz H., Kunze W, *Umweltanalytik mit Spektrometrie und Chromatographie*, 3. Auflage, Wiley-VCH, 2004, 249

[6] Heinz H., Kunze W, *Umweltanalytik mit Spektrometrie und Chromatographie*, 3. Auflage, Wiley-VCH, 2004, 196 – 201

[7] Kandler K. et al., *Chemical composition and complex refractive index of Saharan Mineral Dust at Izana, Tenerife (Spain) derived by electron microscopy, Atmospheric Environment, 41(37), 8058-8074*

[8] Greilinger M. et al., *Contribution of Saharan Dust to Ion Deposition Loads of High Alpine Snow Packs in Austria (1987–2017)*, Front. Earth Sci., 2018, 6

[9] Kau D. et al., *Thermal-optical analysis of snow samples – challenges and perspectives introduced via the occurrence of mineral dust,* Diploma thesis, TU Wien, 2021

[10] Wang W. et al., *Characterizing Surface Albedo of Shallow Fresh Snow and Its Importance for Snow Ablation on the Interior of the Tibetan Plateau,* Journal of Hydrometeorology Vol. 21, 2020, 815–827

[11] Ales Hall, *The Role of Surface Albedo Feedback in Climate, journal of Climate*, Vol. 17, 2004, 1550–1568

[12] Chaoliu Li et al., *Re-evaluating black carbon in the Himalayas and the Tibetan Plateau: concentrations and deposition,* Atmos. Chem. Phys., 17, 2017, 11899–11912

[13] M. E. Birch & R. A. Cary, Elemental Carbon-Based Method for Monitoring Occupational Exposures to Particulate Diesel Exhaust, Aerosol Science and Technology, 2007, 226

[14] F. Cavalli et al., *Toward a standardised thermal-optical protocol for measuring atmospheric organic and elemental carbon: the EUSAAR protocol, A*tmos. Meas. Tech., 3, 2010, 79–89

[15] Kirchsteiger B. et al., *Combination of Different Approaches to Infer Local or Regional Contributions to $PM_{2.5}$ Burdens in Graz, Austria,* Applied Sciences, 2020, 4

[16] Zdanowicz C. et al., *Elemental and water-insoluble organic carbon in Svalbard snow: a synthesis of observations during 2007-2018, Atmospheric Chemistry and Physics*, 21, 2021, 3035-3057

[17] Kau D. et al., *Thermal-optical analysis of quartz fiber filters loaded with snow-samples determination of iron based on interferences caused by mineral dust*, Atmospheric Measurement Techniques, 15, 2022, 5207-5217

[18] Meinander O. et al., *Intercomparison Experiment of Water-Insoluble Carbonaceous Particles in Snow in a High-Mountain Environment (1598 m a.s.l.)*, Geosciences, 2022, 12(5), 197

[19] S. Lim et al*., Refractory black carbon mass concentrations in snow and ice: method evaluation and inter-comparison with elemental carbon measurement*, Atmos. Meas. Tech., 2014, 7, 3307-3324

[20] Mário Cerqueira et al., *Particulate carbon in precipitation at European background sites*, Aerosol Science, 2010, 41, 51-61

[21] Jonas Svensson et al., *Light-absorption of dust and elemental carbon in snow in the Indian Himalayas and the Finnish Arctic,* Atmospheric Measurement Techniques, 2018, 11, 1403-1416

[22] Sarah J. Doherty et al., *Black carbon and other light-absorbing particles in snow of central North America,* Journal of Geophysical Research: Atmospheres, 2014, 119, 12807-12831

[23] Vukicevic A., *Thermo-optische Analyse von Schnee und Aerosolproben aus den Hohen Tauern (Sonnblick Observatorium),* Bachelor's thesis, TU Wien, 2022

[24] Greilinger M. et al., *Temporal changes of inorganic ion deposition in the seasonal snow cover for the Austrian Alps (1983-2014)*, Atmospheric Environment, 2016, 132, 141-152